Fall 12-2011

Chemical, Biological, and Preliminary In Vitro Studies of Novel Vanadium(IV) Complexes with Schiff Bases and Thiosemicarbazone Ligands

Nerissa Abigail Lewis
University of Southern Mississippi

The University of Southern Mississippi

CHEMICAL, BIOLOGICAL AND PRELIMINARY *IN VITRO* STUDIES OF NOVEL VANADIUM(IV) COMPLEXES WITH SCHIFF BASES AND THIOSEMICARBAZONE LIGANDS

by

Nerissa Abigail Lewis

A Thesis
Submitted to the Graduate School
of The University of Southern Mississippi
in Partial Fulfillment of the Requirements
for the Degree of Master of Science

Approved:

Alvin A. Holder
_____
Director

Douglas S. Masterson
_____

Wujian Miao
_____

Susan A. Sultanen
_____
Dean of the Graduate School

December 2011

ABSTRACT

CHEMICAL, BIOLOGICAL AND PRELIMINARY *IN VITRO* STUDIES OF NOVEL VANADIUM(IV) COMPLEXES WITH SCHIFF BASES AND THIOSEMICARBAZONE LIGANDS

by Nerissa Lewis

December 2011

9-Anthraldehyde-N(4)-methylthiosemicarbazone (MeATSC), potassium (E)-2-(2-hydroxybenzylideneamino)-3-(1H-indol-3-yl)propanoate (K[(Sal-*L*-tryp)] and 2-(2-hydroxybenzylamino)-3-(1H-indol-3-yl)propanoic acid (the reduced Schiff base) were prepared using known synthetic procedures. Two novel thiosemicarbazone ligands, *(E)*-*N*-ethyl-2-(4-hydroxy-3-methoxybenzylidene)hydrazinecarbothioamide (*N*-Ethhymethohcarbthio) and (*E*)-*N*-ethyl-2-(1-(thiazol-2-yl)ethylidene)hydrazinecarbothioamide (acetylethTSC), were also prepared. All ligands were characterized by FT IR and electrochemistry. *N*-Ethhymethohcarbthio were characterized by elemental analysis whereas the reduced Schiff base and K[(Sal-*L*-tryp)] were characterized by ESI MS. X-ray crystallography was also used to characterize acetylethTSC. The ligands were then reacted with [VO(Sal-*L*-tryp)(H_2O)] **(1)** (Sal-*L*-tryp = *N*-salicylidene-*L*-tryptophanate) to produce the novel complexes, [VO(Sal-*L*-tryp)(MeATSC)].1.5C_2H_5OH **(2)**, [VO(Sal-*L*-tryp)(*N*-Ethhymethohcarbthio)].H_2O **(3)**, and [VO(Sal-*L*-tryp)(acetylethTSC)].0.75C_2H_5OH **(4)**, respectively. All complexes were characterized by elemental analysis, ESI MS, IR, UV-visible, ^{1}H and ^{13}C NMR spectroscopy, and electrochemistry. Oxidized DMSO and DMSO-d_6 solutions of each

complex were also characterized by ESI MS and ^{1}H NMR spectroscopy. [VO(Sal-*L*-tryp)(MeATSC)].1.5C_2H_5OH, [VO(Sal-*L*-tryp)(*N*-Ethhymethohcarbthio)].H_2O, and [VO(Sal-*L*-tryp)(acetylethTSC)].0.75C_2H_5OH were observed to exhibit anti-proliferative activity against three colon cancer cell lines, HTC-116, Caco-2, and HT-29. When the anti-proliferative effects were compared with that of non-cancerous colonic myofibroblasts, less inhibition was observed. The results obtained suggest that these compounds can be used as potential chemotherapeutic agents.

ACKNOWLEDGMENTS

I wish to extend sincere gratitude to all who assisted and supported me throughout this journey. The accomplishment of this thesis would have been impossible without the help of Almighty God and the support of several special people. I would therefore like to take this opportunity to acknowledge and thank those persons who assisted me throughout this project.

Firstly, I want to thank the Department of Chemistry and Biochemistry for allowing me the opportunity to pursue my graduate career. To my research advisor, Dr. Alvin Holder, I thank you for all your assistance and guidance, and for allowing me the opportunity to conduct research in your laboratory. I would also like to thank my committee members: Dr. Douglas Masterson and Dr. Wujian Miao, for all their advice and assistance, and also Dr. Robert Bateman for temporarily sitting in on an emergency meeting at short notice.

Appreciation must also be expressed to the Mississippi INBRE (P20RR016476), which is funded by the National Center for Research Resources, National Institutes of Health, U.S.A., the USM Lucas Endowment Grant, and the ExxonMobil Research and Engineering Company through Dr. John Robbins.

Special thanks to Dr. Vijayaraghavan Rangachari and his research group for the use of their Cary Eclipse fluorescence spectrophotometer and JASCO J-815 CD spectrometer and also to Anthony Magnusen and Travis Erves for their significant contribution to the synthesis of all V(IV) complexes. Anthony Magnusen and Travis Erves played an important role in designing a successful synthetic pathway for our

novel compounds, and they are therefore responsible for the mobilization of this project. To Dr. Wujian Miao and Dr. Suman Parajuli, special thanks for the guidance and assistance with the interpretation of the electrochemical data. I would also like to thank Dr.William Jarret and Mr. Gary Cook for allowing us use the respective NMR spectrophotometers and for assisting with the NMR spectral analysis.

I would also like to thank Dr. Ramaiyer Venkatraman and Dr. Floyd A. Beckford for assistance with the synthesis of our novel thiosemicarbazone ligands. Special thanks to Dr. Don VanDerveer and Dr. Frank Fronczek for the collection and structural analysis of X-ray crystallographic data for acethylethTSC. Thanks to Dr. Antonio González-Sarrías for performing the *in vitro* studies of compounds **1-4** .

My deepest gratitude is extended to my mom, Gale Lewis; my dad, Oswald Lewis; and my two brothers, Kishon and Devon Lewis; and the rest of my family and friends at home for all their prayers and support. Also, I will like to thank Connie and Willie Trotter and Francine Clemons for all their encouragement, prayers, guidance and support during my time of need.

I thank my fellow colleagues La Crissia Bridges, Joshua Phillip and Monique Taylor, as well as the other members of my group, for all their help and support. I would also like to thank Dr. Varma Rambaran for his advice and assistance during the short period he spent in our research group.

TABLE OF CONTENTS

LIST OF TABLES

Table

LIST OF ILLUSTRATIONS

Figure

LIST OF SCHEMES

Scheme

LIST OF ABBREVIATIONS

$acac^-$	Acetylacetonate
ATP	Adenosine-5'-Triphosphate
bpy = bipy	2,2'- Bipyridine
Carboplatin	(Diamine[1,1-Cyclobutanedicarboxylato(2-)]-*O,O´*-Platinum(II))
Cp	Cyclopentadienyl
diars	*o*-Phenylenebisdimethylarsine, *o*-$C_6H_4(AsMe_2)_2$
dmpe	1,2-Bis(dimethylphosphino)ethane
DNA	Deoxyribonucleic acid
EAT	Ehrlich ascites tumour
E. Coli	*Escherichia coli*
EtOH	Ethanol
Hz	Hertz
Me	Methyl
MeOH	Methanol
NMR	Nuclear Magnetic Resonance
NADP	Nicotinamide Adenine Dinucleotide Phosphate
NADV	Nicotinamide Adenine Dinucleotide Vanadate
NADH	Reduced Nicotinamide Adenine Dinucleotide
NAD^+	Nicotinamide Adenine Dinucleotide
NMR	Nuclear Magnetie Resonance
pp_i	Inorganic Phosphate

ppm	Parts per Million
PTP	Protein Tyrosine Phosphatase
py	Pyridine
RNA	Ribonucleic Acid
RR	Ribonucleotide Reductase
THF	Tetrahydrofuran

CHAPTER I

INTRODUCTION

Vanadium History

Vanadium was first discovered by the Spanish-Mexican mineralogist Andrés del Río in the year 1813.[1,2] The element was given the name vanadium, after Vanadis, the Norse goddess of love and beauty (Figure 1), due to the variety of colors formed in solution upon changes in concentration and pH.[1-3] Vanadium is therefore the only element in the periodic table that is named after a goddess.[4]

Figure 1. A painting of "Vanadis" the Norse goddess of love and beauty.[5]

Vanadium is a widely dispersed element found at generally low concentrations in approximately 65 minerals including patronite (VS_4), vanadinite ($Pb_5(VO_4)_3Cl$) and carnotite ($K_2(UO_2)_2(VO_4)_2.3H_2O$).[6] As a trace element, vanadium is known to occur at extremely low concentrations in mammalian tissues and is essential for many mammalian species distributed on earth.[3,7,8] Although the exact function of this element remains unclear, vanadium is known to be beneficial and possibly essential for humans and some living organisms.[3,9-13]

Vanadium Chemistry

Vanadium is the 23rd element of the periodic table and is known to possess numerous chemical and biochemical properties.[3,4,7] Vanadium, a typical first row transition metal, is a silvery grey metal which has an electronic configuration of [Ar] $3d^3 4s^2$.[14,15] Vanadium displays a wide variety of oxidation states and varying geometries (Table 1).[4,7,16] The most common oxidation states of vanadium are V^{2+}, V^{3+}, V^{4+} and V^{5+} for which the corresponding electronic configurations are [Ar] $3d^3$, [Ar] $3d^2$, [Ar] $3d^1$ and [Ar] $3d^0$, respectively.[14] Given the varying possible oxidation states of vanadium, the partial pressure of oxygen $p[O_2]$ is a very strong factor for reactions involving vanadium.[14] In aqueous solutions, (V(III)) is the lowest oxidation state of vanadium that is relatively stable.[3]

The aqueous chemistry of V(II) are very sparse in literature. The most commonly mentioned aqua V(II) species is the $[V(H_2O)_6]^{2+}$ as shown in Table 1. The aqueous chemistry of V(III) has been studied to a much lesser extent than that of V(IV) and V(V).[3,17-20] V(III) complexes are known to form numerous mononuclear, binuclear, and

Table 1

Variety of oxidation states and geometries exhibited by vanadium.[16]

Oxidation State	Coordination number	Geometry	Examples
V^{-1}, d^6	6	Octahedral	$V(CO)^-_6$, $Li[V(bipy)_3].4C_4H_8O$
V^0, d^5	6	Octahedral	$V(CO)^-_6$, $V(bipy)_3$, $V[C_2H_4(PMe_2)_2]_3$
V^1, d^4	6	Octahedral	$[V(bipy)_3]^+$
		Tetragonal pyramidal	μ^5-$C_5H_5V(CO)_4$
	7	Monocapped octahedral	$[V[(CO)_3(PMe_3)_4]^+$, $V(CO)_2(dmpe)_2Cl$
	4	Almost planar	$[Li(THF)]_2V$(2,6-diisopropylphenolate)$_4$]
V^{II}, d^3	5	*Sp*	$(2,6\text{-}Ph_2C_6H_3O)_2V(py)_3$
	6[a]	Octahedral	$[V(H_2O)_6]^{2+}$, $[V(CN)_6]^{4-}$
	3	Planar	$V[N(SiMe_3)_2]_3$, $V[CH(SiMe_3)_3]_3$
	4	Tetrahedral	$[VCl_4]^-$
V^{III}, d^2	5	*tbq*	*trans*-$VCl_3(SMe_2)_2$, $VCl_3(NMe_3)_2$
	6[a]	Octahedral	$[V(NH_3)_6]^{3+}$, $[V(C_2O_4)]^{3-}$, VF
	7	Pentagonal bipyramidal	$K_4[V(CN)_7].2H_2O$
V^{IV}, d^1	4	Tetrahedral	VCl_4, $V(NEt_2)_4$, $V(CH_2SiMe_3)_4$
	5	Tetragonal pyramidal	$VO(acac)_2$, $PCl_4^+VCl_5^-$
		sp	$[V_2O_4(OH)_2(PhPO_3)_4]^{2+}$
		tbp	$VOCl_2$ trans-$(NMe_3)_2$
	6	Octahedral	VO_2(rutile), K_2VCl_6, $VO(acac)_2(py)$, $VO(acac)_2Cl_2$
	8	Dodecahedral	$VCl_4(diars)_2$, $V(S_2CMe)_4$
	4	Tetrahedral	$VOCl_3$
	5	*tbp*	$VF_5(g)$, $VNCl_2$(quinuclidine)$_2$
		sp	$CsVOF_4$
V^V, d^0	6a	Octahedral	$VF_5(s)$, VF_6^-, V_2O_5, $[VO_2(ox)_2]^{3-}$,V_2S_5
	7	Pentagonal bipyramidal	$VO(NO_3)_3.CH_3CN$, $VO(Et_2NCS_2)_3$

species of high nuclearities which introduces ambiguity when attempting to identify the actual species that is present in solution.[21]

Due to the presence of unpaired electrons, vanadium compounds of lower oxidation states are paramagnetic in nature and generally exist as colored compounds.[22] V(III) complexes are therefore NMR silent, leading to further complications in the analysis of the species present in solution.[21] V(III) solutions are also easily oxidized (E^0 = +0.34 V (vs NHE)) (Equation 1)[23] and therefore requires stringent anaerobic conditions during speciation studies.[3]

$$VO^{2+} + 2H^{+} + 2e^{-} \leftrightarrow V^{3+} + H_2O \qquad \text{…….. (1)}$$

V(III) compounds therefore require strongly acidic conditions or the presence of a potent chelator in order to exist in aqueous solutions.[3] These compounds generally form octahedral complexes, such as $[V(H_2O)_6]^{3+}$, $[VCl_2(MeOH)_4]^{+}$, $[V(NCS)_6]^{3-}$, and $[VCl_2(THF)_2(H_2O)_2]^{+}$.[3,24]

The aqua V(III) ion, $[V(H_2O)_6]^{3+}$, is greenish blue in color and is mainly obtained from electrolytic or chemical reduction of V(IV) and V(V).[3] Under strongly acidic conditions, V(III) ions predominate as $[V(H_2O)_6]^{3+}$ ions (at pH < 1) and as $[V(OH)(H_2O)_5]^{2+}$ ions (at pH = 1.0 - 3.5) (Figure 2).[3] As the pH increases further (1.0 < pH < 3.5), V(III) ions undergo dimerization to form $[V_2(\mu_2\text{-}O)(H_2O)_{10}]^{4+}$ (Figure 2).[3,18] Upon further increase in pH, the trinuclear $[V_3(OH)_8(H_2O)_{10}]^{+}$ and tetranuclear

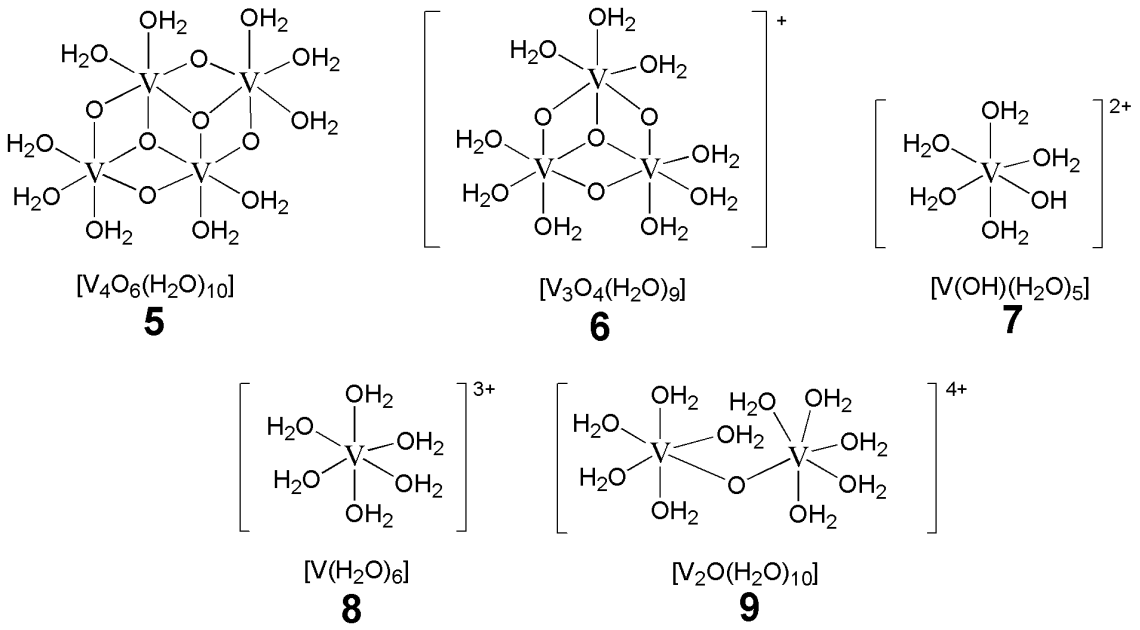

Figure 2. Polymeric V(III) species.[3]

$[V_4(OH)_{12}(H_2O)_{12}]$ species are formed at pH > 3.5 (Figure 2).[3,18] As the pH exceeds a value of 4.5 (pH > 4.5), an insoluble solid usually referred to as $(V(OH)_3)_n$ then begins to form in solution which emphasizes the need for a strong chelation to remove soluble V(III) that may still be present at neutral pH.[3,25,26]

V(IV) complexes are paramagnetic in nature and generally forms compounds that are colorless, pale yellow or red in color.[22] V(IV) compounds exists primarily in a square pyramidal or peuedo-octahedral coordination, as the hydrated vanadyl cation, $[VO(H_2O)_5]^{2+}$ (VO^{2+}) (Figure 3).[3,27] The vanadyl cation, formed by dissolving $VOSO_4$

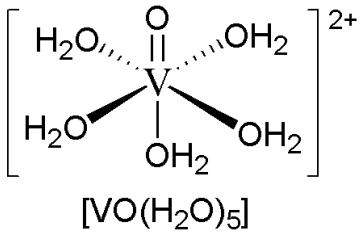

Figure 3. Structure of the most common vanadyl cation.[3]

in acidic aqueous solutions, is probably the most stable diatomic ion and is known to be present in approximately 98% of all V(IV) solid compounds and aqueous solutions.[24,27-29]

The VO^{2+} cation is known to form many complexes and the identity of this ion is retained throughout a wide variety of reactions.[24] This cation is very stable under acidic conditions and is the main species present in solution at pH 3.[3,30] As the pH is increased into the physiological range, several oligomeric and polymeric spin-paired species are then formed.[27] The speciation of V(IV) species at nanomolar to submicromolar and at millimolar concentrations of V(IV) is shown in Schemes 1 and 2, respectively.[3] As shown in Schemes 1 and 2, as pH increases (pH ~ 4), a proton is loss resulting in the formation of the hydrolyzed species, $[VO(H_2O)_4(OH)]^+$ species.[3]

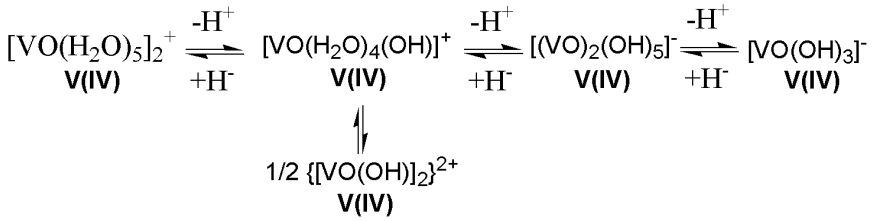

Scheme 1. Aqueous $[VO(OH_2)_5]^{2+}$ Hydrolysis Products at Nano to Submicromolar Concentrations of V(IV).[3] The insoluble hydroxide $\{VO(OH)_2\}_n$ is in equilibrium with the positively and negatively charged monomeric species.

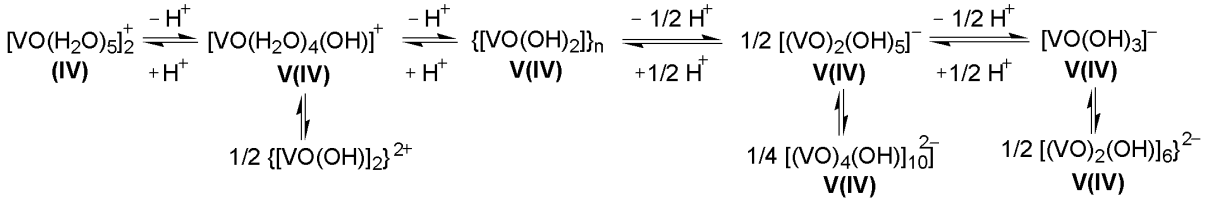

Scheme 2. Aqueous $[VO(OH_2)_5]^{2+}$ Hydrolysis Products at Micro to Millimolar Concentrations of V(IV).[3]

As the pH increases further (pH>5), an insoluble $\{VO(OH)_2\}_n$ species is formed, which dissolves to form a binuclear species ($[(VO)_2(OH)_5]^-$), and a subsequent monomeric species $[VO(OH)_3]^-$ upon further increase in pH.[3,31] In the speciation diagram (Figure 4), the existence of negatively charged monomeric V(IV) species at neutral pH is clearly illustrated.[3] Figure 4 displays a diagram of the V(IV) species that generally exist in aqueous solutions.[3] Extensive studies have been carried out on the aqueous chemistry of V(V) ions, which are readily solvated in aqueous solutions to form the hydrated $[V(OH_2)_n]^{5+}$ species.[32] According to thermodynamic evidence, when compared with

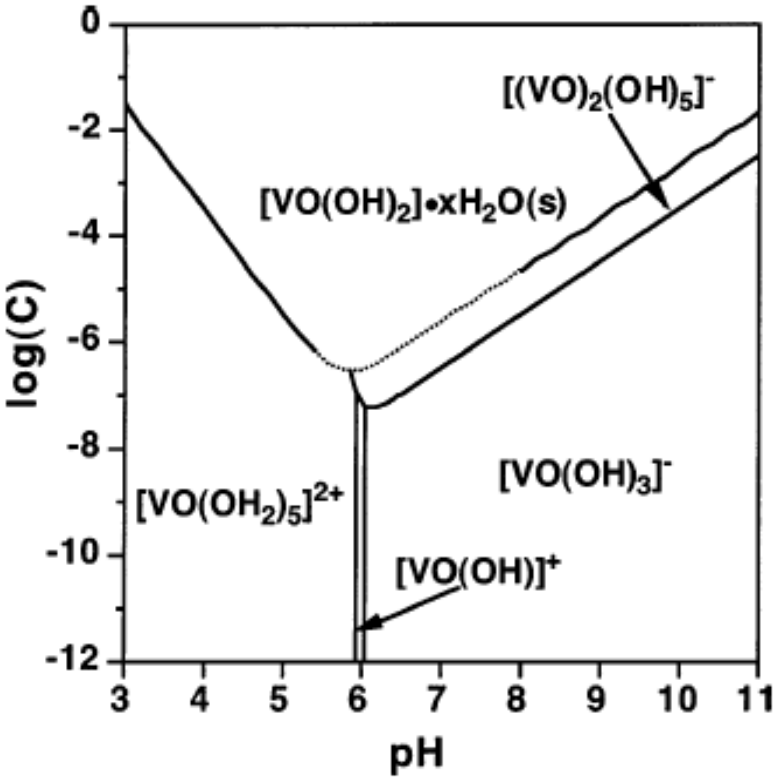

Figure 4. Predominance area diagram for aqueous V(IV) species, which is represented as the logarithm of the total molar concentration of vanadium(IV) against pH. Solid lines represent the condition where the concentrations of two soluble species in equilibrium.[3] "Reprinted with permission from Crans, D. C.; Smee, J. J.; Gaidamauskas, E.; Yang, L. *Chem. Rev.* **2004**, *104*, 849. Copyright 2004 by the American Chemical Society."

H_3VO_4, the high stability of the vanadate ion (VO_4^+) is often accounted for by an increase in coordination number.[3,33] The pH of the solution and the concentration of the vanadium oxide are two critical factors for determining the identity of the specific vanadium oxide present in aqueous solution.[7,15] V(V) readily hydrolyzes to form twelve different species consisting of both monomeric and polymeric species.[15,34] The strong polarizing power of the V(V) ion leads to an increase in the acidity solutions due to the partial dissociation of coordinated water molecules (Equation 2).[32]

$$[V^V(OH_2)_6]^{5+} + nH_2O \longrightarrow [V^V(OH)_n(OH_2)_{6-n}]^{(5-n)+} + nH_3O^+ \quad \text{……...} \quad (2)$$

The existence of various oxides of vanadium at varying pH is illustrated in the Pourbaix diagram shown in Figure 5.[30] The Pourbaix diagram clearly indicates the existence of V(V) species at higher pH and the subsequent existence of V(IV) species at low pH.[3,35,36] In Figures 5a and 5b, it is also observed that vanadium exists mainly as cationic species at pH < 3, and as anionic species pH > 3.5.30 In aqueous solutions, the decameric species, [V10O28]6-, and its protonated forms are the major V(V) species present.[3,37] Due to the instability of this compound, [V10O28]6- often serves as a thermodynamic sink in solutions at pH = 3-6.[3,37]

V(V) compounds generally forms a variety of polyoxoanions and may exist in a tetrahedral (VO_4), pentahedral (VO_5) or octahedral (VO_6) coordination environments.[3] At physiological pH, the vanadate mononuclear species exists predominantly in the monomeric form as the $H_2VO_4^-$ ion.[3,27,38,39] In the presence of nucleophillic ligands,

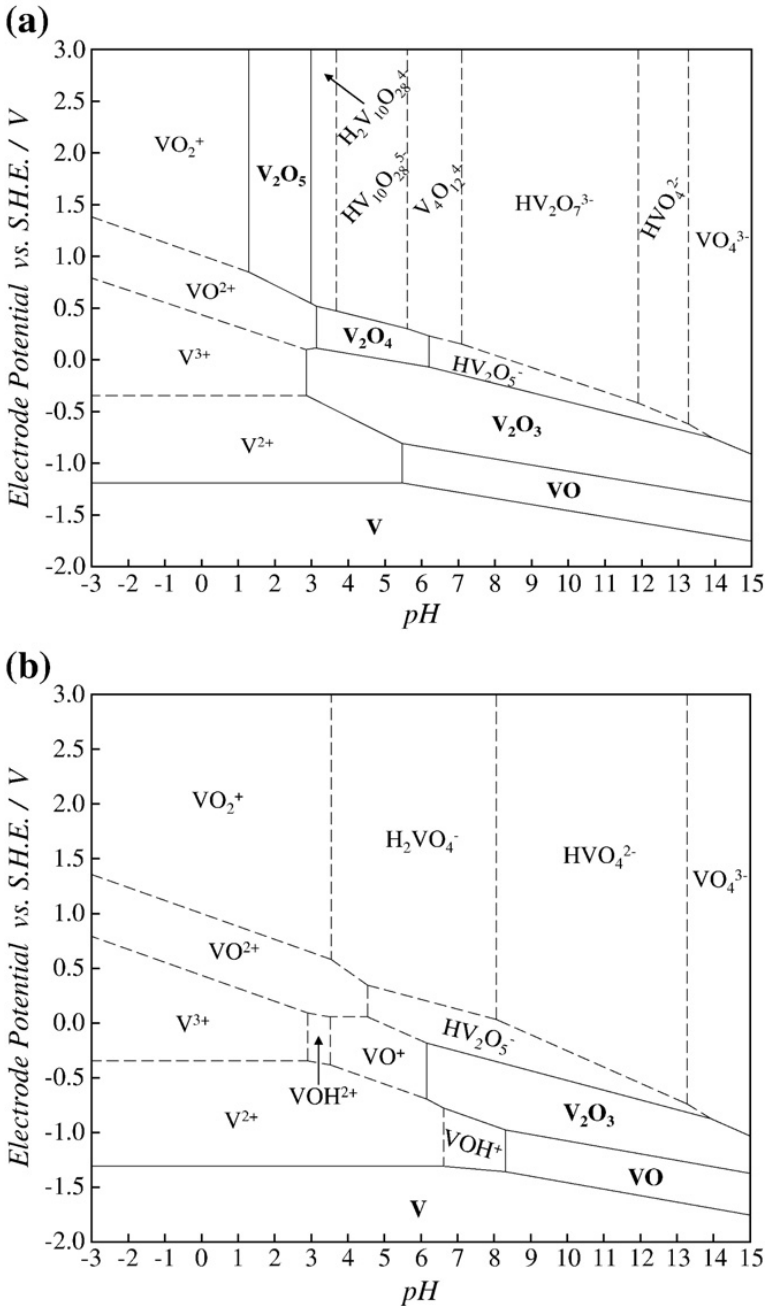

Figure 5. Potential–pH diagrams for the vanadium–water system at 298.15 K: (a) activities of dissolved vanadium of 10^{-2} and (b) activities of dissolved vanadium of 10^{-6}.[30] Reproduced with permission from *Hydrometallurgy* 2011, *106*,105. Copyright 2011 by Elsevier.

monomeric vanadate readily undergoes various condensation reactions to form numerous species in solution (Figure 6).[3]

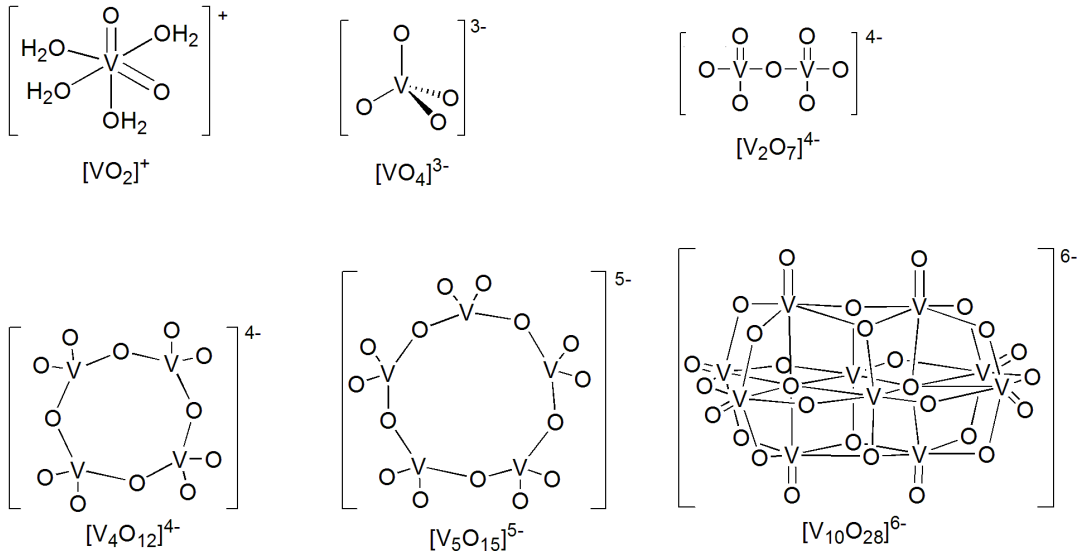

Figure 6. Structures of the major deprotonated oxovanadium(V) ions.[3,41,42]

Vanadium pentoxide (V_2O_5) is amphoteric in nature and readily dissolves in strong aqueous alkali to form colorless solutions, consisting mainly of VO_4^{3-}.[40] As the acidity of the solution is increased, the colorless solution deepens in color, and changes from orange to red (just below neutral pH).[40] As the acidity is further increased, a brown precipitate of V_2O_5 is formed, which readily dissolves at lower pH to give a pale-yellow solution.[40] The existence of various vanadate species in aqueous solutions is *dependent* on the pH and total concentration of vanadium in solution.[40] The predominant oligomer formed under acidic conditions ($2 \leq pH \leq 6$) is the yellow-orange decavanadate ion $[V_{10}O_{28}]^{6-}$ (V_{10}) which is capable of existing in several protonated forms (Scheme 3).[16] Upon further addition of acid, the $[V_{10}O_{28}]^{6-}$ readily forms the dioxovanadium(V) ion (VO_2^+).[16] The main oligomeric species present from pH 6 to 10 includes the dimeric $[V_2O_7]^{4-}$ ion (V2), the cyclic tetrameric $[V_4O_{12}]^{4-}$ ion (V4), and the cyclic pentameric $[V_5O_{15}]^{4-}$ ion (V5), which are all colorless.[27,43,44]

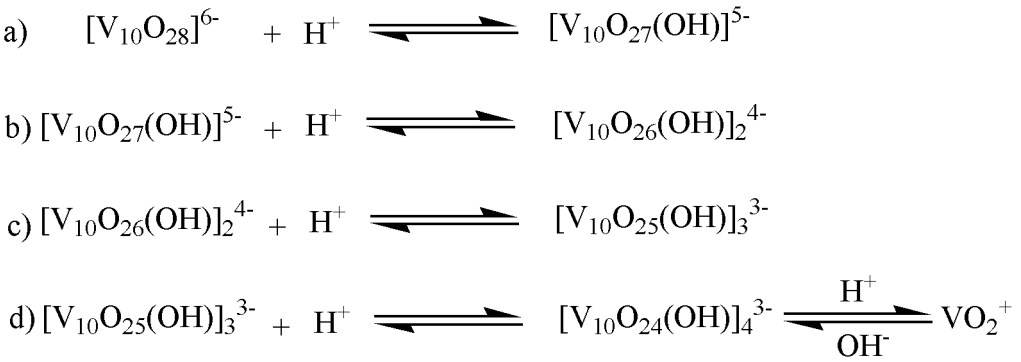

Scheme 3. Protonated forms of decavanadate ion.[16]

Schiff Base Complexes of Vanadium

Schiff bases are considered to be a very important class of compounds that are widely used due to their good solubility properties and their remarkable versatility.[45] Schiff bases and their metal complexes are known to exhibit a broad variety of biological activity such as anti-viral,[46] anti-parasitic,[47] anti-bacterial,[48] anti-inflammatory,[49] anti-tumor,[50,51] anti-HIV,[52] anti-cancer,[53] etc.

According to Sen *et al*.,[54] metal complexes containing salen-type Schiff bases are capable of exhibiting unusual coordination, high thermodynamic stability and kinetic inertness.[54] Schiff bases display interesting asymmetric catalytic activity, and their metal complexes are of great interest as enzyme models since they are capable of mimicking biological sites.[54]

Recently, the use of heterogenized $V^{IV}O$ and $V^{V}O_2$ complexes as catalysts for the functionalization of alkenes were reported by Maurya *et al.*[55] Previously, the encapsulation of $[V^{V}O_2(Sal\text{-}aebmz)]$ (Hsal-aebmz = Schiff base derived from salicylaldehyde and 2-aminoethylbenzimidazole) in zeolite-Y (where the zeolite acts as a protein mantle) was shown to significantly improve the catalytic activity of the zeolite by yielding a higher turnover frequency. This catalyst (or catalyst precursor) was also found

to be easily recyclable and maintain their activity for several cycles of catalytic use.[55] In their present study, the catalytic activity of similar $V^{IV}O$ and $V^{V}O_2$ complexes containing ligands **10** (Hpydx-aebmz) and **11** (Hpydx-ambmz) (Figure 7) were also investigated.[55]

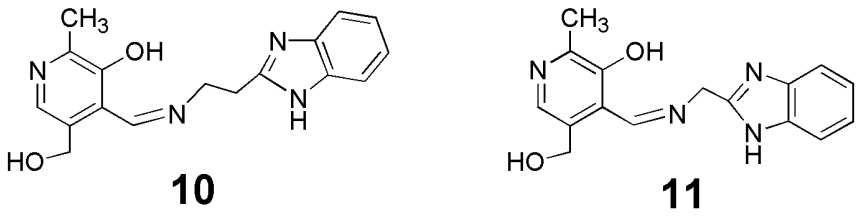

Figure 7. Structural formula of Schiff base ligands used for catalytic activity.[55]

Similarly, both complexes exhibited similar catalytic properties when compared to that of [VVO2(Sal-aebmz)].[55]

Extensive research has been carried out on complexes of *N*-salicylideneamino acids, typified by their vanadium compounds.[56-59] V(IV) and V(V) complexes containing Schiff base ligands generally exhibit coordination geometry such as that of compounds **12** and 1**3** shown in Figure 8. The formation of dinuclear oxo-bridged $V^{IV}–O–V^{V}$ or $V^{V}–O–V$ compounds (such as compound **14** in Figure 8) has also been reported.[59-61] When methanolic solutions of $[V^{IV}O(sal–aa)(H_2O)]$ complexes (sal–aa = *N*-salicylidene-amino acidato) were allowed to stand in air, the complexes were spontaneously oxidized to form $[V^{V}O(sal–aa)(OMe)(OHMe)]$ (**13)**. Similarly, the presence of bpy in solution during aerial oxidation, results in the formation of compound **15,** formed from the coordination of bpy ligand to the $[V^{IV}O]^{2+}$ metal center.[59-61]

Due to their potential pharmacological applications, there is now a growing interest in the chemistry of hydrazine and hydrazone compounds.[62] In the past,

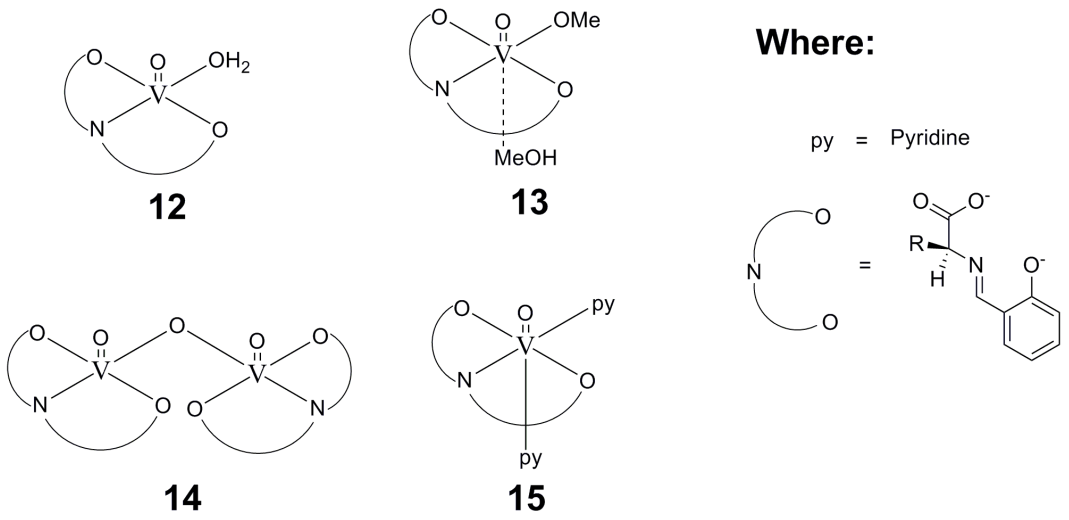

Figure 8. Structure of V(IV) and V(V) complexes containing Schiff base ligands.[59]

great interest has aroused in the mode of chelation of acid hydrazides R-CO-NH-NH_2 and their corresponding aryolhydrazones R-CO-NH-N=CHR with transition metal ions.[62] In 2008, Mishra and Soni reported the synthesis, characterization and biological activity of VO(II) and Co(II) complexes synthesized from the reaction of methyl isobutyl ketone with nicotinamide (mna)/2-amino-4-chlorophenol (map) and 2-hydroxy acetophenone with nicotinamide (han)/isoniazide (hai) (Figure 9).[62] The Schiff base ligands and the

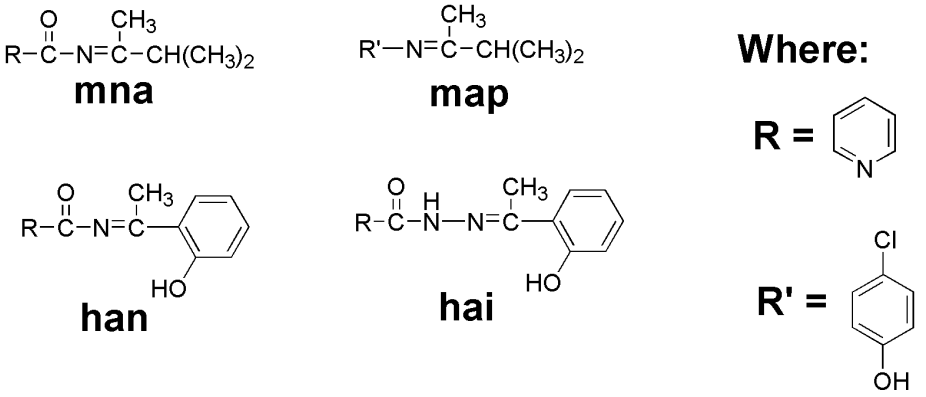

Figure 9. The structure of Schiff base ligands containing acid hydrazides and aryolhydrazones.[62]

respective VO(II) and Co(II) complexes (Figure 10) were shown to exhibit significant antibacterial and antifungal activity.[62] Chelation was suggested to have a major effect on the enhancement or suppression of the biochemical activity since the majority of the complexes were observed to be more active than their respective Schiff bases.[62]

Due to the stability of the quinazoline nucleus, quinazolinones are also an excellent reservoir of bioactive substances.[63] 4(*3H*)-quinazolinones is known to

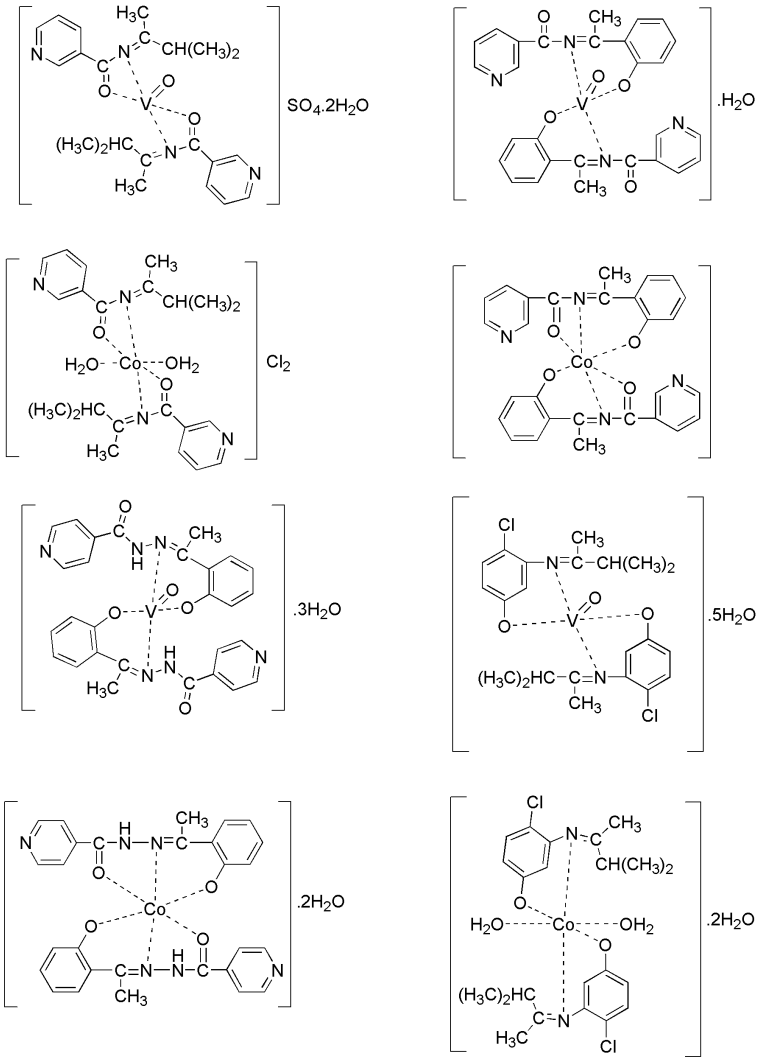

Figure 10. Proposed structures of VO(II) and Co(II) complexes containing Schiff base ligands.[62]

possess many potential pharmalogical applications.[58,59] Hence, there is now a considerable interest in the chemistry of 4(*3H*)-quinazolinones.[63,64] Studies involving vanadium chemistry with4-(*3H*)-quinazolinones ring systems are very scarce in literature.[63] Very recently, Prasad *et al*.[63] reported the synthesis of two newly synthesized Schiff base ligands (Figure 11), viz., 2-methyl-3-(pyridine-2

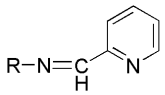

2-methyl-3-(pyridine-2-ylmethyleneamine)quinazolin-4(3H)-one

Where:

R =

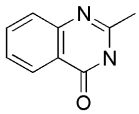

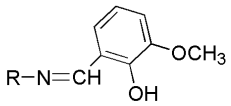

3-(4-hydroxy-3-methoxybenzylideneamino)-2-methylquinazolin-4(3H)-one

Figure 11. The structure of 4(*3H*)-quinazolinone Schiff base ligands.[63]

ylmethyleneamine)quinazolin-4(*3H*)-one and 3-(4-hydroxy-3-methoxybenzylideneamino)-2-methylquinazolin-4(*3H*)-one with 1,10-phenanthroline.

Biological studies carried out by Prasad *et al*.[63] has also demonstrated the ability of Schiff base ligands to bind to CT-DNA in intercalative mode.[63] According to Prasad *et al*.,[63] oxovanadium(IV) complexes containing the two newly synthesized Schiff base ligands (Figure 12), can readily bind to CT-DNA in intercalative mode.[63] Schiff base transition metal complexes are currently used in the design and development of synthetic restriction enzymes, foot printing agents, chemotherapeutic agents, site specific cleavers, spectroscopic probes, and molecular photo switches.[63] The interaction of these Schiff base-transition metal complexes with nucleic acids is a therefore major area of research to medicinal chemists.[63]

Vanadium and Cancer

Cancer or neoplasia is the term used to define diseases characterized by uncontrolled proliferation and the spread of abnormal forms of the body cells.[65]

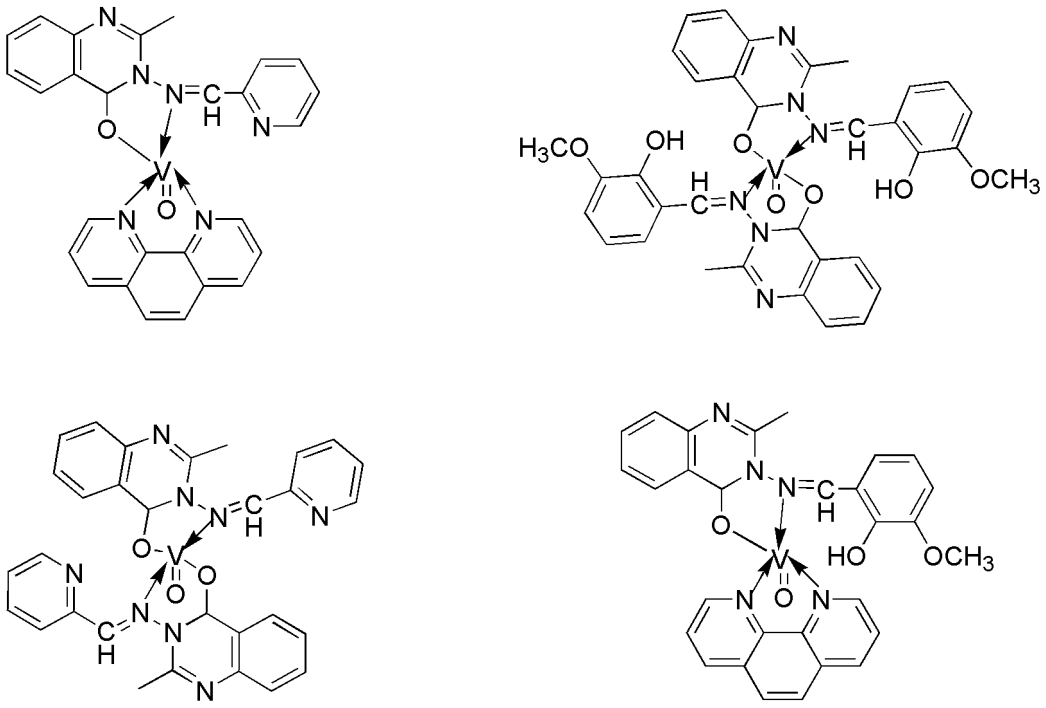

Figure 12. Oxovanadium(IV) complexes containing two synthesized Schiff base ligands that can bind to CT-DNA in intercalative mode.[63]

Neoplastic cells possesses the ability to continually divide and proliferate which leads to the formation of localized tumors.[65] The invasiveness of these cells and the ability to metastasize, results in the growth of tumors at secondary sites, which undergoes uncontrolled growth and later spreads throughout the entire body leading to starvation and death of normal tissue cells.[65]

Chemotherapeutic cancer treatment involves the use of drugs that are capable of selectively targeting rapidly proliferating neoplastic cells (in preference to healthy body cells) used in combination with surgery and/or radiation therapy.[66] An in depth

understanding of the mechanism by which the regulation of cell division and proliferation is disrupted by neoplastic cells is critical for advances in new cancer treatment.[66] The activity of anticancer drugs is generally exerted by the inhibition of one or more processes occurring in the normal cell cycle.[65]

The study of metal containing antitumor agents began in the year 1969 following the detection of the antitumor properties of cisplatin [*cis*-diamminedichloroplatinum(II)] (Figure 13).[67] Cisplatin is one of the most successful anticancer drugs and is effective in

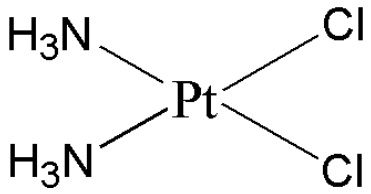

Figure 13. Structure of cisplatin.[68]

the treatment of a variety of cancers (with a cure rate greater than 90% in the case of testicular cancer).[68-70] The clinical success of cisplatin as an antitumor agent is limited by factors including acquired or intrinsic drug resistance, and the lack of selectivity for tumor tissues, which leads to severe side effects including renal impairment, neurotoxicity and cytotoxicity.[71,72] The development of non-platinum metal based drugs has received considerable interest and a few of these compounds are currently in undergoing clinical studies.[73,74] A range of metal complexes, such as gold, iron, ruthenium, rhodium, palladium, gallium, and tin have demonstrated interesting antitumor activity but have not yet entered clinical trial.[75]

In 1983, English *et al.*[76] and Thompson *et al.*[77] discovered that vanadium exerted an inhibitory effect on the terminal differentiation of murine erythroleukemia cells.[78] Dietary administration of ammonium vanadate was shown to inhibit chemically-induced

mammary carcinogenesis.[77,78] Since then, the use of vanadium in the treatment of human diseases has been widely investigated.[79-82]

In 1965, the first discovery of the anticancer effect of vanadium salts were reported by Kieler *et al*.[83] Since then, several studies have been carried out to determine the biochemical and molecular mechanism underlying the antitumor vanadium salts.[7,84,85] Vanadium was shown to be effective in the prevention and/or reduction of chemically induced preneoplastic and neoplastic development in various target organs.[85] The putative therapeutic effects of vanadium on the growth and metastatic potential of tumor cells have also been reported in literature.[85]

Vanadium compounds are capable of exerting anti-carcinogenic effects in several different ways as shown in Figure 14.[7] Although very few vanadium complexes have been tested for antitumor activity, several peroxovanadium and vanadocene complexes are known to exert anti-proliferative and proliferative activity on various cell types.[78] In 2004, peroxovanadium complexes including potassium bisperoxo(1,10-phenanthroline)oxovanadate(V) and potassium bisperoxo(pyridine-2-carboxylato)oxovanadate(V) (Figure 15) were shown to reduce proliferative activity of neuroblastoma NB41 and glioma C6 cell lines.[7,86] The biological effect of vanadium in various cell lines were also enhanced by the concomitant treatment of vanadate(IV) and peroxide due to the formation of peroxovanadate.[78] *In vitro* studies also demonstrated a marked increase in protein tyrosine phosphorylation and phosphoinositide breakdown, combined with the selective inhibition of protein tyrosine phosphatase and phosphotyrosine phosphatase activities.[78] The inhibitory effect of peroxovanadium

complexes is proposed to be 100-1000 times greater than that of sodium orthovanadate *in vitro.*[78]

Vanadium compounds generally exert their anti-proliferative effects on normal or malignant cell lines through cell cycle arrest.[78] This was demonstrated by Zhang *et al.*,[88]

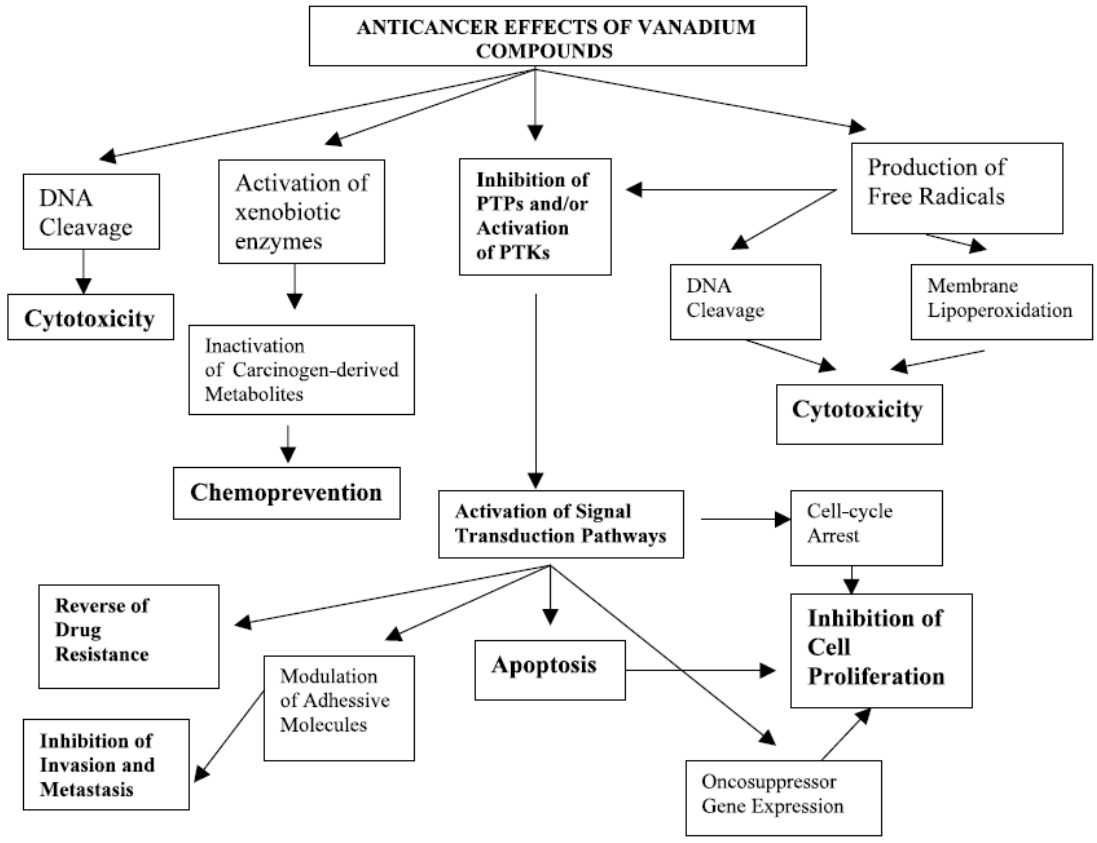

Figure 14. Schematic presentation of the actions, through which the antitumor effects of vanadium are exerted.[7] (PTPs - Protein Tyrosine Phospahatases and PTKs - Protein Tyrosine Kinases). Reproduced with permission from *Crit. Rev. Oncol. Hematol.*, 2002, *42*, p.255. Copyright 2002 by Elsevier.

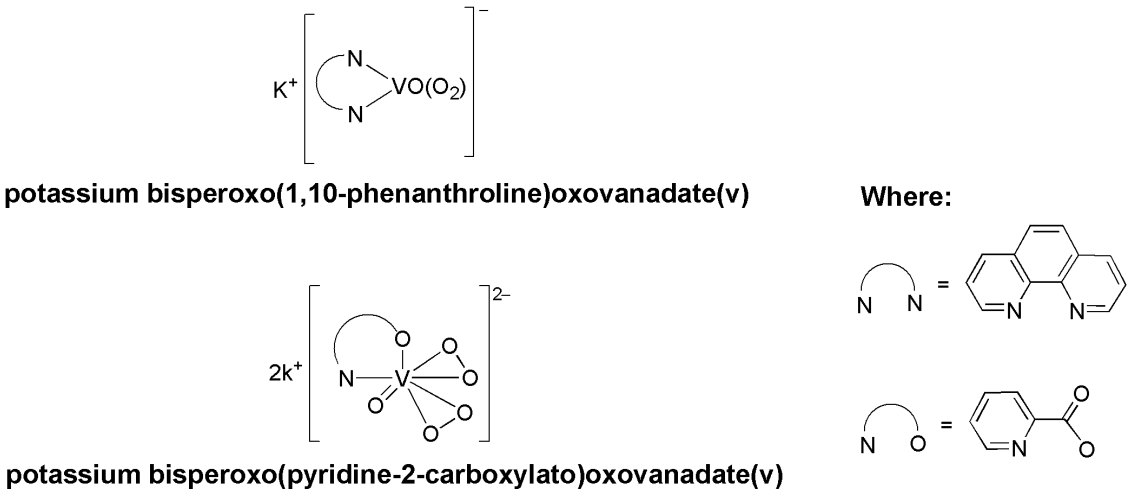

Figure 15. Peroxovanadium complexes that exhibit proliferative activity.[87]

when vanadate was shown to both induce G2/M-phase arrest in p53-deficient mouse embryo fibroblasts and promote S-phase entry in the corresponding p53 wild-type cells.[78,88] Anti-proliferative and cytotoxic effects of vanadium compounds may also be exerted via interactions with DNA.[7] Vanadocene complexes, including vanadocene dichloride (Figure 16), are known to interact with the phosphate groups of DNA nucleotides to form a labile outer sphere complex.[7]

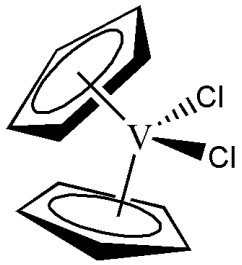

Figure 16. The structure of vanadocene dichloride.[89]

Bis(4,7-dimethyl-1,10-phenanthroline) sulfatooxovanadium(IV) ([$VO(SO_4)(Me_2$-$Phen)_2$]) (metvan) was also recently identified as an active apoptosis inducing agent with

potent *in vitro* antitumor activity (Figure 17).[79,90-92] Apoptosis (programmed cell death) is characterized by nuclear fragmentation, membrane blebbing, nuclear and cytoplasmic condensation, and by the appearance of apoptotic bodies.[7,93] Metvan induces apoptosis in multiple myeloma cell lines, leukemic cell lines, and solid tumor cell lines derived from breast cancer, glioblastoma, and testicular cancer patients at nanomolar to low micromolar concentrations.[79,90,91] Metvan is highly effective against cisplatin-resistant ovarian and testicular cancer cell lines and represents the first vanadium complex as a

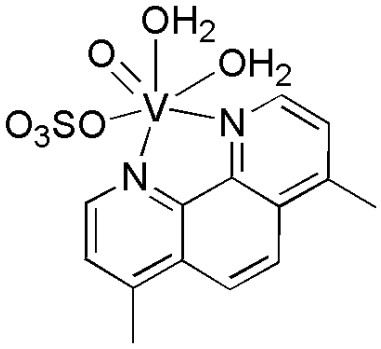

Figure 17. Structure of Metvan.[144]

possible alternative to platinum-based chemotherapy.[94] Metvan induced apoptosis is mediated by the depolarization of mitochondrial membranes, the depletion of glutathione, and the generation of reactive oxygen species.[79,94]

Thiosemicarbazone Ligands and Metal Complexes

Thiosemicarbazones are a very unique class of compounds due to their pharmacological applications and their versatility in coordination chemistry.[95] Thiosemicarbazones and their metal complexes have long been recognized for their potential antiviral, antibacterial, antifungal, antimalarial, and antitumor activities.[96-100] Thiosemicarbazones are versatile mixed hard-soft oxygen/nitrogen-sulfur chelating

ligands, exhibiting various binding modes with transition and some main group metals.[101,102] The presence of amide, thione and imine groups makes them potential polydentate ligands.[103]

Thiosemicarbazones usually coordinate to metal centers in a bidentate mode via the imine nitrogen and the sulfur atom of the thioamide moiety. The coordination mode can be increased however by the incorporation of an additional donor groups as heterocyclic substituents.[95] The most common donor set involves the ONS or NNS atoms in which one or two ligands are attached to the metal center, which is bridged through either thiolate sulfur or a non-thiosemicarbazone coligand (i.e.N_3, Cl, NCS, CH_3COO, etc.).[95,104] Depending on the disposition of substituents about the imine and thioamide groups, α-pyridyl thiosemicarbzones are known to exist in three isomeric forms (Figure 18).[105] Intramolecular hydrogen bonding plays a very important role in the structural determination of the isomeric forms of thiosemicarbazones.[105]

As reported in literature, the anticancer activity of thiosemicarbazone metal derivatives is much more effective than that of the free ligand.[95] This is due to the change in the binding affinity of metals to proteins and enzymes that occur following the coordination of a thiosemicarbazone ligand to a metal center.[95] This results in a change in the interaction of the respective complex with DNA thereby causing an effect on DNA replication and cell proliferation.[95]

Following the discovery of the antileukemic activity2-formylpyridine thiosemicarbazone (Figure 19) in the 1950s, the antineoplastic activity of α-*N*-heterocyclic thiosemicarbazones has since been thoroughly investigated.[106]

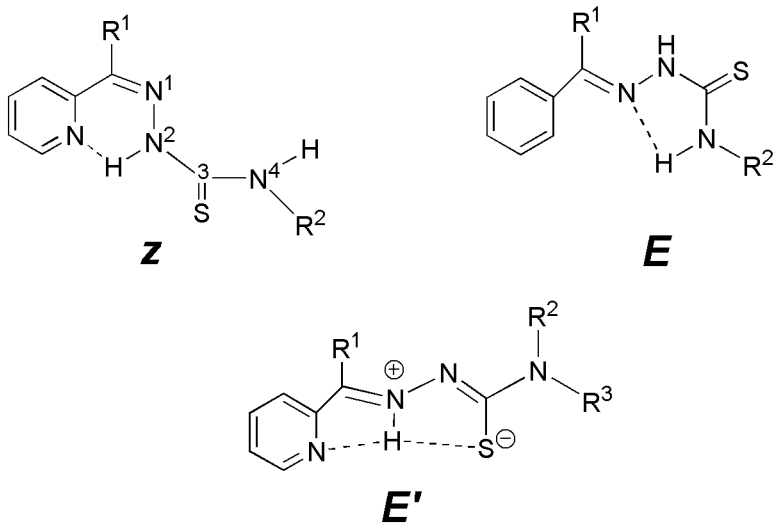

Figure 18. Isomeric forms of α-pyridyl thiosemicarbzones showing *Z*, E (anti, anti) and *E'* (syn,syn) isomeric forms.[105]

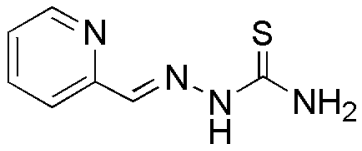

Figure 19. Structure of 2-formylpyridine thiosemicarbazone.[105]

Several reports have recently documented the preparation and biological activity of transition metal complexes containing thiosemicarbazone ligands.[105] Ribonucleotide reductase (RR) (a mammalian enzyme) has been identified as a principal target for thiosemicarbazones.[102,107] In 1961, Peter Reichard reported the discovery of the enzyme RR in E. *coli*.[108,109] This enzyme was later found in all growing cells of every living organism and in several species of viruses.[108,110]

Thiosemicarbazones are the strongest known inhibitor of RR both in cell-free assay and in intact tumor cells.[101] The inhibition of RR is results in the pronounced antineoplastic efficacy of thiosemicarbazones.[105,111] RR catalyzes the reductive conversion of ribonucleotides to deoxyribonucleotides, which is a crucial, rate-limiting

step in the pathway leading to the biosynthesis of DNA.[112] The reaction involves the replacement of the C2'-hydroxyl group on the ribose moiety by a hydrogen atom (Scheme 4).[108]

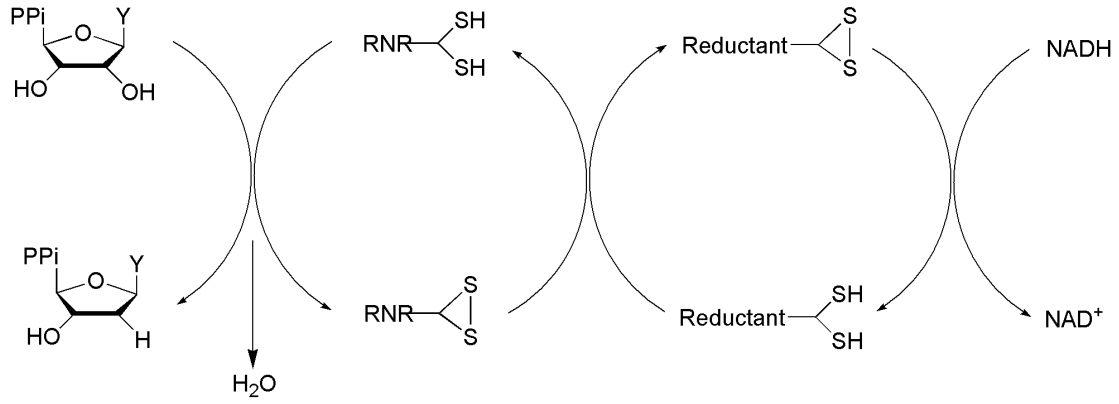

Scheme 4. Ribonucleotide reduction catalysed by ribonucleotide reductase.[108]

RR is produced at the transition from G_1 to the S phase of the cell cycle as a prerequisite for DNA replication and is highly active in proliferating tumor cells, making it an excellent target for tumor chemotherapy.[101,113] Mammalian (class 1a) RR consists of two non-identical subunits called R1 (α_2 homodimer) and R2 (β_2 homodimer).[101] The R1 subunit harbors the catalytically active center consisting of redox active cysteines regenerated by the action of thioredoxin.[101] The R2 subunit contains a tyrosyl radical and a diiron center, both of which are essential for the initiation of the reductive process at the active site in R1.[101,114]

RR inhibitors are divided into four classes depending on the mode of action: radical scavengers, chelating molecules, and nucleoside analogs.[101] The inhibitory effect of thiosemicarbazone is often attributed to their pronounced iron-chelating properties.[101,107] The chelation of iron from the R2 subunit of the enzyme, results in the

formation of an active iron complex, which is responsible for the inhibition of the RR enzyme.[101,107]

The ability of thiosemicarbazones to chelate metal ions is solely dependent on the presence of a N,N,S tridentate "soft donor" coordination system, which allows for the coordination of iron, copper, zinc and several other transition metals.[105,111] The antitumor activity of thiosemicarbazones is therefore assumed to originate from the capability of these compounds to form stable metal complexes.[115] According to Thelander and Graslund,[116] the existence of an active iron complex confirms the proposed mechanism, which involves the reduction of an iron(III) complex (containing 1-formylisoquinoline thiosemicarbazone) to form a stable iron(II) complex (in the presence of dithioreitol).[116]

Presently, gemcitabine and hydroxyurea (HU) (Figure 20) are the only known clinically approved inhibitors of RR.[112,117,118] Recently, Sartorelli and coworkers also reported the synthesis and biological evaluation of 3-aminopyridine-2-carboxaldehyde thiosemicarbazone (3-AP) and 3-aminopyridine-4-methyl-2-carboxyaldehyde thiosemicarbazone (3-AMP) (Figure 21).[119] 3-AP (triapine) is the first reported thiosemicarbazone to enter phase II clinical trials as an antineoplastic agent.[102] A comparative study of 3-AP and HU demonstrated a greater inhibitory potency for 3-AP against L1210 leukemia cells, both in vitro and in vivo.[105,120,121] 3-AP was also observed to be active against HU-resistant cells.[105,120] This observation lead to the suggestion of other possible modes of action, which may include radical reactions or inhibition of topoisomerase II.[101]

The high general toxicity and the consequent low therapeutic index are the major disadvantages associated with the use of thiosemicarbazones as antineoplastic agents.[101]

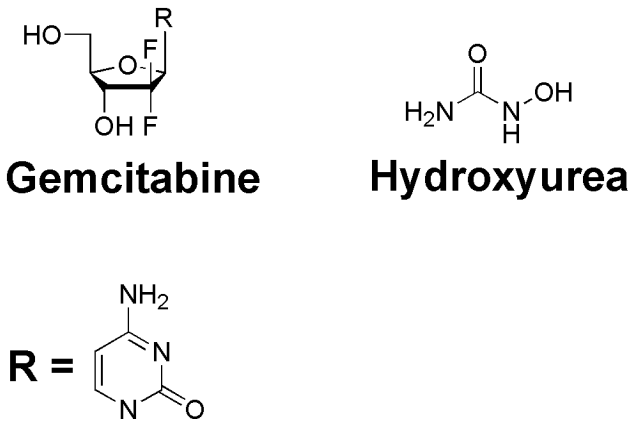

Figure 20. Structure of gemcitabine and hydroxyurea. [112,117,118]

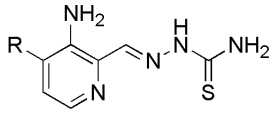

16) R = H (3-AP)
17) R = Me (3-AMP)

Figure 21. Structure of 3-AP and 3-AMP.[119]

The entry of 3-AP into clinical stages, however, has led to a renewed interest in the antineoplastic effects of thiosemicarbazone complexes.[101] Recently, the biological activity of several metal complexes containing α-pyridyl and salicyladehyde (and their analogues) thiosemicarbazones (Figure 22) have been reported in literature.[101,105] Gallium(III) complexes has been reported to possess clinically useful antipoliferative properties.[122,123] The synthesis of a series of gallium(III) and iron(III) complexes with N-substituted α-N-heterocyclic thiosemicarbazones were recently reported by Kowol *et al* (Figure 23).[122] The ligand binding affinity of gallium(III) is very similar to that of iron(III), which often leads to an upset in the availability of intracellular iron.[122] Gallium interacts directly with RR and competes with iron for the binding site in the R2 unit of

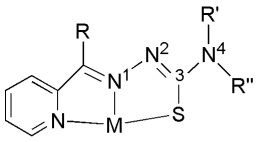

a-pyridyl thiosemicarbazones
M = Re, Mn, Fe, Ni, Cu, Zn, Ru, Pd, Pt, Cd, Hg, Pb, Al, Co, Au, Tl, Ga, Bi, Sb, Sn, V, U

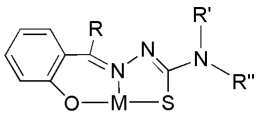

salicylaldehyde thiosemicarbazones
M = Ni, Cu, Zn, Ru, Pd, Pt, Cr, Fe, Co, Rh, Ru, Ir V, Mn, Sn, V, Mo

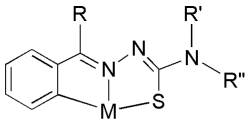

benzaldehyde/benzophenone thiosemicarbazones
M = Ru, Pd, Pt

Figure 22. Structure of the α-Pyridyl Thiosemicarbazone, Salicylaldehde Thiosemicrbazone, and Benzaldehyde/Benzophenone Thiosemicarbazone Metal Complexes.[105]

the enzyme.[122,124,125]

Pronounced differences in the cytotoxic effect were observed upon variation in the central metal ion.[101] Gallium(III) was shown to enhance cytotoxicity due to the synergistic action of the two components.[101] The complexation to iron(III), however,

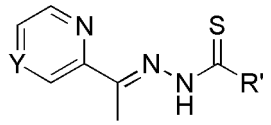

Y = CH, N
R' = $N(CH_2)_2$, $N(C_4H_8)$, $N(C_5H_{10})$

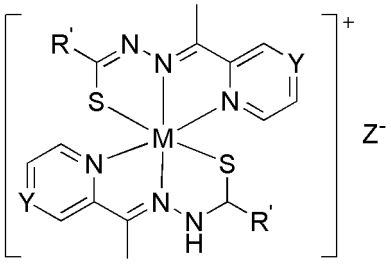

$[ML_2][Y]$
M = Fe, Z = $FeCl_4^-$, PF_6^-
M = Ga, Z = PF_6^-

Figure 23. Structure of thiosemicarbazones and their gallium(III) and iron(III) complexes.[122]

resulted in a marked attenuation of the antiproliferative activity.[101] The design of metal complexes in which both the metal and the ligand is directed at the same molecular target produces highly potent RR inhibitors due to the synergistic action of the two components.[122]

The antimicrobial and DNA cleavage activity of a series of Co(II), Ni(II), and Cu(II) complexes with Schiff bases derived from *m*-chloro/nitro substituted thiosemicarbazides and 2-methoxy benzaldehyde (possessing sulfur and azomethine nitrogen donors) (Figure 24) were reported by Patil et al.[126] Although a significant

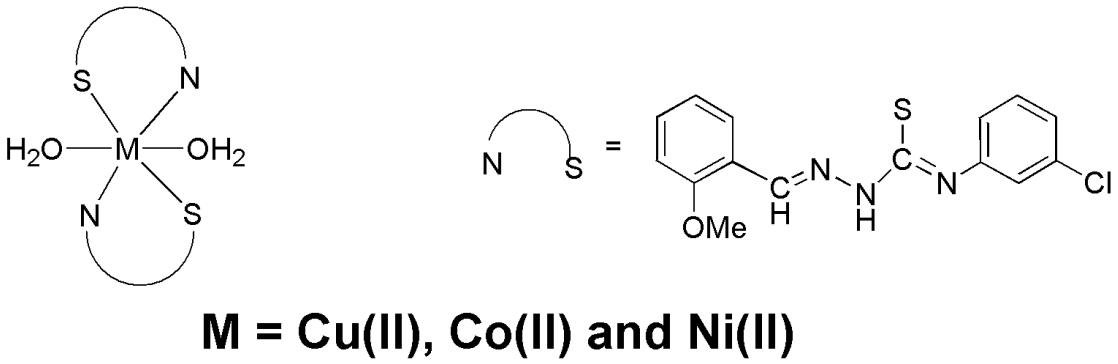

Figure 24. Structure of Co(II), Ni(II), and Cu(II) complexes containing thiosemicarbazone ligands.[126]

increase in activity was observed upon coordination, both the Schiff base ligands and their metal complexes were shown to be highly active against some of the antifungal and antibacterial species.[126]

Ruthenium complexes are believed to have low toxicity and good selectivity for tumors.[127,128] As such, ruthenium complexes are widely studied as metallodrugs.[127,128] Ruthenium has been reported to possess several favorable anticancer properties and several of these ruthenium containing complexes are known to interaction with DNA and RNA causing a reduction in tumor growth.[129-131] Imidazolium *trans*-[tetrachlorido(1H-imidazole)-(S-dimethyl sulfoxide)ruthenate(III)] (NAMI-A) and indazolium *trans*-[tetrachlorobis(1H-indazole)ruthenate(III)] (KP1019) (Figure 25) are two of the most promising ruthenium based complexes for clinical use as anticancer agents.[132] Both

NAMI-A and KP1019 have successfully completed phase 1 clinical trials and are currently undergoing phase II studies.[132] NAMI-A is known to exert an inhibitory effect

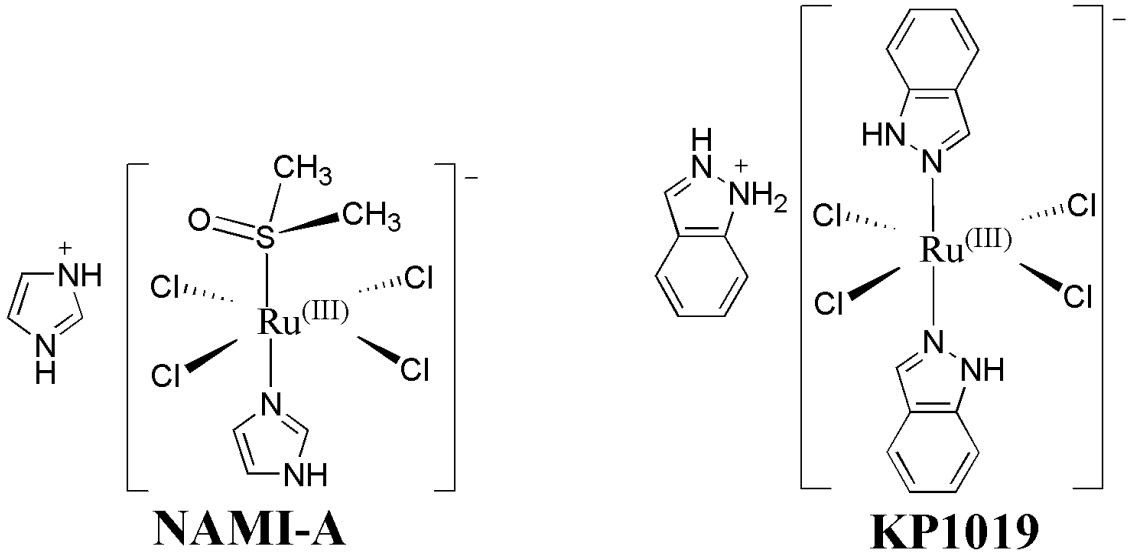

Figure 25. Structure of NAMI-A and KP1019.[132]

on metastases formation and causes a reduction in the weight of metastasis without affecting the primary tumor.[133] The application of KP1019, however, is mainly aimed at the treatment of solid tumors such as colorectal carcinoma.[133]

Several researchers have demonstrated interest in the possibility of identifying a new anticancer drug among ruthenium complexes containing thiosemicarbazone ligands.[134,135] Recently, the cytotoxicity of a series of mixed-ligand diimine ruthenium complexes of the type $[(bipy)_2Ru(TSC)](PF_6)_2$ and $[(phen)_2Ru(TSC)](PF_6)_2$ (Figure 26) was reported by Beckford *et al.*[128] All complexes were observed to interact with DNA via weak to moderate intercalation, and they all showed good cytotoxicity against a variety of human cancer cell lines including MCF-7 and MDA-MB-231 (breast adenocarcinoma) and HCT 116 and HT-29 (colorectal carcinoma) cell lines.[128]

In 2006, the synthesis, characterization and antiamoebic properties of several

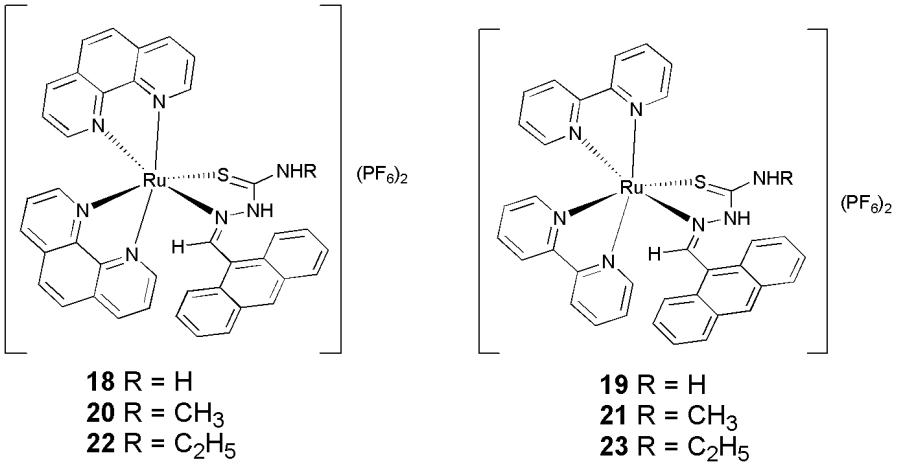

Figure 26. Ruthenium(II) complexes containing thiosemicarbazone ligands.[128]

neutral dioxovanadium(V) complexes $[VO_2(HL)]$ (H_2L = I: **24**, H_2L = II: **25** and H_2L = III: **26**; H_2L are the thiosemicarbazones H_2pydx-tsc (I), H_2pydx-chtsc (II) and H_2pydx-clbtsc (III); pydx = pyridoxal, tsc = thiosemicarbazide, chtsc = N4-cyclohexylthiosemicarbazide, clbtsc = N4-(2-chloro)benzylthiosemicarbazide) (Figure 27) were reported by Maurya *et al*.[136] Upon heating, methanolic solutions of these complexes readily dimerized to form the respective μ-oxo binuclear complexes $[(VOL)_2\ \mu\text{-}O]$ (H_2L = I: **27**, H_2L = II: **28**, H_2L = III: **29**) as shown in Figure 27.[136]

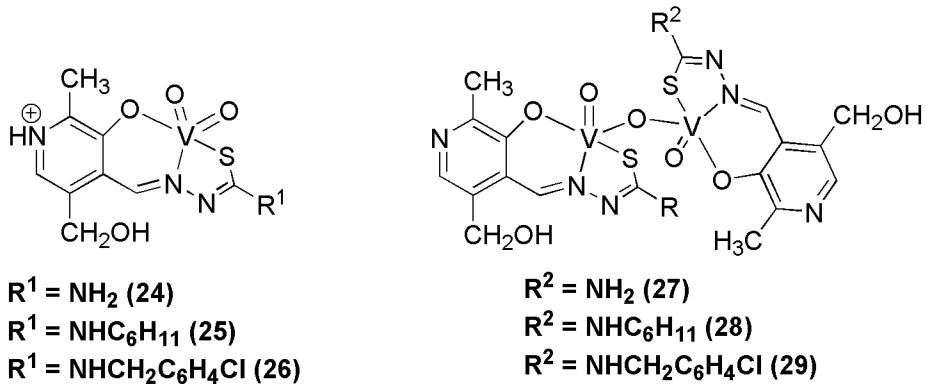

Figure 27. Structure of neutral dioxovanadium(V) complexes containing thiosemicarbazone ligands.[136]

Research Aim

The main aim of this project is to synthesize, characterize and investigate the anti-proliferative properties of a series of novel V(IV) compounds containing thiosemicarbzone ligands. In this study, three thiosemicarbazone ligands will be synthesized. The three thiosemicarbazone ligands will then be coordinated to [VO(Sal-*L*-tryp)(H_2O)] (**1**), to produce three novel V(IV)-containing complexes. All ligands and complexes will be characterized using electrochemical and several spectroscopic techniques.

Preliminary *in vitro* studies will also be carried out in order to investigate the anti-proliferative activity of the novel compounds. *In vitro* studies will be carried out using colon cancer cell lines, and the results obtained will be compared with that of normal non-cancerous colonic myofibroblasts. These compounds are proposed to have the potential to be used as anticancer agents. Stability studies in DMSO solvent to ascertain the oxidation numbers of the vanadium-containing species. Spectroscopic techniques will be used in order to determine the identity of the products formed upon aerial oxidation in DMSO. The hypotheses are as follows:

- Vanadium(IV) complexes are resistant to aerial oxidation.
- Vanadium(IV) complexes do exhibit anti-proliferative properties against colon cancer cell lines.

CHAPTER II

EXPERIMENTAL

Materials

Analytical or reagent grade chemicals were used throughout this study. All reagents and solvents were obtained from Sigma-Aldrich (St. Louis, MO, USA) or other commercial vendors, and used as received.

Instrumentation and Techniques

Microanalyses (C, H, N) were performed by Desert Analytics, Tucson, U.S.A. and Columbia Analytical Services, 3860 S. Palo Verde Road Suite 303, Tucson, AZ 85714, U.S.A. All FT IR spectra were acquired on a Nicolet 6700 FT IR spectrophotometer in the range 4000-400 cm^{-1} using the ATR accessory (with a diamond crystal). ^{1}H- and ^{13}C-NMR spectra were acquired in DMSO-d_6 on a Bruker 400 MHz spectrometer operating at ambient temperature. The residual ^{1}H- and ^{13}C-present in DMSO-d_6 (2.49 and 39.7 ppm, respectively) were used as internal references. Electronic absorption spectra were recorded on a HP8452 diode array spectrophotometer using quartz cuvettes and DMSO as the solvent. Fluorescence spectra were acquired on a Cary Eclipse fluorescence spectrophotometer (Varian Inc.) using a slit width of 10 nm.

Electrospray Ionization Mass Spectrometry (ESI MS)

ESI MS data was collected on an HP Agilent 1956b single-quadrupole mass spectrometer. Samples were dissolved in an acetic acid/methanol mixture and introduced by direct injection using a syringe pump at a flow rate of 100 $\mu L\ s^{-1}$ while sweeping the cone voltage from 0 to 200 V at a rate of 10 V min^{-1}. All m/z ratios and

percentages presented as ESI MS data were determined using the MestReNova software.

Electrochemical Studies

Cyclic voltammetric (CV) and square wave (SQW) data were collected on a Bioanalytical Systems Inc. Episilon workstation on a C3 cell stand at 296 K. Measurements were carried out using a three-electrode system consisting of a 1.6 mm platinum working electrode, a platinum wire auxiliary electrode, and a Ag/Ag^+ (0.01 M $AgNO_3$ and 0.10 M TBAP in acetonitrile) reference electrode. The working electrode was polished before each experiment with alumina slurry. DMSO solutions (1.0 mM) containing 0.10 M tetra-*n*-butylammonium hexafluorophosphate (TBAP) as supporting electrolyte were saturated with argon for 15 minutes prior to each run. A blanket of argon gas was maintained throughout the measurements and ferrocene was used as an internal standard ($E_{1/2}$ = 0.09 V versus Ag/Ag^+).

X-ray Crystallography

X-ray crystallographic data collection, structure analysis and refinement, and intensity data of the acetylethTSC were obtained by Dr. Don VanDerveer and Dr. Frank R. Fronczek of Clemson University and Louisiana State University, respectively. Crystallographic data were collected at 90 K on a Bruker Kappa Apex-II CCD diffractometer equipped with CuKα radiation and an Oxford Cryosystems Cryostream cooler. The structure of acetylethTSC was solved using SHELXS[137] and refined using the SHELX97[138,139] software packages. All H atoms were visible in difference maps. Coordinates of the NH hydrogen atoms were refined individually while those on C were placed in idealized positions with torsional parameters refined

for the methyl groups. Crystal data: $C_8H_{12}N_4S_2$, FW = 228.34, monoclinic, space group = C2/c, a =10.4549(10), b = 10.8970(10), c = 18.7694(15) Å, β = 91.544(5)º, V = 2137.6(3) $Å^3$, Z = 8, T = 90.0(5)K, μ = 4.25 mm^{-1}, d_{calc} = 1.419 g cm^{-3}, colourless parallelepiped, dimensions = 0.18 x 0.17 x 0.09 mm, reflections collected = 8017, unique reflections = 1901, observed reflections ($I > 2\sigma(I)$) = 1738, R_{int} = 0.026, No. of parameters = 136, R_1 = 0.028, R_2 = 0.069, GOF(F^2) = 1.065, CCDC No. = 812348.

Cell Culture

All *in vitro* studies were done by Dr. Antonio González-Sarrías of the University of Rhode Island. All cell lines were obtained from the American Type Culture Collection (ATCC, Rockville, MD, U.S.A.) and maintained at the University of Rhode Island, U.S.A. Cell lines used included three human colon cancer cells: HCT116 (human colon carcinoma), HT-29 (human colon adenocarcinoma) and Caco-2 (human epithelial colorectal adenocarcinoma). Non-cancerous human colon cells, CCD-18Co (human colon fibroblasts) were also used in this study. Caco-2 cells were grown in EMEM medium supplemented with 10% v/v fetal bovine serum, 1% v/v L-glutamine, 1% v/v nonessential amino acids, and 1% v/v antibiotic solution (Sigma-Aldrich). HT-29 and HCT-116 cells were grown in McCoy's 5a medium supplemented with 10% v/v fetal bovine serum, 1% v/v non-essential amino acids, 2% v/v HEPES and 1% v/v antibiotic solution. CCD-18Co cells were grown in EMEM medium supplemented with 10% v/v fetal bovine serum, 1% v/v non-essential amino acids, 1% v/v *L*-glutamine, and 1% v/v antibiotic solution and were used from PDL = 26 to PDL = 35 for all experiments. Cells were maintained in an incubator at 37 ºC under an atmosphere of 5% CO_2/95% air atmosphere at constant humidity and maintained in the linear phase of growth. The pH of the culture medium inside the

incubator was determined using pH indicator paper (pHydrionTM Brilliant, pH 5.5-9.0, Micro Essential Laboratory, NY, U.S.A.). Prior to addition to the culture mixture, all test samples were dissolved in DMSO (<0.5 % in the culture medium) by sonication and then filter sterilised (0.2 μm). Control cells were also carried out in parallel sequences and subjected to the same changes in medium with a 0.5 % DMSO.

Cytotoxicity Assay

This assay was carried out as described by Cory et at.[140] in order to measure the IC_{50} values for samples. The *in vitro* cytotoxicity of samples were briefly assessed in tumour cells by a tetrazolium-based colorimetric assay taking advantage of the metabolic conversion of MTS [3-(4,5-dimethylthiazol-2-yl)-5-(3-carboxymethoxyphenyl)-2-(4-sulfenyl)-2H-tetrazolium, inner salt] to a reduced form that absorbs light at 490 nm. Cells were counted using a hemacytometer and were plated at 2000-5,000 cells per well, depending on the cell line, in a 96-well format for 24 hours prior to drug addition. All test samples and a positive control, etoposide 4 mg ml^{-1} (Sigma-Aldrich), were dissolved in DMSO (by sonication) and diluted with media to the desired treatment concentration and the final DMSO concentration per well did not exceed 0.5%. Control wells were also included on all plates. Following a 24, 48, or 72 hour drug-incubation period of the serially diluted test compounds at 37 °C, MTS, in combination with the electron coupling agent, phenazine methosulphate, was added to the wells and cells were incubated at 37 ˚C in a humidified incubator for three hours. Absorbances at 490 nm (OD_{490}) were acquired on a spectrophotometer (SpectraMax M2, Molecular Devices Corp., operated by SoftmaxPro v.4.6 software, Sunnyvale, CA, U.S.A.) to obtain the number of surviving cells relative to control

populations. The results are expressed as the median cytotoxic concentrations (IC_{50} values) and were calculated from six-point dose response curves using 4-fold serial dilutions. Each point on the curve was tested in. Data are expressed as mean ± SE for three replications on each cell line.

Synthesis of Ligands

9-anthraldehyde-N(4)-methylthiosemicarbazone (MeATSC) was prepared by Dr. Floyd Beckford of Lyon College.[128]

N-Ethhymethohcarbthio. This ligand was initially synthesized by Dr. Floyd Beckford and Dr. Ramaiyer Venkatraman. This synthesis reproduced during the course of this research project. 4-ethyl-3-thiosemicarbazide (2.35 g, 19.7 mmol) and *o*-Vanillin (3.00 g, 19.7 mmol) were placed in a 250 mL round bottom flask followed by absolute ethanol (100 mL). Approximately 10 drops of glacial acetic acid were added to the off-white suspension, and the reaction mixture was heated to reflux solvent for three hours. The reaction mixture was then cooled to room temperature and filtered through a sinistered glass crucible. The white solid obtained was washed with ethanol (3 x15 mL) followed by ether (3 x10 mL) and allowed to air dry. Yield = 4.97 g (99%). The purity was checked by elemental analysis. Calc. for $C_{10}H_{13}N_3O_2S$: C, 52.15; H, 5.97; N, 16.59. Found: C, 52.53; H, 6.16; N, 17.02; Infrared spectrum (ν/cm^{-1}): FT IR (ν/cm^{-1}): 3304 (m) ($-N^1H$), 3300 (m) ($-N^2H$), 3130 (br) (OH), 1155 (m) (N-N), 1606 (m) (TSC (C=N)), (1267) (m) and (831) (m) (C=S). δ_H (400 MHz; DMSO-d_6); 1.15 (t) (3H) ($-CH_3$), 3.46 (s) (1H) ($-CH_3$-OAr), 3.60 (q) (2H) (CH_2), 7.57 (s) (1H) (azomethine -CH=N), 6.78 (t) (CH_{ar}), 6.94 (dd) (CH_{ar}), 8.43 (s) (3H) (aminic NH), 9.19 (s) (1H) (ArOH), 11.42 (s) (1H) (hydrazinic-NH); ^{13}C (400 MHz; DMSO-

d_6); δ 172.90 (C=S), 165.73 (CH=N), 163.26 (-$COCH_{3ar}$), 136.21 (ROH), 120.61 ($CCH=N_{ar}$), 118.31 (CH_{ar}), 118.04 (CH_{ar}), 111.57 (CH_{ar}), 56.02 (OCH_3), 29.95 (CH_2), 15.06 (CH_3).

AcetylethTSC. AcetylethTSC was synthesized and characterized by Dr. Ramaiyer Venkatraman from Jackson State University. This synthesis was also repeated during the course of this research project. 2-Acetylthiazole (0.636 g, 0.518 ml 5.0 mmol) was placed in a 100 ml round bottomed flask followed by anhydrous methanol (25 mL). 4-Ethyl-3-thiocarbazide (0.596 g, 5.0 mmol) in anhydrous methanol (25 mL) was slowly added to the solution of 2-acetylthiazole follwed by a few drops of concentrated hydrochloric acid. The reaction mixture was stirred and heated to reflux solvent for two hours, then evaporated to a minimum volume to form a yellow solid. The mixture was filtered and the residue was washed with ether and air-dried. Yield = 0.750 g (66%). A single cystal for X-ray crystallography was grown by slow evaporation from methanol. FT IR (ν/cm^{-1}): 3164 (m) (-N^1H), 3054 (m) (-N^2H), 1059 (m) (N-N), 1543 (m) (TSC (C=N)), (1296) (m) and (813) (m) (C=S). δ_H (400 MHz; DMSO-d_6); 1.16 (t) (3H) (-CH_3), 2.42 (s) (3H) ($CH_3CH=N$), 3.61 (d) (2H) (CH_2), 7.39 (d) (CH_{ar}), 7.89 (d) (CH_{ar}), 8.34 (s) (3H) (aminic NH), 10.61 (s) (1H) (hydrazinic-NH).

Reduced Schiff base (2-(2-hydroxybenzylamino)-3-(1H-indol-3-yl)propanoic acid). The reduced Schiff base was prepared using a known procedure involving salicylaldehyde, amino acids, and $NaBH_4$, but with *L*-trptophan using the following synthetic procedure:[141] *L*-tryptophan (2.042 g, 10.0 mmol) and potassium hydroxide (0.56 g, 10.0 mmol) were added to a 125 mL Erlenmeyer flask, followed by deionised

water (10 mL). Salicylaldehyde (1.029 mL, 10.0 mmol) in absolute ethanol (10 mL) was slowly added to the mixture. The yellow solution was then stirred for thirty minutes prior to cooling in an ice bath. The intermediate Schiff base formed *in situ* was then reduced with an excess of sodium borohydride (0.46 g, 12 mmol) in water (5 mL) containing 10 drops of 2 M sodium hydroxide. The solution was stirred for ten minutes, and the yellow color slowly discharged. The solution was then acified with concentrated HCl to pH 4.68 and the resulting solid was filtered off, washed with ethanol (2 x 30 mL) and diethyl ether (2 x 30 mL), and dried. The white solid obtained was recrystalized twice from water/ethanol (1:1). Yield = 1.08 g (35%). m/z (ESI) (+ve mode) 311.08 (100.00%, $[M+H]^+$), 242.42 (13.04%, $[M-CHO_3 + H]^+$), 620.36 (12.77%, $[2M + H]^+$), 930.39 (5.02%, $[3M+H]^+$), 1240.92 (3.92%, $[4M + H]^+$). FT IR (ν/cm^{-1}): 3392 (m) (indolic NH), 3055 (br) (OH), 1208 (m) (C-O)), 1494 (m) (COO_s) and 1592 (m) (COO_{as}). δ_H (400 MHz; DMSO-d_6); 2.67 (d) (2H) (H (j)), 3.21 (d) (2H) ((H (h)), 3.05 (d) (2H) (H (g)), 5.91 (t) (1H) (H (d)), 6.15 (d) (1H) (H (b)), 6.31 (d) (1H) (H (l)), 6.62 (m) (1H) (H (n)), 6.62 (m) (1H) (H (o)), 6.62 (m) (1H) (H (p)), 6.62 (m) (1H) (H (q)), 6.90 (d) (1H) (H (a)) and 7.18 (d) (1H) (H (c)); ^{13}C (400 MHz; DMSO-d_6); 28.57 (C (j)), 46.72 (C (g)), 63.61 (C (h)), 110.66 (C (n)), 111.57 (C (k)), 113.46 (C (d)), 118.50 (C (o)), 118.69 (C (q)), 121.37 (C (b)), 123.85 (C (p)), 123.89 (C (l)), 126.95 (C (f)), 127.78 (C (c)), 128.16 (C (a)), 128.34 (C (r)), 135.97 (C (m)), 164.55 (C (e)), 182.05 (C (i)).

K[(Sal-L-tryp)]. This complex was prepared using an analogous synthesis as reported by Vanco *et al.*,[142] but in our case, *L*-tryptophan was used instead of β-alanine. To a mixture of *L*-tryptophan (3.07 g, 15.0 mmol) and potassium hydroxide

(0.85 g, 15.0 mmol) dissolved in water (5 mL), the solution of salicylaldehyde (1.57 mL, 15.0 mmol) in 10 mL of ethanol was added with stirring. The resulting yellow solution was stirred at room temperature for 24 hours, and then, it was diluted by ethanol (25 mL). Upon slow evaporation of solvent, a yellow oil was formed, which was then tertuated with diethyl ether. Solution was then filtered and dried under vacuum to give a yellow powder. Yield = 4.85 g (93%). *m/z* (ESI) (+ve mode) 344.05 (39.65%, $[M + H]^+$), 300.03 (100.00%, $[M - OH - K + H]^+$), 281.14 (46.08%, $[M - OH - O - K + H]^+$), 262.12 (1.51%, $[M - COO - K + H]^+$), 242.62 (64.65%, $[M - COO - OH - K + H]^+$) and 205.20 (50.43%, $[M - C_7H_6O - K + H]^+$). FT IR (ν/cm^{-1}): 3407 (m) (indolic NH), 3169 (br) (OH), 1194 (m) (C-O)), 1521 (m) (COO_s), 1604 (m) (COO_{as}) and 1570 (m) (TSC (C=N)). δ_H (400 MHz; DMSO-d_6); 3.13 (t) (2H) (H (k)), 3.62 (d) (1H) ((H (i)), 4.07 (s) (1H) (H (g)), 6.59 (s) (1H) (H (t)), 6.72 - 7.06 (m) (1H) (H (b)), 6.72 - 7.06 (m) (1H) (H (d)), 7.20 (s) (1H) (H (n)), 7.20 (m) (1H) (H (o)), 7.20 (m) (1H) (H (p)), 7.20 (m) (1H) (H (q)), 7.35 - 7.58 (m) (1H) (H (c)), 7.35 - 7.58 (m) (1H) (H (e)) and 11.17 (s) (1H) (H (s)); ^{13}C (400 MHz; DMSO-d_6); 30.16 (C (k)), 64.82 (C (i)), 72.43 (C (q)), 111.39 (C (l)), 111.56 (C (p)), 115.74 (C (b)), 117.62 (C (d)), 117.99 (C (n)), 118.31 (C (t)), 118.33 (C (f)), 120.59 (C (o)), 123.38 (C (m)), 127.36 (C (c)), 131.77 (C (r)), 132.01 (C (e)), 163.27 (C (a)) and 172.88 (C (j)).

Synthesis of Complexes

[Zn(Sal-L-tryp)(H_2O)].0.25 H_2O. **[**Zn(Sal-*L*-tryp)(H_2O)].0.25H_2O was prepared as by Garcia-Raso *et.al*. with minor modifications to the general procedure.[143] *L*-tryptophan (5 mmol, 1.024 g) and absolute ethanol (10 mL) was placed in a 250 mL

round bottomed flask and the mixture was heated and stirred at 60-70 ˚C. Salicylaldehyde (5 mmol, 0.52 mL) in absolute ethanol (10 mL) was slowly added to the mixture. The resulting yellow solution was stirred vigorously on a magnetic stirrer for 30 minutes and an aqueous solution of zinc(II) acetate dihydrate (5 mmol, 1.098 g) in water (30 mL) was added dropwise to the solution. The solution was simultaneous neutralized to pH 7 with 0.5 M KOH. The resulting solution was stirred for 1 h and the yellow precipitate formed was filtered, washed with water, and dried under vacuum. The resulting solid was crystallized from methanol and rotary evaporated to dryness. Yield: 1.2608g (64%). *m/z* (ESI) (+ve mode) 395.11 (13.93%, $[M + H]^+$) and 1152.92 (92.74%, $[Zn_3O_2(Sal\text{-}L\text{-}tryp)_3 + H]^+$). FT IR ($\nu/cm^{-1}$): 3405 (m) (indolic NH), 3256 (br) (OH), 1551 (m) (C-O)), 1473 (m) (COO_s), 1597 (m) (COO_{as}) and 1581 (m) (TSC (C=N)). δ_H (400 MHz; DMSO-d_6); 4.15 (d) (1H) (H (b)), 7.13 (m) (1H) ((H (c)), 7.06 (t) (1H) (H (d)), 7.34 (d) (1H) (H (e)), 7.25 (s) (1H) (H (g)), 3.90 (d) (1H) (H (i)), 3.19 (d) (2H) (H (j)), 6.62 (m) (1H) (H (n)), 6.62 (m) (1H) (H (o)), 6.62 (m) (1H) (H (p)), 10.70 (s) (1H) (H (r)) and 6.62 (m) (1H) (H (q)); ^{13}C (400 MHz; DMSO-d_6); 30.64 (C (j)), 48.66 (C (i)), 69.07 (C (k)), 109.58 (C (p)), 111.42 (C (d)), 118.28 (C (m)), 118.28 (C (n)), 118.44 (C (f)), 118.86 (C (o)), 120.90 (C (b)), 122.22 (C (l)), 124.44 (C (s)), 127.05 (C (c)), 132.87 (C (e)), 134.50 (C (q)), 136.19 (C (g)), 167.14 (C (a)) and 179.60 (C (h)).

[VO(Sal-L-tryp)(H_2O)] ***1***. This complex was prepared as by Costa Pessoa *et al.*[144] *L*-tryptophan (1.14 g, 5.60 mmol) and sodium acetate trihydrate (1.47 g, 10.8 mmol) was placed in a 250 mL round bottomed flask with deionized water (100 mL). The mixture was stirred and heated at 50 ˚C to completely dissolve the *L*-tryptophan. Salicylaldehyde (0.59 mL, 5.6 mmol) in absolute ethanol (14 mL) was slowly added

to the mixture. The resulting yellow solution was stirred vigorously on a magnetic stirrer and an aqueous solution of $VOSO_4.xH_2O$ (0.78 g, 4.8 mmol) in water (2 mL) was added dropwise to the solution. The solution was stirred for 30 minutes. A deep dark brown precipitation developed immediately, and then, a heavy precipitation was observed. The resulting solution was then filtered under vacuum. The grey solid formed was washed with water (30 mL) followed by a ethanol-water mixture (50:50) (30 mL) and dried. Yield = 1.19 g (63%). The purity was checked by elemental analysis. Calc. for $C_{18}H_{16}N_2O_5V$: C, 55.25; H, 4.12; N, 7.16. Found: C, 55.16; H, 4.31; N, 6.87 (lit.[144] Calc. for $C_{18}H_{16}N_2O_5V$: C, 55.25; H, 4.12; N, 7.16. Found: C, 55.2; H, 4.2; N, 7.1). FT IR (ν/cm^{-1}): 3478 (m) (indolic NH), 3014 (br) (OH), 1540 (m) (C-O), 1490 (m) (COO_s), 1597 (m) (COO_{as}), 1600 (m) ([(Sal-*L*-tryp)] C=N), and 997 (s) (V=O) (lit.[144] 3480 (m) (indolic NH), 3065 (br) (OH), 1630 (m) ([(Sal-*L*-tryp)] (C=N)), 1600 (m) (C-O)) and 970 (s) (V=O)). UV-Visible spectrum (MeOH), $\lambda_{max.}/nm$ ($\varepsilon/M^{-1}\,cm^{-1}$): 558 (44) and 758 (27); (lit.[144] UV-Visible spectrum (DMSO), $\lambda_{max.}/nm$ ($\varepsilon/M^{-1}\,cm^{-1}$): 275 (15400) and 375 (4850), 520 (45) and 730 (20)). Compounds **2-4** were initially synthesized by Mr. Anthony Magnusen. However, during this research project, the following syntheses were reproduced to give higher purity and improved yields. Compounds were also fully characterized for the first time.

[VO(Sal-L-tryp)(MeATSC)].1.5C_2H_5OH ***2***. A 250 mL round bottom flask was thoroughly dried; then, (E)-2-(anthracen-9-ylmethylene)-N-methylhydrazinecarbothioamide (0.15 g, 0.51 mmol) and [VO(Sal-L-tryp)(H_2O)] (0.20 g, 0.51 mmol) were placed in the 250 mL round bottom flask. Absolute ethanol

(100 mL) was added to the flask and the solution was heated to reflux solvent while stirring under argon for two hours in an oil bath at 110 ˚C. An orange-blue solution, which was produced, was then rotary evaporated to dryness. Diethyl ether was added to the product and the mixture was filtered under vacuum and dried. A green solid was collected. Yield = 0.23 g (68%). The purity was checked by elemental analysis. Calc. for $C_{38}H_{38}N_5O_{5.5}$ SV: C, 62.03; H, 5.21; N, 9.52. Found: C, 62.62; H, 5.25; N, 9.33. *m/z* (ESI) 666.17 (100.00%, $[M + H]^+$), 577.08 (33.10%, $[[M - C_2H_5N_2S] + H]^+$, 405.14 (31.86%, $[[M - C_{17}H_{17}N_3] + H]^+$), 292.14 (54.60%, $[MeATSC + H]^+$). FT IR (ν/cm^{-1}): 3308 (m) (indolic NH), 3340 (m) ($-N^1H$), 2976 (m) ($-N^2H$), 1148 (m) (N-N), 1544 (m) (C-O)), 1491 (m) (COO_s), 1600 (s) (COO_{as}), 1624 (m) (TSC (C=N)), 1590 (m) ([(Sal-*L*-tryp)] (C=N)), (1225) (m), (829) (m) (C=S), (455) (m) (V-S), and 980 (s) (V=O). UV-Visible spectrum (DMSO), $\lambda_{max.}/nm$ ($\varepsilon/M^{-1}cm^{-1}$): 226 (74835), 292 (sh) (17954), 316 (sh) (10046), 388 (15013), 550 (54), 592 (sh) (45), 756 (28).

[VO(Sal-L-tryp)(N-Ethhymethohcarbthio)].H_2O ***3***. A 250 mL round bottom flask was thoroughly dried; then, (*E*)-2-(4-hydroxy-3-methoxybenzylidene)-*N* methylhydrazinecarbothioamide (0.065 g, 0.26 mmol) and [VO(Sal-*L*-tryp)(H_2O)] (0.10 g, 0.26 mmol) were placed in the 250 mL round bottom flask. Absolute ethanol (40 mL) was added to the flask and the solution was refluxed with stirring under argon for two hours in an oil bath at 110 ˚C to form a blue-green solution. The blue-green solution was rotary evaporated to dryness; then, diethyl ether was added to the product and the mixture was filtered under vacuum and dried. Yield = 0.12 g (78%).The purity was checked by elemental analysis. Calc. for $C_{29}H_{30}N_4O_7$ SV: C, 53.33; H, 4.64; N, 11.11. Found: C, 53.18; H, 5.21; N, 11.09. *m/z* (ESI) 624.87

(100.00%, [M - H]$^-$), 431.90 (64.75%, [M - $C_{11}H_{10}N_2O$ - H]$^-$), 407.85 (20.99%, [M - $C_{11}H_{15}N_3O_2S$ - H]$^-$), 287.88 (12.70%, [[$C_{11}H_{15}N_3O_2S$ – C_8H_7N] - H]$^-$), 252.00 (25.74%, [*N*-Ethhymethohcarbthio - H]$^-$). FT IR (ν/cm^{-1}): 3210 (m) (indolic NH), 3306 (m) (-N^{1}H), 2970 (m) (-N^{2}H), 3010 (br) (OH), 1154 (m) (N-N), 1540 (m) (C-O)), 1480 (m) (COO_s), 1600 (s) (COO_{as}), 1620 (m) (TSC (C=N)), 1580 (m) ([(Sal-*L*-tryp)] (C=N)), (1270) (m), (802) (m) (C=S), (454) (m) (V-S) and 976 (s) (V=O). Visible spectrum (DMSO), $\lambda_{max.}$/nm (ε/M^{-1}cm^{-1}): 270 (sh) (10984), 288 (sh) (13874), 330 (24837), 390 (sh) (18250), 620 (852).

[VO(Sal-L-tryp)(acetylethTSC)].0.75C_2H_5OH ***4***. A 250 mL round bottom flask was thoroughly dried; then, 2-acetylthiozole-4,4'-dimethylthiosemicarbazone (0.12 g, 0.51 mmol) and [VO(Sal-*L*-tryp)(H_2O)] (0.20 g, 0.51 mmol) were placed in the 250 mL round bottom flask. Absolute ethanol (40 mL) was added to the flask and the solution was refluxed with stirring under argon for two hours in an oil bath at 110 ˚C. An orange-blue solution which was produced was then rotary evaporated to dryness. Diethyl ether was added to the product and the mixture was filtered under vacuum and dried. Yield = 0.18 g (57%).The purity was checked by elemental analysis. Calc. for $C_{27.5}H_{30.5}N_6O_{4.75}S_2V$: C, 51.92; H, 4.83; N, 13.21. Found: C, 52.49; H, 4.72; N, 10.91. *m/z* (ESI) 600.25 (2.71%, [M+H]$^+$), 513.57 (100.00%, [M - C_3H_7NS + H]$^+$), 482.38 (37.11%, [M - C_7H_5NO] + H]$^+$), 336.06 (4.13%, [[M - $C_{17}H_{15}N_2O$] + H]$^+$, 636. 82 (2.75%, [M + 0.75 C_2H_5OH + H]$^+$). FT IR (ν/cm^{-1}): 3229 (m) (indolic NH), 3310 (m) (-N^{1}H), 2976 (m) (-N^{2}H), 1149 (m) (N-N), 1545 (m) (C-O)), 1480 (m) (COO_s), 1600 (s) (COO_{as}), 1624 (m) (TSC (C=N)), 1580 (m) ([(Sal-*L*-tryp)] (C=N)), (1287) (m), (819) (m) (C=S), (455) (m) (V-S) and 982 (V=O). Visible spectrum

(DMSO), $\lambda_{max.}$/nm (ε/$M^{-1}cm^{-1}$): 276 (21969), 352 (14227), 558 (80), 590 (sh) (70), 756 (38).

*Oxidized [VO(Sal-L-tryp)(H_2O)] (compound **1**) in DMSO*. [VO(Sal-*L*-tryp)(H_2O)] **1** (0.1 g, 0.26 mmol) and dimethylsulfoxide (10 mL) was placed in an evaporating dish and the resulting solution was left to evaporate for 32 days. Yield = 0.09 g. *m/z* (ESI) (+ve mode) 468.60 (1.67, $[M + H]^+$), 242.41 (100.00, [M - OH - DMSO - C_8H_7N + H]$^+$), 451.05 (48.25, $[M - OH + H]^+$), 763.68 (30.06, [[V_2O_3(Sal-*L*-tryp)$_2$] + H]$^+$), 776.77 (49.36, [[V_2O_3(Sal-*L*-tryp)$_2$(H_2O)] + H]$^+$) and 918.28 (3.13, [[V_2O_3(Sal-*L*-tryp)$_2$(DMSO)$_2$] + H]$^+$). FT IR (ν/cm^{-1}): 3185 (m) (indolic NH), 3194 (br)(OH), 1551 (m) (C-O)), 1497 (m) (COO_s), 1618 (s) (COO_{as}), 1667 (m) (TSC (C=N)), 1581 (m) ([(Sal-*L*-tryp)] (C=N)), 1164 (m), 1213 (m) (S=O), 949 (s) (V=O). δ_H (400 MHz; DMSO-d_6); 2.52 (d) (3H) (H (a)), 2.52 (d) (3H) ((H (b)), 10.89 (s) (1H) (H (c)), 7.06 (S) (1H) (H (d)), 7.22 (m) (1H) (H (e)), 7.22 (m) (1H) (H (f)), 7.52 (d) (1H) (H (g)), 8.06 (d) (2H) (H (h)), 3.36 (s) (1H) (H (i)), 3.00 (s) (2H) (H (j)), 7.22 (m) (1H) (H (k)), 7.22 (m) (1H) (H (l)), 7.22 (m) (1H) (H (m)), 7.22 (m) (1H) (H (n)), 9.93 (s) (1H) (H (o)) and 7.06 (s) (1H) (H (p)).

*Oxidized [VO(Sal-L-tryp)(N-Ethhymethohcarbthio)].H_2O (compound **3**) in DMSO*. [VO(Sal-*L*-tryp)(*N*-Ethhymethohcarbthio)].H_2O **3** (0.1 g, 0.16 mmol) and dimethylsulfoxide (10 mL) was placed in an evaporating dish and the resulting solution was left to evaporate for 32 days. Yield = 0.09 g. *m/z* (ESI) (+ve mode) 470.01 (0.50, $[M + H]^+$), 252.26 (100.00, [*N*-Ethhymethohcarbthio + H]$^+$), 451.96 (2.97, $[M - OH + H]^+$), 702.75 (2.15, [M - OH + *N*-Ethhymethohcarbthio + H]$^+$), 763.22 (0.74, [[V_2O_3(Sal-*L*-tryp)$_2$ + H]$^+$), 775.40 (1.08, [[V_2O_3(Sal-*L*-tryp)$_2$(H_2O)] +

H]$^{+}$) and 916.44 (0.75, [[V_2O_3(Sal-*L*-tryp)$_2$(DMSO)$_2$] + H]$^{+}$). FT IR (ν/cm^{-1}): 3193 (br)(OH), 1666 (m) (C=N), 1600 (C=O), 1550 (m) (C-O)), 1133 (m), 1157 (m) (S=O), 946 (s) (V=O). δ_H (400 MHz; DMSO-d_6); 2.52 (d) (3H) (H (a)), 2.52 (d) (3H) ((H (b)), 10.43 (s) (1H) (H (c)), 6.96 (s) (1H) (H (d)), 7.22 (m) (1H) (H (e)), 7.22 (m) (1H) (H (f)), 7.42 (d) (1H) (H (g)), 8.00 (d) (2H) (H (h)), 3.34 (s) (1H) (H (i)), 3.00 (s) (2H) (H (j)), 7.22 (m) (1H) (H (k)), 7.22 (m) (1H) (H (l)), 7.22 (m) (1H) (H (m)), 7.22 (m) (1H) (H (n)), 9.95 (s) (1H) (H (o)) and 6.96 (s) (1H) (H (p)).

CHAPTER III

RESULTS AND DISCUSSIONS

Synthesis and Characterization of the Ligands

Two novel thiosemicarbazones (*E*)-*N*-ethyl-2-(4-hydroxy-3 methoxybenzylidene)hydrazinecarbothioamide (*N*-Ethhymethohcarbthio) and (*E*)-*N*-ethyl-2-(1-(thiazol-2-yl)ethylidene)hydrazinecarbothioamide (acetylethTSC) were synthesized as shown in Scheme 5.

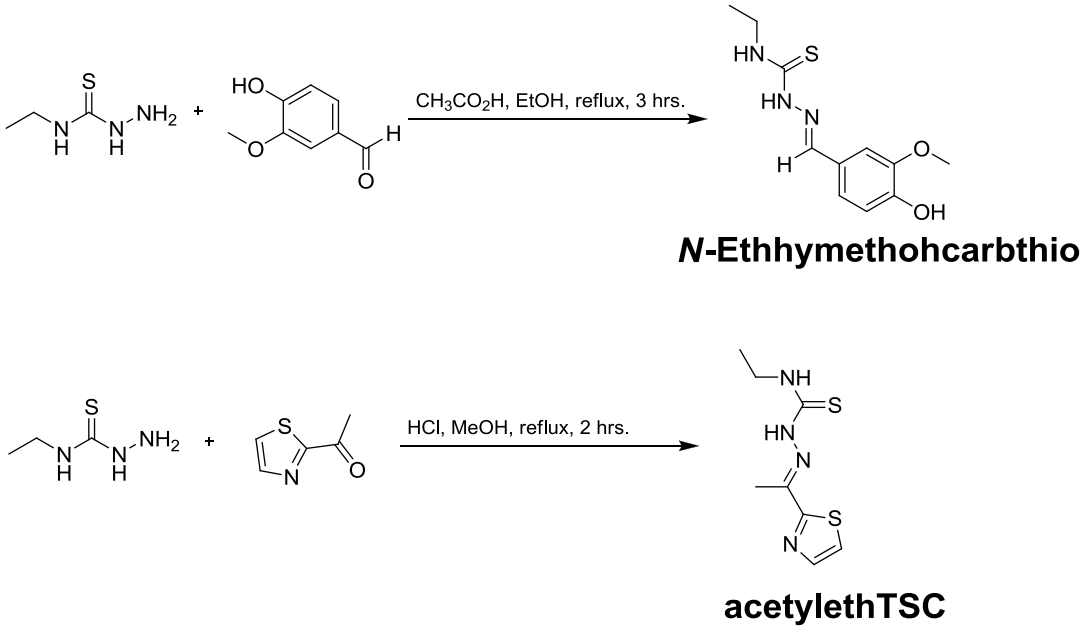

Scheme 5. Synthesis of the thiosemicarbazones.

9-Anthraldehyde-*N*(4)-methylthiosemicarbazone (MeATSC) was synthesized as by Beckford et al.[128] 2-(2-hydroxybenzylamino)-3-(1H-indol-3-yl)propanoic acid (the reduced Schiff base) was also prepared using a known procedure[141] involving salicylaldehyde, amino acids, and $NaBH_4$, but with *L*-tryptophan (Scheme 6).

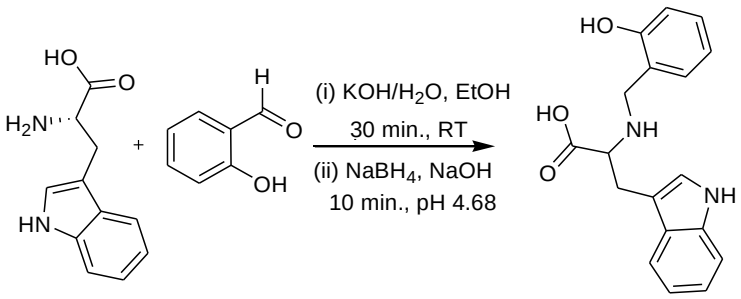

Scheme 6. Synthesis of 2-(2-hydroxybenzylamino)-3-(1H-indol-3-yl)propanoic acid.

Elemental and Mass Spectroscopic Analyses

Elemental analyses were carried out on *N*-Ethhymethohcarbthio, and the percentage values found for C, H, and N as an assessment of the purity are discussed in this chapter. ESI MS spectroscopic data were acquired for the reduced Schiff base and K[(Sal-*L*-tryp)] (See Appendix, Figures A1 and A2) and the data is presented in Table 2.

The ESI MS data for the reduced Schiff base and K[(Sal-*L*-tryp)] were acquired in the positive ion mode of the mass spectrometer. The ESI MS spectrum acquired for the reduced Schiff base (using $NH_4OH/NH_4CH_3CO_2$ at pH 9.65 as solvent) revealed a base peak at *m/z* = 311.08, corresponding to $[M + H]^+$ ion. Four peaks assigned to the fragments $[M - CHO_3 + H]^+$, $[2M + H]^+$, $[3M + H]^+$ and $[4M + H]^+$ were also observed at *m/z* = 242.42, *m/z* = 620.36, *m/z* = 930.39, and *m/z* = 1240.97, respectively. The ESI MS spectrum of K[(Sal-*L*-tryp)], acquired in methanol, revealed a base peak at *m/z* = 300.03, which is attributed to the $[M - HO - K + H]^+$ ion. The peak at *m/z* = 344.05 was assigned to the $[M + H]^+$ ion while the fragments at *m/z* = 205.20, *m/z* = 242.62, *m/z* = 262.12 and *m/z* = 281.14 were assigned to $[M - C_7H_6O - K + H]^+$, $[M - COO - OH - K + H]^+$, $[M - COO - K + H]^+$ and $[M - OH - O - K + H]^+$, respectively.

Table 2

Mass spectroscopic data of the Reduced Schiff base (2-(2-hydroxybenzylamino)-3-(1H-indol-3-yl)propanoic acid) and K[(Sal-L-tryp)].

Species	*Exact Mass/gmol^{-1}*	*Species*	*m/z*	*Relative Intensity*
Reduced Schiff Base #	310.13	$[M+ H]^+$	311.08	100.00
		$[M - CHO_3 + H]^+$	242.42	13.04
		$[2M + H]^+$	620.36	12.77
		$[3M + H]^+$	930.39	5.02
		$[4M + H]^+$	1240.92	3.92
K[(Sal-*L*-tryp)] #	346.07	$[M + H]^+$	344.05	39.65
		$[M - OH - K + H]^+$	300.03	100.00
		$[M - OH - O - K + H]^+$	205.20	50.43
		$[M - COO - K + H]^+$	242.62	64.65
		$[M - COO - OH - K + H]^+$	262.12	1.51
		$[M - C_7H_6O - K + H]^+$	281.14	46.08

- positive mode

X-ray Crystallographic Studies on AcetylethTSC

A single crystal of acetylethTSC was grown by slow evaporation of a solution containing methanol as solvent. The molecular structure with the atomic numbering scheme of acetylethTSC is shown in Figure 28 while Table 3 shows the crystal data and structure refinement (see Appendix, Figures AJJ-AMM for selected bond lengths and angles).

The molecule was observed to be nearly planar with its 14 non-hydrogen atoms having a mean deviation of 0.029 Å from their mean plane. The largest deviation is 0.0719(4) Å for S2 as a result of a very slight tilt of the thiazole ring from the rest of the molecule as given by the S2-C3-C2-N1 torsion angle, 3.3(2)º. The near-planarity of the

molecule is likely due to the N3-H...N1 intramolecular interaction with N...N distance 2.588(2) Å, H...N distance 2.20(2) Å, and a rather small N-H...N angle for a hydrogen

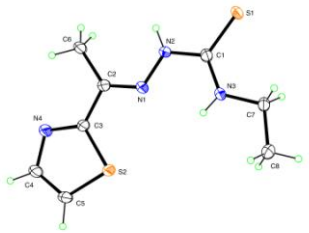

Figure 28. An ORTEP diagram of acetylethTSC (identification code = Venkat35).

Table 3

Crystal data and structure refinement for acetylethTSC (identification code = Venkat35).

Identification code	Venkat35
Empirical formula	$C_8H_{12}N_4S_2$
Formula weight	228.34
Temperature	90.0(5) K
Wavelength	1.54178 Å
Crystal system, space group	Monoclinic, C2/c
Unit cell dimensions	a = 10.4549(10) Å, α = 90º b = 10.8970(10) Å, β = 91.544(5)º c = 18.7694(15) Å, γ = 90º Volume 2137.6(3) $Å^3$
Z, Calculated density	8, 1.419 Mg/m^3
Absorption coefficient	4.251 mm^{-1}
F(000)	960
Crystal size	0.18 x 0.17 x 0.09 mm
Theta range for data collection	5.8 to 68.1º

Table 3 (continued).

Identification code	Venkat35
Limiting indices	-12<=h<=12, -12<=k<=13, -22<=l<=22
Reflections collected / unique	8017 / 1901 [R_{int} = 0.026]
Completeness to theta = 66.6º	99.1%
Absorption correction	Semi-empirical from equivalents
Max. and min. transmission	0.701 and 0.515
Refinement method	Full-matrix least-squares on F^2
Data / restraints / parameters	1901 / 0 / 136
Goodness-of-fit on F^2	1.065
Final R indices [I>2σ(I)]	R_1 = 0.0276, wR_2 = 0.0691
R indices (all data)	R_1 = 0.0312, wR_2 = 0.0715
Extinction coefficient	0.00011(3)
Largest diff. peak and hole	0.257 and -0.262 e Å $^{-3}$

bond, 110(2)º. The N1=C2 formal double bond has distance 1.284(2) Å, the N1-N2 distance is 1.3691(18) Å, and the thione distance C1=S1 is 1.6814(16) Å. It is known that the thiosemicarbazone group can present a thione-thiol tautomerism.[128] The C(1)-S(1) distance (1.6814 Å) is similar to that found in a methyl analogue of 2-acetyl-2-thiazoline thiosemicarbazone which is in the thione form as a solid,[145] which indicates that acetylethTSC is in that form. The N2-H group donates an intermolecular hydrogen bond to thione S1, forming centrosymmetric hydrogen-bonded dimers with N...S distance

3.4651(15) Å. Thiazole N atom N4 is not involved in hydrogen bonding as shown in Figure 29.

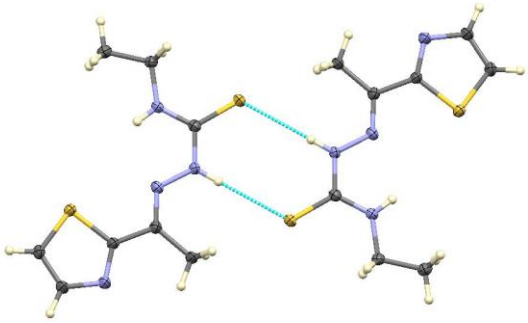

Figure 29. Hydrogen bonding in acetylethTSC (identification code = Venkat35).

FT IR Spectroscopy

Thiosemicarbazones are known to exhibit characteristic bands in specific energy regions corresponding to various functional groups.[128,146] FT IR spectra were acquired for each ligand (see Appendix, Figures A3-A7) and significant FT IR spectral bands of the free ligands are shown in Table 4. FT IR spectral data obtained for the reduced Schiff base and K[(Sal-*L*-tryp)] are also presented and used to confirm the existence of various spectral bands observed in the FT IR spectra of the free ligands.

The stretching frequencies of the ν(N-H), ν(C=N), and ν(C=S) functional groups are very useful when determining the mode of coordination of the thiosemicarbazone ligands.[147] The corresponding spectral bands occur in the regions 3100 - 3500 cm-1, 1580 - 1630 cm-1, 1000 - 1200 cm-1 and 820 - 900 cm-1, respectively.[147] Thiosemicarbazones have been shown to exhibit thione-thiol

Table 4

FT IR data for the ligands.

Compound	Indolic ν(NH) /cm^{-1}	–N^{1}H$_2$ ν(NH) /cm^{-1}	N^{2}H ν(NH) /cm^{-1}	ν(N-N) /cm^{-1}	ν(C-O) /cm^{-1}	ν_s(COO) /cm^{-1}	ν_{as}(COO) /cm^{-1}	TSC ν(C=N) /cm^{-1}	Sal-*L*-tryp ν(C=N) /cm^{-1}	ν(C=S) /cm^{-1}	ν(V-S) /cm^{-1}	ν(OH) /cm^{-1}
MeATSC	-	3399 (m)	3201 (w)	1075 (m)	-	-	-	1621 (m)	-	1255 (m), 841 (m)	-	-
N-Ethhymethohcarbthio	-	3304 (m)	3300 (w)	1155 (m)	-	-	-	1606 (m)	-	1267 (m), 831 (m)	-	3130 (br)
AcetylethTSC	-	3164 (m)	3054 (w)	1059 (m)	-	-	-	1543 (m)	-	1296 (m), 813 (m)	-	-
K[(Sal-*L*-tryp)]	3407 (m)	-	-	-	1194 (m)	1521 (m)	1604 (m)	-	1570 (m)	-	-	3169 (br)
Reduced Schiff base ligand	3392 (m)	-	-	-	1208 (m)	1494 (m)	1592 (m)	-	-	-	-	3055 (br)

tautomerism due to the presence of a thioamide -NH-C=S functionality (Figure 30).[148] Recently, it was reported that thiosemicarbazones can coordinate to metal centers

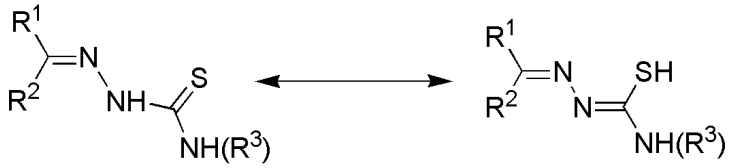

Figure 30. Tautomerism in thiosemicarbazones.[128]

either as a neutral (thione) or as a mono-anionic (thiolate) ligand.[128] The question of thione-thiol tautometism in the ligands were ruled out due to the absence of a characteristic ν ((S-H) spectral band (in the region 2600 to 2500 cm^{-1}) in the respective FT IR spectra.[147,149-151] The FT IR spectra of the ligands in our case also exhibited two stretching frequencies in the ν(N-H) region, confirming that the ligands are coordinated as the thione form.[128,148,152-154]

When evaluating the nature of the bonding in thiosemicarbazone complexes, the ν(N-H) stretching frequency is known to play a very important role.[155] The bands assigned to ν(N-H) can be split into two regions: (i) 3450 to 3210 cm^{-1} due to the -N^1H_2 group, (ii) 3180 to 3150 cm^{-1} due to the -N^2H group.[146] The ν(N-H) stretching frequency of the -N^1H_2 group was observed at 3399 cm^{-1}, 3304 cm^{-1}, and 3164 cm^{-1} for MeATSC, *N*-Ethhymethohcarbthio, and acetylethTSC, respectively. The ν(N-H) stretching frequency of the -N^2H group was observed 3201 cm^{-1}, 3300 cm^{-1}, 3054 cm^{-1} and 2831 cm^{-1} for MeATSC, *N*-Ethhymethohcarbthio, acetylethTSC, and the reduced Schiff base, respectively.

Stretching frequencies observed in the regions 1620 to 1605 cm^{-1} are

commonly assigned to the ν(C=N) moiety of the thiosemicarbazone ligands.[148,152,153,156] Spectral bands corresponding to ν(C=N) moiety were observed at 1621 cm^{-1}, 1606 cm^{-1}, and 1543 cm^{-1} for MeATSC, *N*-Ethhymethohcarbthio, and acetylethTSC, respectively.[128] A similar stretching frequency was also observed at 1570 cm^{-1} in the FT IR spectrum of K[(Sal-*L*-tryp)], corresponding to the azomethine group of the Sal-*L*-tryp moiety.[142] The absence of a similar ν(C=N) stretching frequency in the FT IR spectra of the reduced Schiff base suggested that the ligand was successfully formed and confirmed the accuracy of the assignment.

Spectra bands of medium intensity observed in the regions 841-816 cm^{-1} and 1255-1295 cm^{-1} for each thiosemicarbazone ligand was assigned to the stretching frequency ν(C=S) moiety.[152,157,158] Stretching frequencies assigned to the ν(C=S) moiety were observed at 841 cm^{-1}, 831 cm^{-1} and 813 cm^{-1}, and 1255 cm^{-1}, 1267 cm^{-1} and 1296 cm^{-1} for MeATSC, *N*-Ethhymethohcarbthio and the acetylethTSC, respectively.

NMR Spectral Studies

NMR spectral data were acquired for *N*-Ethhymethohcarbthio ligand, acetylethTSC, the reduced Schiff base, and K[(Sal-*L*-tryp)]. Based on the solubility of our ligands, *N*-Ethhymethohcarbthio, acetylethTSC and K[(Sal-*L*-tryp)] were dissolved in DMSO-d_6 whereas the reduced Schiff base was dissolved in D_2O/NaOD at pH 9. Figure 31 shows the lettering system used for the assignments of protons and carbons in the experimental section for the reduced Schiff base and K[(Sal-*L*-tryp)] (see Appendix, Figures A8 to A11).

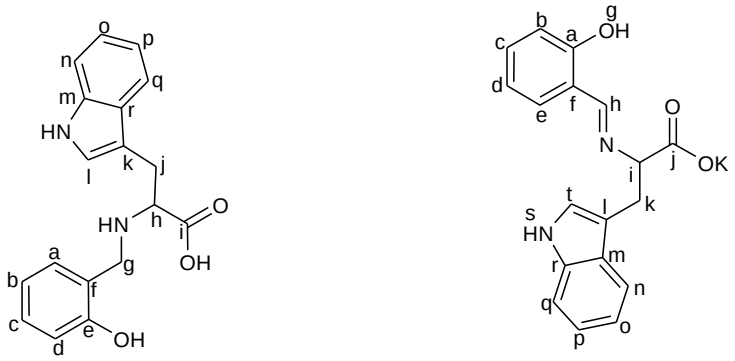

Figure 31. Assignments used for the ^{1}H and ^{13}C NMR data acquired for the reduced Schiff base and K[(Sal-*L*-tryp)] in DMSO-d_6.

N-Ethhymethohcarbthio and AcetylethTSC

The ^{1}H NMR spectra of *N*-Ethhymethohcarbthio and acetylethTSC are shown in Figures 32 and 33. The basic component of thiosemicarbazone ligand system is generally represented by the moiety: $-C^{2}=N^{3}-N^{2}H-C^{1}$.[146] In order to demonstrate the usefulness of NMR in the characterization of metal-ligand bonding, the NMR (^{1}H and^{13}C) data of the rings at C^{2} carbon of *N*-Ethhymethohcarbthio and acetylethTSC is briefly delineated.[146]

In the 1H NMR spectra of N-Ethhymethohcarbthio and acetylethTSC, a singlet at 11.42 ppm and 10.61 ppm, similar to the previously reported data of MeATSC and ATSC thiosemicarbazone ligands, was also present.[128,147,159] Based on spectroscopic data available in the literature, these signals are inferred to be due to the N(2)-H protons.[152,159,160] The hydrazinic protons (N(2)-H) of "free" thiosemicarbazone ligands are known to appear as single broad peaks in a fairly wide range (δ = 8.7 -15 ppm) depending on the nature of the substituents at C2 carbon atom.[146,161-164] This signal is therefore used as a diagnostic test for the identification of isomers.[128]

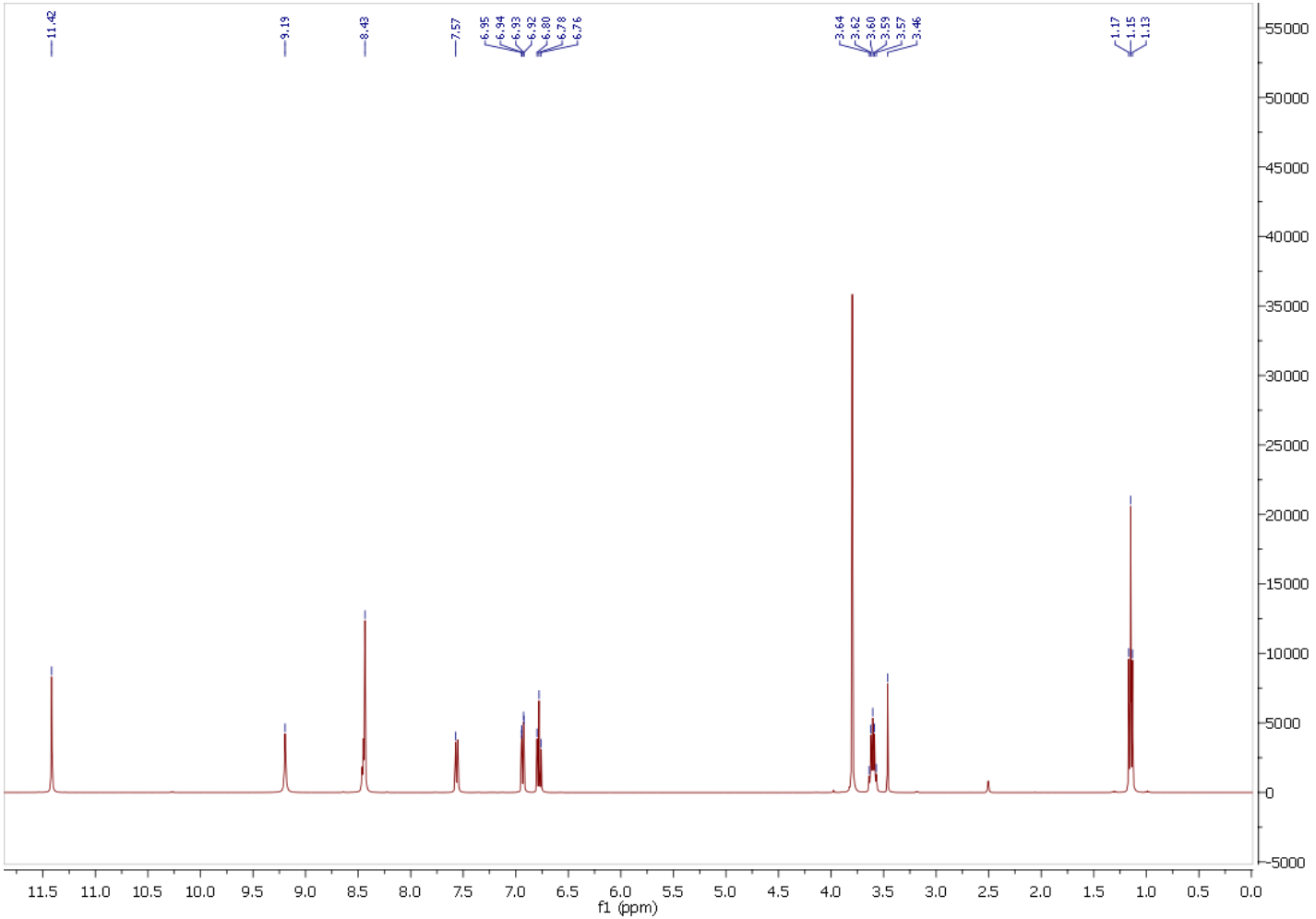

Figure 32. ^{1}H NMR spectra of *N*-Ethhymethohcarbthio in DMSO-d_6.

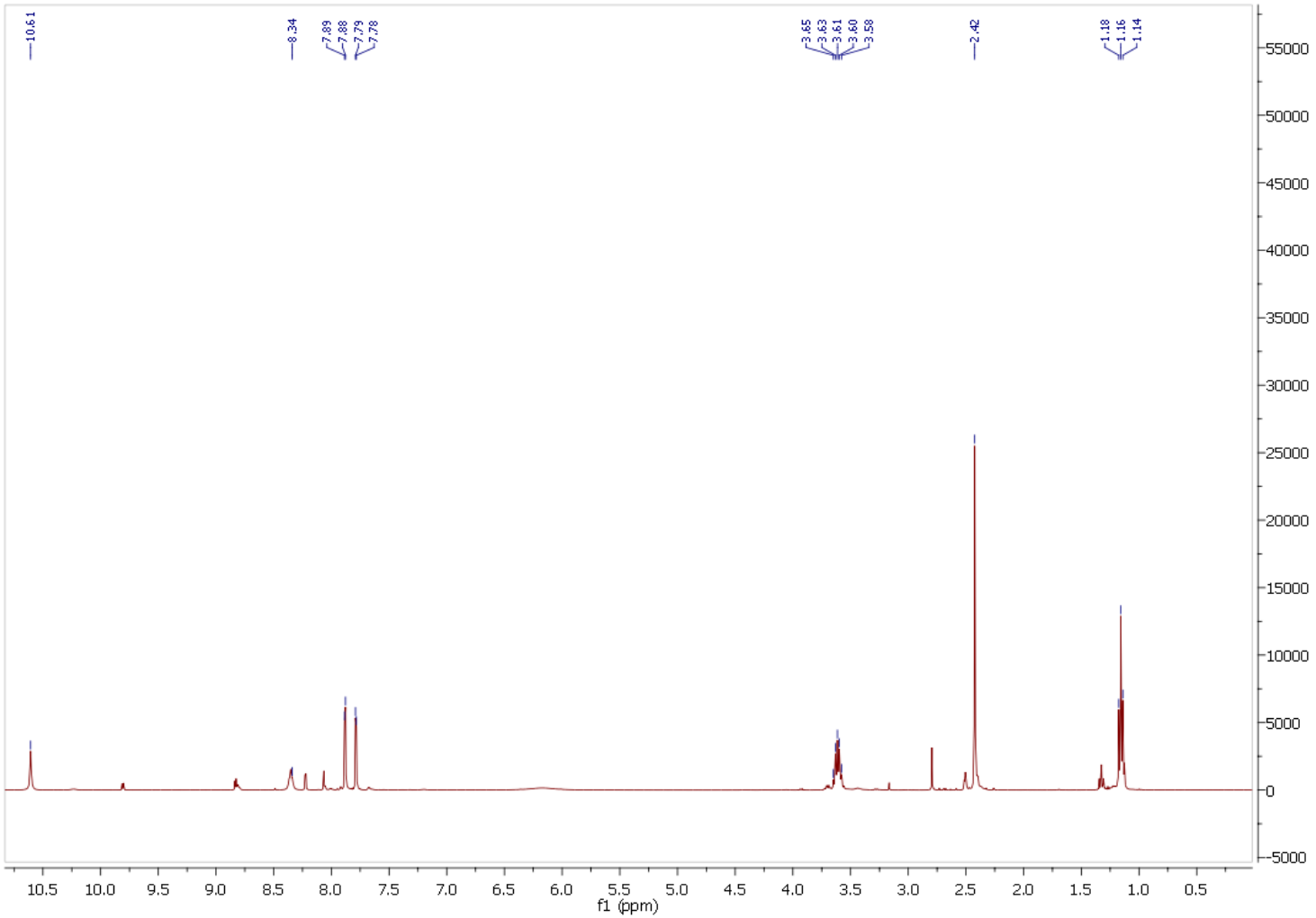

Figure 33. ^{1}H NMR spectra of acetylethTSC in DMSO-d_6.

According to Afrasiabi,[165] a resonance signal in the range δ = 13-15 ppm, suggests that the ligand is in the E form. A resonance signal in the range δ = 9-12 ppm, however, suggests that the ligand is in the Z form. Based on this analysis, the *N*-Ethhymethohcarbthio and acetylethTSC ligands both existed as the respective Z isomers. The lack of a resonance signal at ca. δ = 4.0 ppm attributable to a -SH proton resonance confirmed that both ligands existed in the thione form when in solution (even a solvent as polar as DMSO).[128] An X-ray crystallographic study on acetylethTSC also confirmed the existence of the thione moiety

. The azomethine (-C^2H) protons of free thiosemicarbazone ligands have been reported to resonate in the range δ = 6.6 to 7.9 ppm.[146,147] The singlet observed at δ = 7.57 ppm in the NMR spectrum of the *N*-Ethhymethohcarbthio ligand was therefore assigned to the azomethine moiety. Although a similar peak was absent in the ^{1}H NMR spectrum of acetylethTSC, a singlet observed at 2.42 ppm was assigned to the methyl group present at C^2 atom.

The resonance signals observed at δ = 8.43 ppm and 8.34 ppm were assigned to proton of the N^1H(R) group (where R = ethyl group) in *N*-Ethhymethohcarbthio and acetylethTSC, respectively.[128] Quintets assigned to methylene protons were observed at δ = 3.60 ppm and δ = 3.61 ppm for *N*-Ethhymethohcarbthio and acetylethTSC, respectively. Adjacent methyl protons were observed as triplets at δ = 1.15 ppm and δ = 1.14 ppm for *N*-Ethhymethohcarbthio and acetylethTSC, respectively. In the^{13}C NMR spectra, the corresponding resonance signals for the methylene and the methyl carbons were also observed at δ = 38.28 ppm and δ = 14.60 ppm, respectively.

In the ^{1}H and ^{13}C spectra of *N*-Ethhymethohcarbthio, a resonance signal observed atδ = 3.46 ppm was assigned to the methoxy protons while the corresponding carbon signal was observed at δ = 58.85 ppm. The resonance signals observed at δ = 11.41 ppm and in the region δ = 6.76-7.57 ppm were assigned to the phenolic proton (PhOH), and the aromatic protons of the *N* Ethhymethohcarbthio ligand, respectively.[147]

The resonance signals assigned to the C^1 and C^2 carbon atoms of free thiosemicarbazones are known to appear in the ranges, δ = 177.40 to 178.86 ppm and δ = 132.56 to 163.43 ppm, respectively.[146] In the ^{13}C NMR spectrum of *N*-Ethhymethohcarbthio, the resonance signals observed at δ = 176.50 ppm and δ = 177.54 ppm were therefore assigned to the C^1 and C^2 carbon atoms, respectively. All other aromatic signals were observed in the range δ = 112 to δ = 146 ppm.[128]

Electrochemical Studies

The electrochemical analysis of thiosemicarbazone ligands is very sparse in literature. In this section we attempted to analyze the electrochemical properties of our "free" ligands. Figures 34 and 35 (See Appendix, Figures A13 and A14 for the square wave voltammograms for the ligands) shows the respective cyclic voltammograms for each ligand. Table 5 shows the data obtained from electrochemical studies of all ligands. The assignment of redox peaks were done using the cyclic voltammograms shown in Figures 34 and 35. Square wave voltammograms within the potential window of 0 to +1.0 V versus Ag/Ag+ (See Appendix, Figures A13 and A14) were used in order to

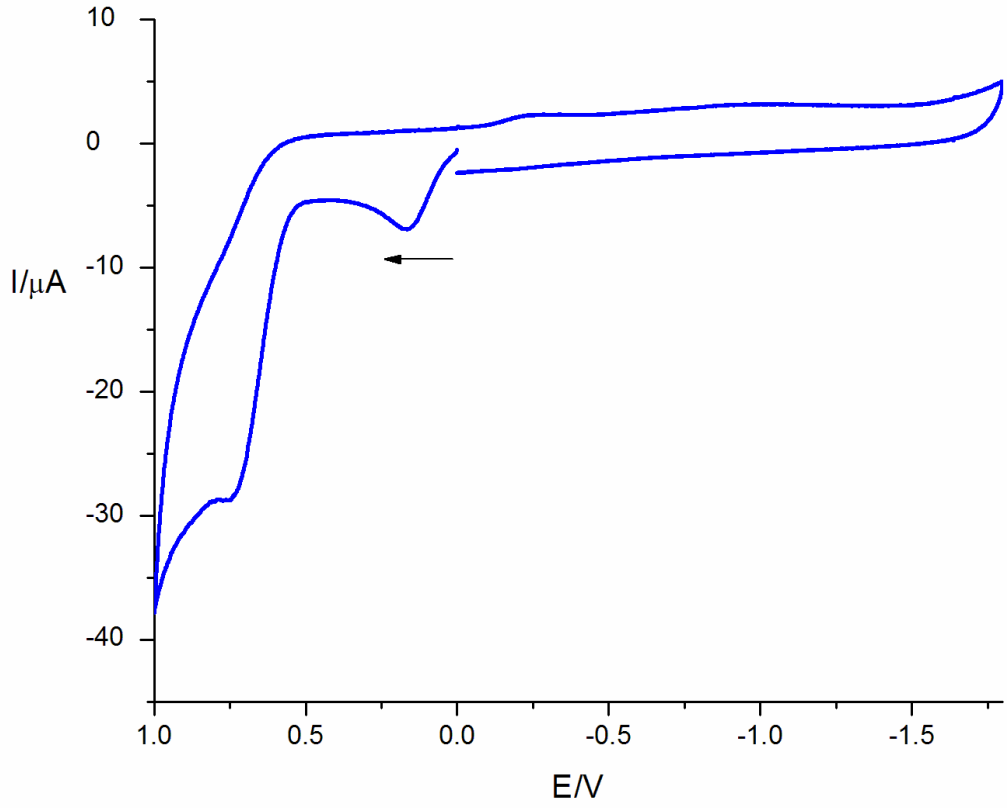

Figure 34. A cyclic voltammogram of a 1.0 mM solution of K[(Sal-*L*-tryp)] in DMSO. Electrodes: platinum working electrode, platinum auxiliary electrode and Ag/Ag^{+} (0.01 M $AgNO_3$ and 0.10 M TBAP in acetonitrile) reference electrode. Supporting electrolyte = 0.1 M TBAP. Scan rate = 100 mV s^{-1}.

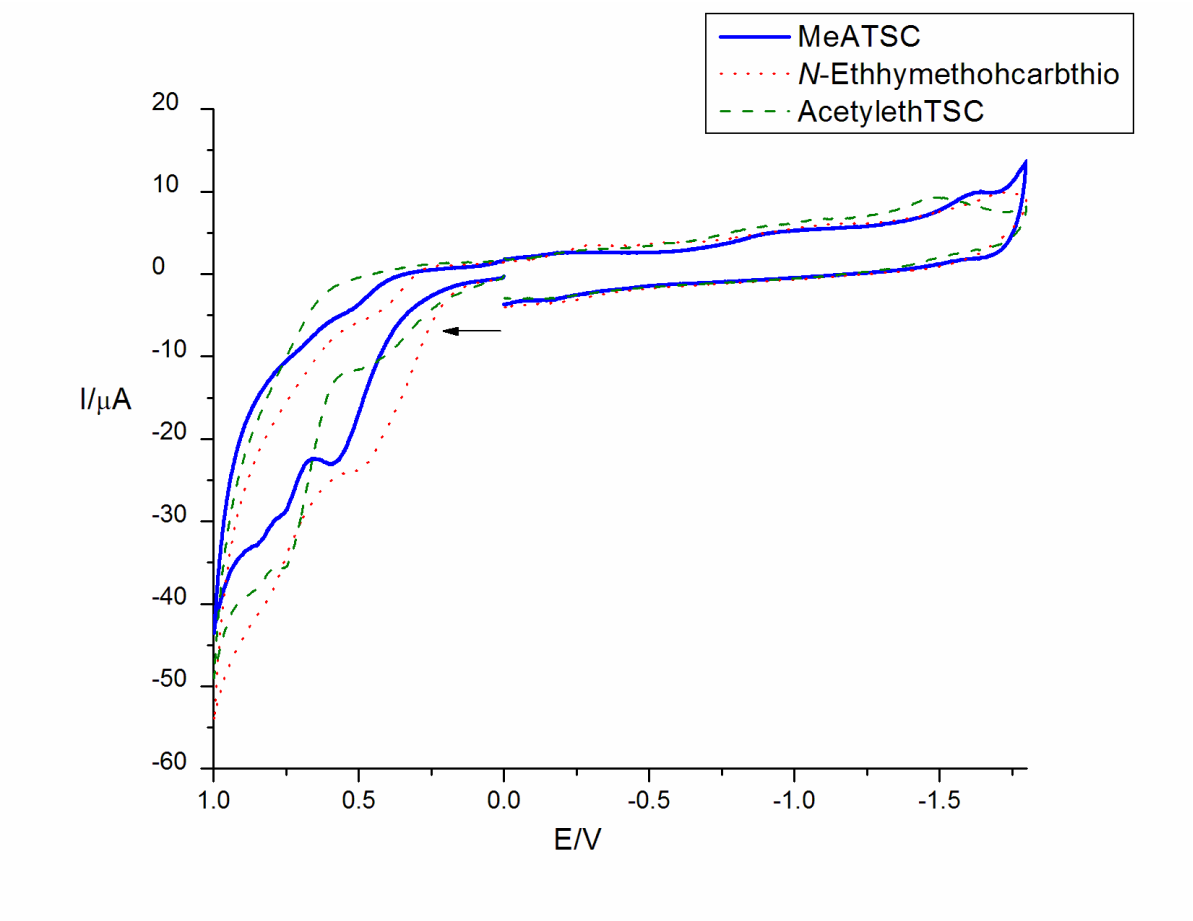

Figure 35. Cyclic voltammograms of 1.0 mM solutions of thiosemicarbazone ligands in DMSO. Electrodes: platinum working electrode, platinum auxiliary electrode and Ag/Ag^{+} (0.01 M $AgNO_3$ and 0.10 M TBAP in acetonitrile) reference electrode. Supporting electrolyte = 0.1 M TBAP. Scan rate = 100 mV s^{-1}.

confirm the assignments made based on cyclic voltammetry. Previously reported electrochemical studies have shown that *L*-tryptophan produces an irreversible anodic peak in the region +0.8 V to +0.9 V versus Ag/Ag^{+} at a scan rate of 100 mV s^{-1}.[166,167] pH studies involving the electrochemical oxidation of *L*-tryptophan have proven that *L*-tryptophan is oxidized via a two electron/two proton process occurring at the amine group (of the indole moiety) and the methyl group (present in the side chain).[168] A similar irreversible anodic peak corresponding to the oxidation of *L*-tryptophan

Table 5

Electrochemical data of 1.0 mM solutions of ligands.

Species	*E*/V	Assignment
[K(Sal-*L*-tryp)]	E_{pa} = +0.75	*L*-tryp$^{0/+}$
	E_{pa} = +0.16	PhO$^{-/\cdot}$
	$E_{1/2}$ = -0.21	PhO$^{-/\cdot}$
	E_{pc} = -0.97	-
	E_{pc} = -1.50	*L*-tryp$^{+/0}$
MeATSC	E_{pa} = +0.84	$R_2C{=}S^{0/+\cdot}$
	E_{pa} = +0.75	Oxidation of anthracene moiety
	E_{pa} = +0.60	$[R_2C{=}S]^{0/+\cdot} \rightarrow [R_2C\text{-}S\text{-}S\text{-}CR_2]^{2+} + 2e^-$
	E_{pa} = -0.17	formation of cation radical
	$E_{1/2}$ = -1.63	$HC{=}N/CH_2\text{-}NH$
	E_{pc} = -0.14	reduction of cation radical
	E_{pc} = -0.49	reduction of disulfide cation
	E_{pc} = -0.93	C=S → C=SH
N-Ethhymethohcarbthio	E_{pa} = +0.80	$R_2C{=}S^{0/+\cdot}$
	E_{pa} = +0.51	$[R_2C{=}S]^{0/+\cdot} \rightarrow [R_2C\text{-}S\text{-}S\text{-}CR_2]^{2+} + 2e^-$
	E_{pa} = +0.37	Oxidation of phenolate in vanillin
	E_{pa} = -0.17	moiety
	E_{pa} = -1.11	formation of cation radical
	$E_{1/2}$ = -1.60	formation of cation radical
	E_{pc} = -0.36	$HC{=}N/CH_2\text{-}NH$
	E_{pc} = -0.52	reduction of cation radical
	E_{pc} = -1.08	reduction of disulfide cation
		C=S → C=SH
AcetylethTSC	E_{pa} = +0.85	$R_2C{=}S^{0/+\cdot}$
	E_{pa} = +0.75	-
	E_{pa} = +0.48	$[R_2C{=}S]^{0/+\cdot} \rightarrow [R_2C\text{-}S\text{-}S\text{-}CR_2]^{2+} + 2e^-$
	E_{pa} = -0.17	formation of cation radical
	E_{pa} = -1.04	formation of cation radical
	E_{pa} = -1.38	-
	E_{pa} = -1.61	$HC{=}N/CH_2\text{-}NH$
	E_{pc} = -0.25	reduction of cation radical
	E_{pc} = -0.53	reduction of disulfide cation
	E_{pc} = -0.86	-
	E_{pc} = -1.07	C=S → C=SH

Note. Electrodes: platinum working electrode, platinum auxiliary electrode and Ag/Ag^+ (0.01 M $AgNO_3$ and 0.10 M TBAP in acetonitrile) reference electrode. Supporting electrolyte = 0.1 M TBAP. Scan rate = 100 mV s^{-1}.

was also observed at +0.75 V in the CV of K[(Sal-*L*-tryp)] (Figure 34). The assignment of this peak was also confirmed by the appearance of a similar anodic redox peak at +0.60 V in the SQW voltammogram of K[(Sal-*L*-tryp)] (see Appendix, A13). The existence of an irreversible cathodic peak, corresponding to catalytic hydrogen reduction, have also been reported during electrochemical studies of *L*-tryptophan.[169-171] In the CV of K[(Sal-*L*-tryp)], the irreversible cathodic peak observed at -1.5 V was assigned to catalytic hydrogen reduction.

Based on similar work reported by Thomas *et al.*,[172] an irreversible anodic redox peak at +0.16 V in the cyclic voltammogram of K[(Sal-*L*-tryp)] was also assumed to be due to the phenolate moieties to form into a phenoxyl radical. This assignment was also confirmed by the appearance of an anodic redox peak at +0.12 V in the square wave voltammogram of K[(Sal-*L*-tryp)]. The redox potential of the one-electron transfer assigned to the oxidation of the phenolate moiety was also observed to vary depending on the electrostatic environment surrounding the redox active phenolate group.[172] A reversible redox wave at $E_{1/2}$ = -0.21 V, attributed to the phenoxyl/phenolate redox couple of the non-coordinated, electron-rich phenolate moiety, was also observed in the cyclic voltammogram of K[(Sal-*L*-tryp)].[172]

Recently, electrochemical studies of thiosemicarbazones has shown the existence of an irreversible cathodic redox peak in the region, -1.26 V to -1.67 V, corresponding to the reduction of the imine moiety of the thiosemicarbazone functional group.[50,159,173] An increase in the electron withdrawing character of substituents present in a compound is known to have a significant effect on the stability of the respective compound.[174] The presence of electron donating substituent

increases the electron density at the reduction centers, making the respective compound more susceptible to oxidation and therefore less stable.[174] The reversible nature of the redox peaks (attributed to the reduction of the imine moiety) observed for our thiosemicarbazone ligands is therefore accounted for by the presence of non electroactive electron withdrawing groups on the iminic carbon of the respective thiosemicarbazone ligands.[174] The cyclic voltammogram of each ligand exhibited a reversible redox waves corresponding to the reduction of the imine moiety.[50,159,173] This reversible redox wave was observed at -1.63 V, -1.60 V and -1.61 V for MeATSC, *N*-Ethhymethohcarbthio, and acetylethTSC ligand, respectively.

Thiocarbonyl compounds, including thioureas, thiocaronates, and mono- and dithiocarbamates, are known to produce stable dimeric dications containing disulphide linkages upon chemical oxidation.[175,176] An outline of the suggested oxidative electron-transfer mechanism of our thiosemicarbazone ligands is shown in Scheme 7. Recently, the cyclic voltammograms of thioureas were shown to exhibit two irreversible anodic redox peaks, as well as an irreversible cathodic redox peak resulting from the reduction of an oxidation product.[175,176]

The cyclic voltammogram of each ligand exhibited two similar irreversible anodic redox peaks and a corresponding irreversible anodic redox peak. These peaks were suggested to be due to the formation of cationic species as shown in Scheme 7. Irreversible anodic redox peaks at were observed at +0.84 V and +0.60 V for MeATSC, +0.80 V and +0.51 V for *N*-Ethhymethohcarbthio and at +0.85 V and +0.48 V for acetylethTSC. The anodic redox peaks observed at +0.60 V, +0.51 V and +0.48 V were suggested to result from the oxidation of the respective thiosemicarbazone ligands to a

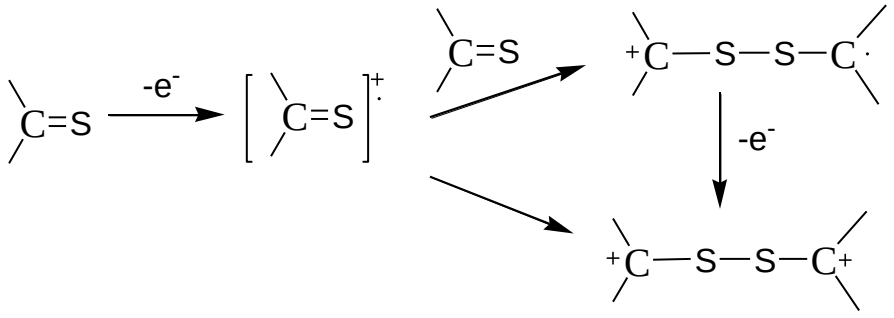

Scheme 7. Electrochemical oxidation of the thione group of a thiosemicarbazone to form a dimeric cation.

highly reactive radical cation followed by the formation of a dimeric species containing a disulphide bond.[176] According to Scheme 7, dimerization occurs either by direct coupling of two radical cations or by the addition of a radical cation to a neutral thiosemicarbazone ligand.[176] The irreversible anodic redox peaks observed at +0.84 V, +0.80 V and +0.85 V were therefore assigned to the one-electron oxidation of the resultant dimeric radical cation.[176]

The reduction of the thione functional group of a thiosemicarbazone moiety, have previously been reported to produce an irreversible cathodic peak at -1.06 V.[177-179] Previously reported electrochemical studies on thiosemicarbazone ligands have also shown the existence of an irreversible cathodic peak at -1.06 V.[177-179] Similar irreversible cathodic peaks (assigned to the reduction of the thione group) were also observed at -0.93 V, -1.08 V and -1.07 V, for MeATSC, *N*-Ethhymethohcarbthio, and acetylethTSC, respectively.

According to Refaey *et al.*,[174] thiosemicarbazones are capable of participating in a series of electrochemical oxidation reactions which eventually leads to the generation of radical cations.[174] Electrochemical oxidative reactions (Scheme 8) were also evident in

our case as illustrated by the presence of at least one irreversible anodic redox peak in the cyclic voltammogram of each thiosemicarbazone ligand. The irreversible anodic redox peaks corresponding to the generation of radical cations were observed at -0.17 V for MeATSC, at -0.17 V and at -1.11 V for *N*-Ethhymethohcarbthio, and at -0.17 V and -1.04 V for acetylethTSC. The previously formed radical cations later react with residual water present in the medium to form adducts, which undergoes the abstraction of a second proton to form thiadiazoles.[174] The appearance of additional irreversible cathodic redox peaks are reported to be attributed to subsequent reduction of the previously formed radical cations.[174] Irreversible cathodic redox peaks, observed at -0.14 V, -0.36 V and –0.25 V, were therefore assigned to the reduction of cation radicals for MeATSC, *N*-Ethhymethohcarbthio, and acetylethTSC, respectively.

According to Li *et al.*,[180] oxidation of vanilllin is also known to proceed through the production of relatively stable carbocation species. The oxidation of vanillin was shown to produce a quasi-reversible redox wave with the oxidative and reductive peak occurring at +0.19 V and +0.14 V, respectively. We are also proposing a similar oxidative reaction for our *N*-Ethhymethohcarbthio thiosemicarbazone ligand. In our case, however, an irreversible anodic redox peak corresponding to the oxidation of the vanillin moiety of the *N*-Ethhymethohcarbthio ligand was observed at +0.37 V. All other ligand based peaks that were not mentioned in this discussion is assumed to be due to the formation of cation radical species.

The cyclic voltammogram of anthracene is known to exhibit a reversible redox wave in the region +0.84 V to +0.90 V.[181,182] An irreversible anodic redox peak at +0.75 V was observed in the cyclic voltammogram of MeATSC. This irreversible anodic

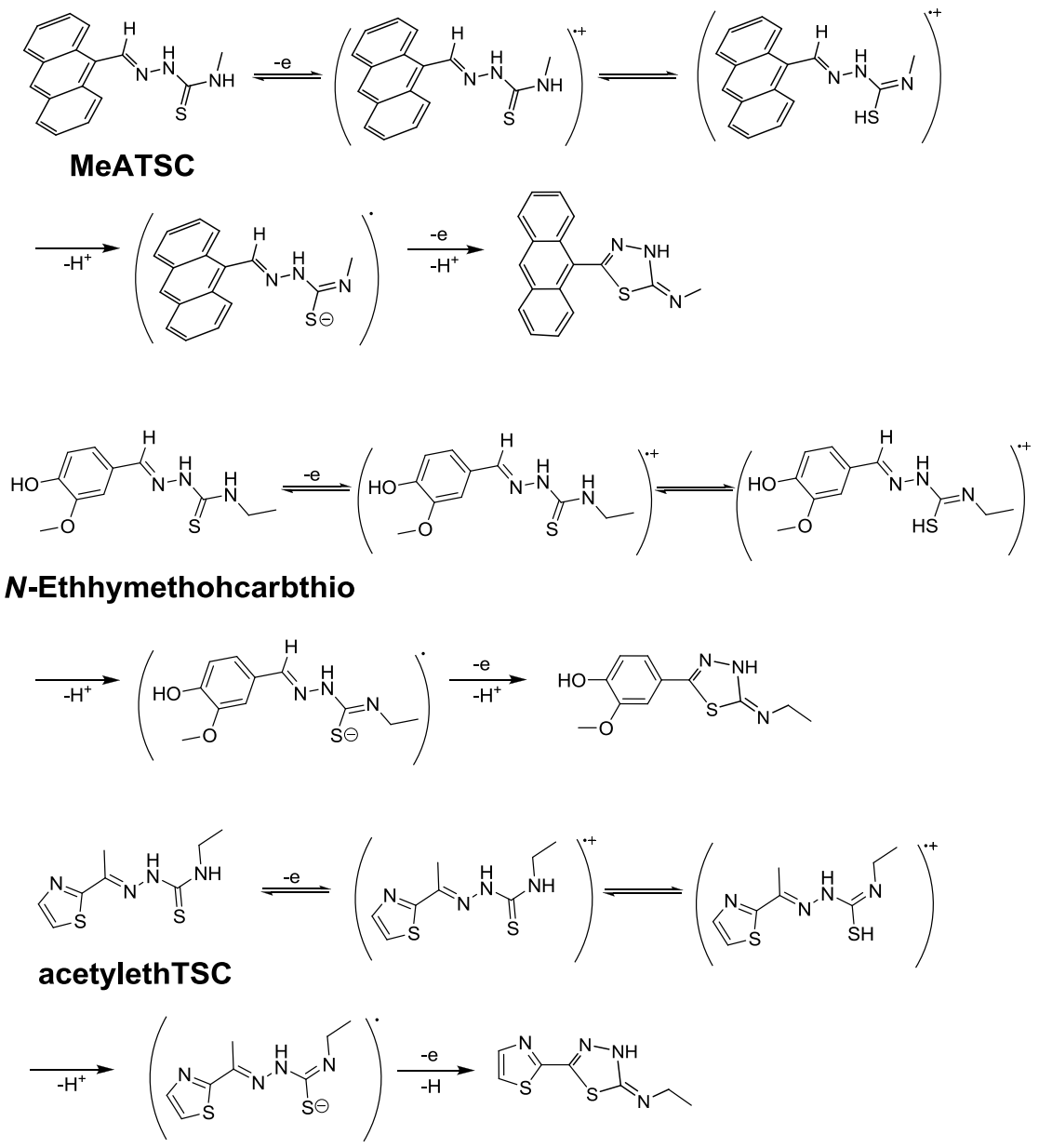

Scheme 8. Proposed electrochemical oxidation of the thione group.[174]

redox peak was assigned to the oxidation of the anthracene moiety present in the MeATSC ligand. This assignment was also confirmed by the appearance of an anodic redox peak at +0.82 V in the square wave voltammogram of the MeATSC ligand.

Synthesis and Characterization of the Complexes

Elemental and Mass Spectroscopic Analyses

Elemental analyses were carried out on compounds **1-4**. Table 6 shows the respective percentage values found for C, H, and N as an assessment of the purity for the respective compounds. The percentage of N found in compound **4** was 10.91% versus the calculated value of 13.21%. This discrepancy is suggested to be due to experimental errors and loss of ethanol as solvate during the elemental analysis. ESI MS analysis of compound **4**, as discussed below proves the existence of the species,

Table 6

*Elemental analysis data for compounds **1-4**.*

Compound		Calculated	Found
1	C	55.25	55.16
	H	4.12	4.31
	N	7.16	6.87
2	C	62.03	62.62
	H	5.21	5.25
	N	9.52	9.33
3	C	53..33	53.18
	H	4.64	5.21
	N	11.11	11.09
4	C	51.92	52.49
	H	4.83	4.72
	N	13.21	10.91

[VO(Sal-*L*-tryp)(acetylethTSC)] and [VO(Sal-*L*-tryp)(acetylethTSC)]0.75C_2H_5OH. ESI MS spectral data were acquired for compounds **2-4**, [Zn(Sal-*L*-tryp)(H_2O)].0.25H_2O and the products obtained from oxidised DMSO solutions of

compounds **1** and **3** (see Appendix, Figures A15-A22). Table 7 shows the ESI MS data acquired for the respective complexes while Schemes 9-11 shows the proposed species formed during ESI MS acquisition compounds **2-4**.

Compounds 2-4 and [Zn(Sal-L-tryp)(H_2O)].0.25H_2O. The ESI MS spectra of compounds **2-4** were acquired in methanol. Each spectra exhibited base peaks corresponding to the respective molecular ions. These peaks were observed at *m/z* = 666.17, *m/z* = 624.87, and *m/z* = 513.57 for compounds **2**, **3**, and **4**, respectively. Base peaks obtained for compounds **2** and **4** were observed in the positive ion mode of the mass spectrometer. The base peak for compound **3**, however, was observed in the negative ion mode of the mass spectrometer due to the deprotonation of the phenol moiety of the *N*-Ethhymethohcarbthio ligand. All other fragments observed for compound **2-4** are assigned as shown in Table 7.

The ESI MS spectrum of [Zn(Sal-*L*-tryp)(H_2O)].0.25H_2O was acquired in the positive mode of the spectrometer and methanol was used as the solvent. The peak at *m/z* = 395.11 was assigned to the $[M + H]^+$ ion. X-ray crystallographic studies of similar [*N*-salicylidene-*L*-aminoacidato)Zn(II)] complexes have proven that these complexes are capable of forming binary and polymeric species.[143] The base peak, attributed to the formation of a trinuclear species, was therefore observed at *m/z* = 1152.92 in the ESI MS spectrum of [Zn(Sal-*L*-tryp)(H_2O)].0.25H_2O. All other peaks (corresponding to the formation of various polymeric species) were assigned as shown in Table 7.

Table 7

Mass spectroscopic data of compounds.

(A) Compounds **1**-**4**, and [Zn(Sal-*L*-tryp)(H_2O)].0.25H_2O.

Species	Exact Mass/$gmol^{-1}$	Species	m/z	Relative Intensity
[VO(Sal-*L*-tryp)(MeATSC)] #	666.14	$[M + H]^+$ $[M - C_2H_5N_2S + H]^+$ $[M - C_{17}H_{17}N_3 + H]^+$ $[MeATSC+ H]^+$	666.17 577.08 405.14 292.14	100.00 33.10 31.86 54.60
[VO(Sal-*L*-tryp)(*N*-Ethhymethohcarbthio)] †	626.13	$[M - H]^-$ $[M - C_{11}H_{10}N_2O - H]^-$ $[M - C_{11}H_{15}N_3O_2S - H]^-$ $[[C_{11}H_{15}N_3O_2S – C_8H_7N] - H]^-$ [*N*-Ethhymethohcarbthio- $H]^-$	624.87 431.90 407.85 287.88 252.00	100.00 64.75 20.99 12.70 25.74
[VO(Sal-*L*-tryp)(acetylethTSC)] #	601.09	$[M + H]^+$ $[M - C_3H_7NS + H]^+$ $[M - C_7H_5NO + H]^+$ $[M - C_{17}H_{15}N_2O + H]^+$	600.25 513.57 482.38 336.06	2.71 100.00 37.11 4.13
[VO(Sal-*L*-tryp)(acetylethTSC)].0.75 C_2H_5OH#	635.62	[[VO(Sal-*L*-tryp)(acetylethTSC)].0.75 C_2H_5OH + $H]^+$	636. 82	2.75
[Zn(Sal-*L*-tryp)(H_2O)].0.25 H_2O #	392.54	$[M+ H]^+$	395.11	13.93

- positive mode

† -negative mode

Table 7 (continued).

(B) Oxidized products isolated from compounds **1** and **3**.

Species	Exact Mass/gmol^{-1}	Species	m/z	Relative Intensity
[VO(Sal-*L*-tryp)(DMSO)(OH)] [a, #]	468.06	$[M + H]^+$	468.60	1.67
		$[M - OH - DMSO - C_8H_7N + H]^+$	242.41	100.00
		$[M - OH + H]^+$	451.05	48.25
		$[[V_2O_3(Sal\text{-}L\text{-}tryp)_2] + H]^+$	763.68	30.06
		$[[V_2O_3(Sal\text{-}L\text{-}tryp)_2(H_2O)] + H]^+$	776.77	49.36
		$[[V_2O_3(Sal\text{-}L\text{-}tryp)_2(DMSO)_2] + H]^+$	918.28	3.13
[VO(Sal-*L*-tryp)(DMSO)(OH)] [b, #]	468.06	$[M + H]^+$	470.01	0.50
		$[N$-Ethhymethohcarbthio $+ H]^+$	252.26	100.00
		$[M - OH + H]^+$	451.96	2.97
		$[M - OH + N$-Ethhymethohcarbthio $+ H]^+$	702.75	2.15
		$[[V_2O_3(Sal\text{-}L\text{-}tryp)_2 + H]^+$	763.22	0.74
		$[[V_2O_3(Sal\text{-}L\text{-}tryp)_2(H_2O)] + H]^+$	775.40	1.08
		$[[V_2O_3(Sal\text{-}L\text{-}tryp)_2(DMSO)_2] + H]^+$	916.44	0.75

a - product obtained from compound **1**

b - product obtained from compound **3**

- positive mode

Scheme 9. Proposed species found during ESI MS acquisition of compound **2**.

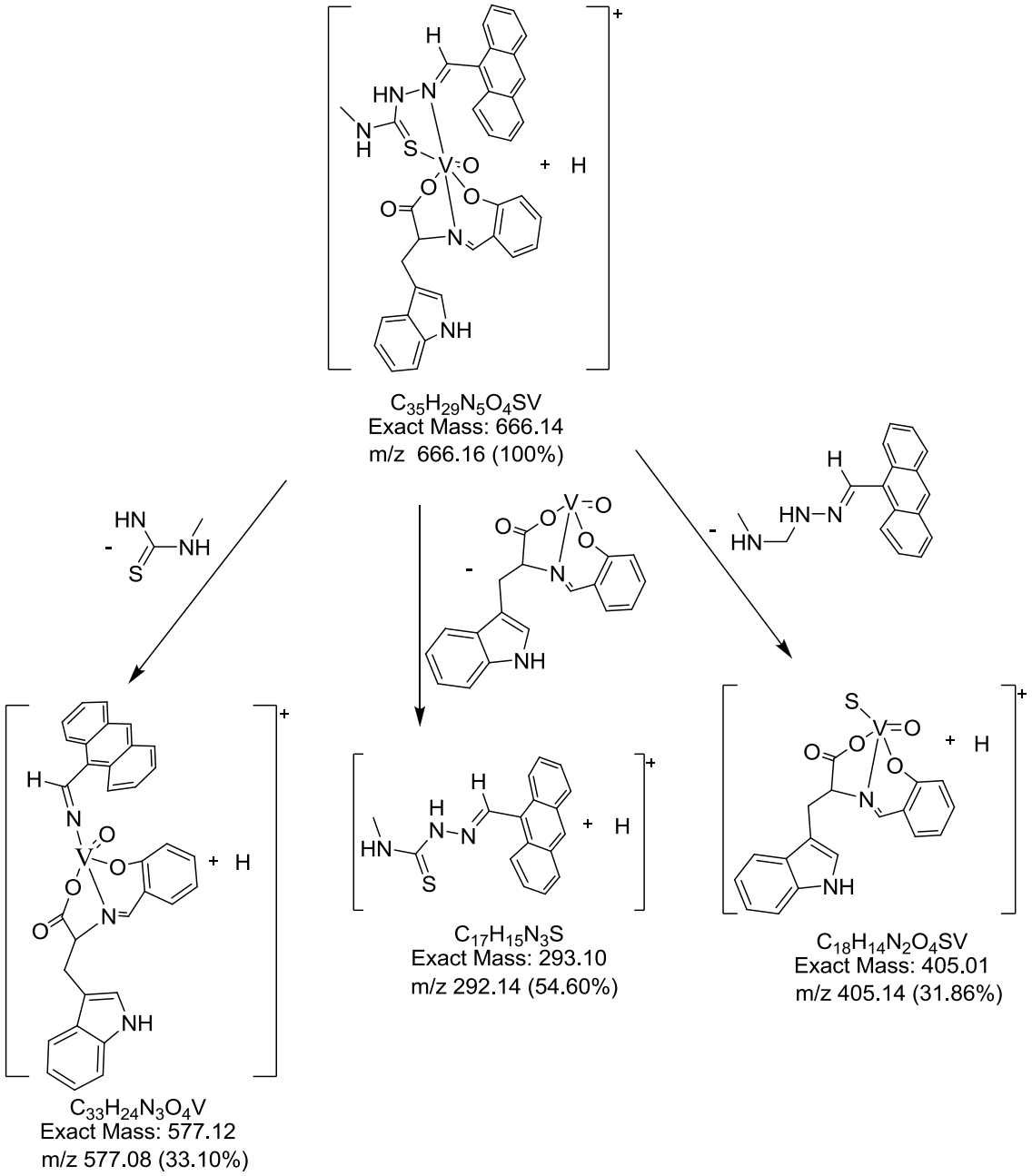

Scheme 10. Proposed species found during ESI MS acquisition of compound **3**.

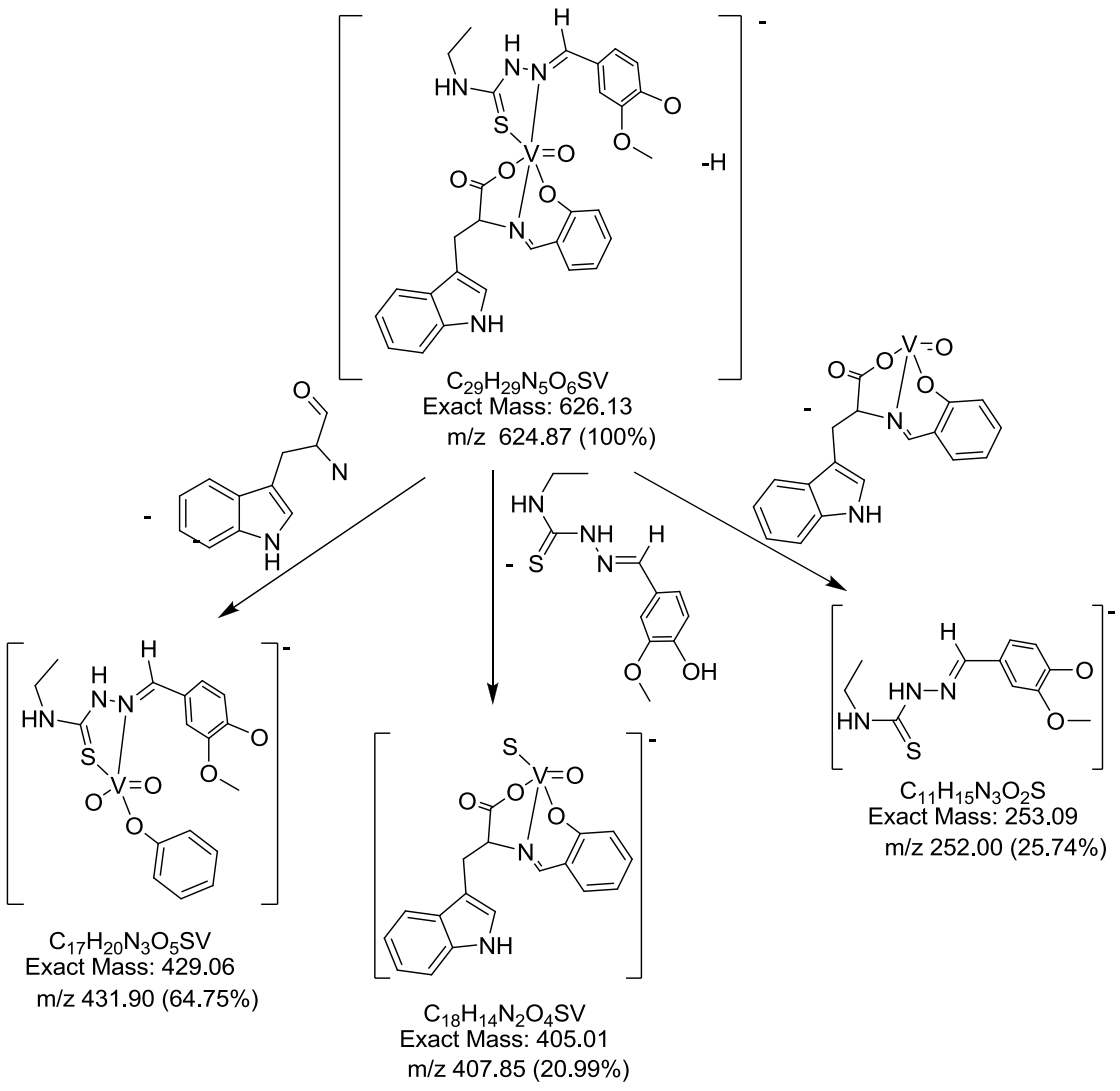

Scheme 11. Proposed species found during ESI MS acquisition of compound **4**.

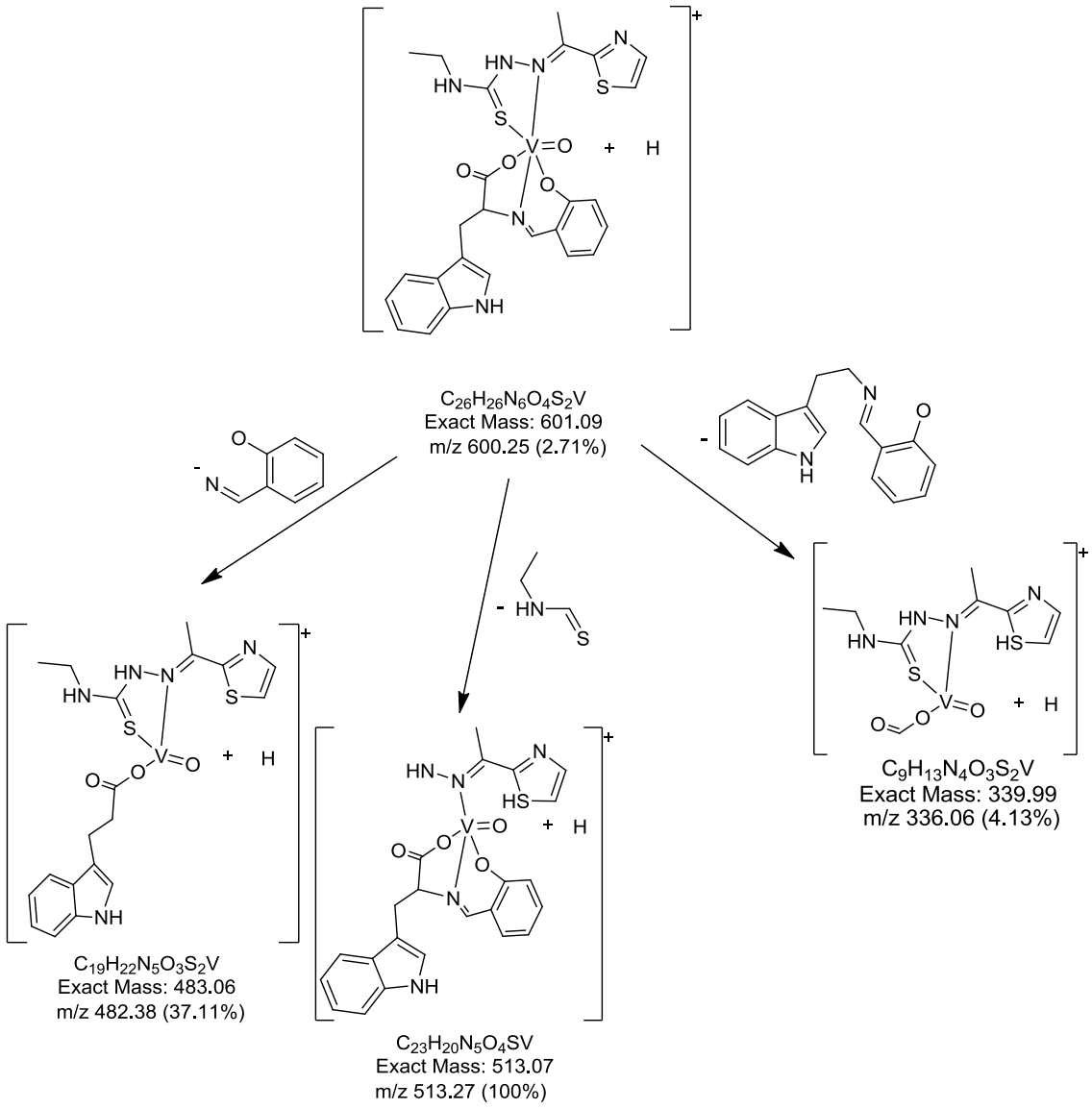

*Oxidized products isolated from Compounds **1** and **3***. Oxovanadium(IV) complexes containing *N*-salicylidene-*L*-aminoacidatos ligands are readily oxidized to form vanadium(V) compounds.[60] Our data suggested that compounds **1**-**4** were readily oxidized to form vanadium(V) upon aerial oxidation in DMSO. In this study, however, we will focus on compounds **1** and **3**. ESI MS spectra of the products obtained from the oxidized solutions of compounds **1** and **3** were acquired in both the positive and negative ion mode of the spectrometer (see Appendix, Figures A19 to A22). Assignments of spectral peaks (as shown in Table 7) were done using the spectra obtained in the positive ion mode of the sprectrometer.

As reported by Cavaco *et al.*,[60] coordinated water molecules present in oxovanadium(IV) complexes, such as [VO(Sal-*L*-ala)(H_2O)], are readily substituted by solvent molecules such as methanol. Upon substitution of solvent molecules, the vanadium(V) species formed readily dimerizes to form binuclear species.[60] It is suggested that our compounds behaved similarly when oxidized. A proposed scheme showing the aerial oxidation of compounds **1** and **3** in DMSO are shown in Scheme 12.

The ESI MS spectra of the products (obtained from oxidized solutions of compounds **1** and **3**) both exhibited spectral peaks attributed to the [VO(Sal-*L*-tryp)(DMSO)(OH) + H]+ ion, when analyzed in the positive mode of the spectrometer. Spectral peaks observed at m/z = 468.60 and m/z = 470.01 were assigned to the [VO(Sal-L-tryp)(DMSO)(OH) + H]+ ion for products obtained from oxidized solutions of compounds 1 and compound 3, respectively (see Table 7). The ESI MS spectra acquired for the oxidized products isolated from compounds 1 and 3 also exhibited peaks

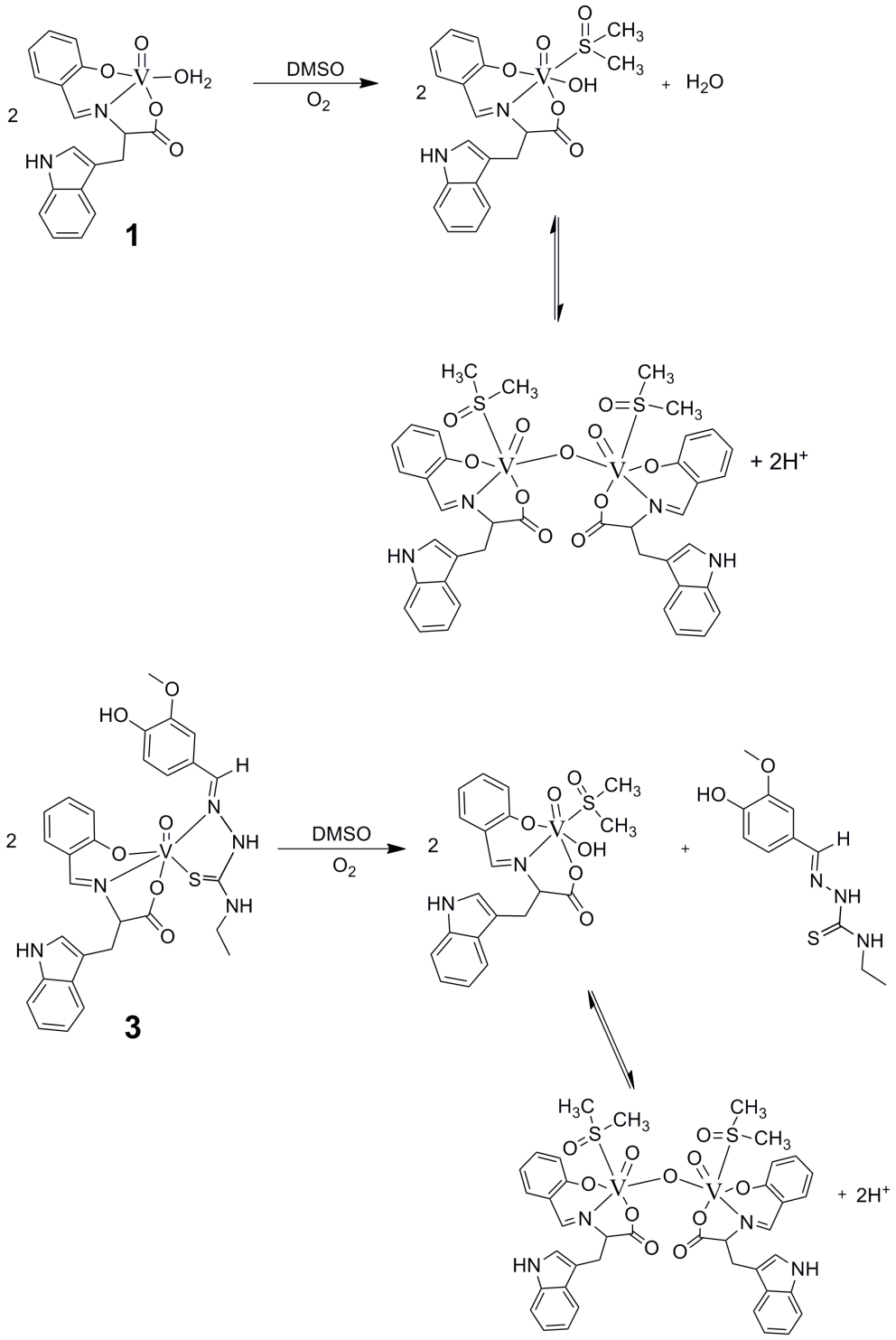

Scheme 12. Proposed mechanism for the formation of the oxidized compounds in DMSO.

attributed to the presence of the vanadium(IV) species, [VO(Sal-*L*-tryp)(OH)]$^-$, at *m/z* = 388.94 and *m/z* = 386.78, respectively. The spectrum acquired for the oxidised product obtained from compound **3** in DMSO also exhibited a base peak at *m/z* = 252.26, which was attributed to the "free" *N*-Ethhymethohcarbthio ion. This presence of this species also confirms the formation of [VO(Sal-*L*-tryp)(DMSO)(OH)] in the proposed mechanism for the formation of the oxidized compounds in DMSO (Scheme 12).

As mentioned earlier, oxovanadium(IV) complexes are known to form vanadium(V) binuclear complexes upon oxidation.[60] The ESI MS spectra acquired for both products obtained from oxidized solutions of compounds **1** and **3**, both exhibited several peaks corresponding to the formation of mixed binuclear species in the positive ion mode of the spectrometer. Peaks assigned to the formation of the binuclear $[V_2O_3(Sal\text{-}L\text{-}tryp)_2(DMSO)_2]$ species were observed at *m/z* = 918.28 and *m/z* = 916.44, for the oxidized products obtained from compound **1** and compound **3**, respectively. The ESI MS spectrum of the product obtained from the oxidized solution of compound **3** also exhibited a peak at *m/z* = 702.75. This peak is proposed to be due to the ion formed when the "free" *N*-Ethhymethohcarbthio ligand coordinates to the [VO(Sal-*L*-tryp)(DMSO)(OH)] species via the phenolate moiety of the "free" *N*-Ethhymethohcarbthio ligand (see Scheme 12).

FT IR Spectroscopy

*Compounds **1**-**4** and [Zn(Sal-L-tryp)(H_2O)].0.25H_2O*. FT IR spectra were acquired for compounds **1**-**4** and [Zn(Sal-*L*-tryp)(H_2O)].0.25H_2O (see Appendix, Figures A23-A27) and significant FT IR spectral bands are shown in Table 8 (A). A general decrease is observed in the ν(N-H) stretching frequency of the -N^1H_2 group

upon coordination of thiosemicarbazone ligands. Coordination of the respective "free" thiosemicarbazone ligands to the vanadium(IV) metal center results in a shift in the the ν(N-H) stretching frequencies from 3399 cm^{-1} to 3308 cm^{-1} for compound **2**, 3340 cm^{-1} to 3306 cm^{-1} for compound **3**, and 3358 cm^{-1} to 3310 cm^{-1} for compound **4**. A decrease was also observed in the ν(N-H) stretching frequencies of the -N^2H group from 3201 cm^{-1} to 2976 cm^{-1} for compound **2**, 3300 cm^{-1} to 2970 cm^{-1} for compound **3**, and 3169 cm^{-1} to 2976 cm^{-1} for compound **4**.

The FT IR spectra of compounds **1-4** and [Zn(Sal-*L*-tryp)(H_2O)].0.25H_2O all exhibited indolic ν(N-H) stretching frequencies at 3350 cm^{-1}, 3200 cm^{-1}, 3210 cm^{-1}, 3229 cm^{-1} and 3229 cm^{-1}, respectively. A comparison between the indolic ν(N-H) stretching frequency observed in the FT IR spectra of compound **1** and [Zn(Sal-*L*-tryp)(H_2O)].0.25H_2O with that of compound **2-4**, illustrated a negative shift upon coordination of the "free" thiosemicarbazone ligand to the metal center.

The FT IR spectra of all complexes exhibited a ν(V-S) stretching frequencies at 455 cm^{-1}, 454 cm^{-1}, and 455 cm^{-1} for compounds **2**, **3**, and **4**, respectively. The presence of ν(V-S) stretching frequencies in the FT IR spectra of compounds **2-4** confirmed that the respective ligands were coordinated to the vanadium metal center via the thiocarbonyl sulphur atom.[58] Similar peaks were absent in the FT IR spectra of the "free" thiosemicarbazone ligands.

Spectral bands observed in the region 1626 to 1615 cm^{-1} were assigned earlier to the ν(C=N) stretching frequency of the thiosemicarbazone ligand.[148,152,153,156] Upon coordination, however, a significant decrease was observed in the ν(C=N) stretching

Table 8

FT IR data for the complexes.

(A) Compounds 1-4 and Zn(Sal-*L*-tryp)(H_2O)].0.25H_2O

Compound	Indolic ν(NH) /cm^{-1}	–N^1H_2 ν(NH) /cm^{-1}	N^2H ν(NH) /cm^{-1}	ν(N-N) /cm^{-1}	ν(C-O) /cm^{-1}	ν_s(COO) /cm^{-1}	ν_{as} (COO) /cm^{-1}	TSC ν(C=N) /cm^{-1}	Sal-*L*-tryp ν(C=N) /cm^{-1}	ν(C=S) /cm^{-1}	ν(V-S) /cm^{-1}	ν(V=O) /cm^{-1}	ν(OH) /cm^{-1}
1	3478 (m)	-	-	-	1540 (m)	1490 (m)	1597 (s)	-	1600 (m)	-	-	997 (s)	3014 (br)
2	3200 (m)	3340 (m),	2976 (w)	1148 (m)	1544 (m)	1491 (m)	1600 (s)	1624 (m)	1590 (m)	1225 (m), 829 (m)	455 (m)	980 (s)	-
3	3210 (m)	3306 (m)	2970 (w)	1154 (m)	1540 (m)	1480 (m)	1600 (s)	1620 (m)	1580 (m)	1270 (m), 802 (m)	454 (m)	976 (s)	3010 (br)
4	3229 (m)	3310 (m)	2976 (w)	1149 (m)	1545 (m)	1480 (m)	1600 (s)	1624 (m)	1580 (m)	1287 (m), 819 (m)	455 (m)	982 (s)	-
Zn(Sal-*L*-tryp)(H_2O)]. 0.25H_2O	3405 (m)	-	-	-	1551 (m)	1473 (m)	1597 (s)	-	1581 (m)	-	-	-	3256 (br)

(B) Oxidized products isolated from compounds 1 and 3

Compound	Indolic ν(NH) /cm^{-1}	ν(C-O) /cm^{-1}	ν_s(COO) /cm^{-1}	ν_{as}(COO) /cm^{-1}	TSC ν(C=N) /cm^{-1}	Sal-*L*-tryp ν(C=N) /cm^{-1}	ν(V=O) /cm^{-1}	ν(OH) /cm^{-1}	ν(S=O) /cm^{-1}
[a] [VO(Sal-*L*-tryp)(DMSO)(OH)]	3185 (m)	1551 (m)	1497 (m)	1618 (s)	-	1581 (m)	949 (s)	3194 (br)	1164 (m), 1213 (m)
[b] [VO(Sal-*L*-tryp)(DMSO)(OH)]	3201 (m)	1550 (m)	1497 (m)	1600 (s)	1666 (m)	1590 (m)	946 (s)	3193 (br)	1133 (m), 1157 (m)

a – oxidized product obtained from compound **1**

b – oxidized product obtained from compound **3**

frequencies for acetylethTSC (1543 to 1624 cm^{-1} in compound **4**) and *N*-Ethylmethocarbthio (1606 to 1620 cm^{-1} in compound **3**). A significant shift in the ν(C=N) stretching frequency was not evident in the FT IR spectrum of compound **2**. A decrease in the ν(C=N) stretching frequency upon coordination of respective ligands suggested tha the nitrogen atom (belonging to the -C=N moiety) was involved in the ligation process.[128,147,150,152,183-186]

A ν(C=N) stretching frequency attributed to azomethine moiety present in the Sal-*L*-tryp entity of compounds **1-4** were also observed in the respective FT IR spectra. A comparison of the respective ν(C=N) stretching frequencies observed in the FT IR spectra of K[(Sal-*L*-tryp)] with that of compounds **1-4** and [Zn(Sal-*L*-tryp)(H_2O)].0.25H_2O, suggested that this moiety is also in the vicinity of the vanadium(IV) metal center. Upon coordination of the respective "free" thiosemicarbazone ligands, a shift was observed in the ν(C=N) stretching frequencies (of the Sal-*L*-tryp moiety) from 1570 cm^{-1} for K[(Sal-*L*-tryp)] to 1580 cm^{-1} for compounds **3** and **4**, 1600 cm^{-1} for compound **1**, 1590 cm^{-1} for compound **2**, and 1581cm^{-1} for [Zn(Sal-*L*-tryp)(H_2O)].0.25H_2O.

Similarly, the involvement of the thiocarbonyl moiety of the thiosemicarbazone ligands in the ligation process was also inferred based on the decrease in the ν(C=S) stretching frequencies upon coordination.[128,183,184] Medium intensity spectral bands in the region 841-816 cm^{-1} were earlier assigned to ν(C=S) stretching frequency.[152,157,158] Upon coordination, a decrease in the order of 12-29 cm^{-1} was observed in the ν(C=S) stretching frequencies of each complex. The magnitude of the shift in the ν(C=S) stretching frequencies confirmed that the

thiosemicarbazone ligands are also coordinated of to the metal center via the neutral thioamide sulphur.[128,147,183] Based on the results presented above, it is evident that the neutral, bidentate thiosemicarbazone ligands are coordinated to the vanadium(IV) metal center via the nitrogen atom of the -C=N group and the sulphur tom of the thiocarbonyl group.[128,183]

Broad spectral peaks attributed to ν(OH) stretching frequencies were observed at 3014 cm^{-1}, 3010 cm^{-1}, and 3256 cm^{-1} for compounds **1** and **3** and [Zn(Sal-*L*-tryp)(H_2O)].0.25H_2O, respectively. The absence of a similar ν(OH) stretching frequencies in the FT IR spectra acquired for compounds **2** and **4** confirmed that the Sal-*L*-tryp moiety was coordinated to the vanadium(IV) metal center via the phenolate anion of the respective group.[148,154]

All complexes exhibited spectral peaks in the region 997-980 cm^{-1} attributed to the ν(V=O) stretching frequencies for typical oxovanadium(IV) complexes.[156,184,187] The ν(V=O) stretching frequencies were observed at 997 cm^{-1}, 980 cm^{-1}, 976 cm^{-1}, and 982 cm^{-1}, for compounds **1**, **2**, **3**, and **4**, respectively. Subsequent to the coordination of the respective thiosemicarbazone ligands to compound **1**, a significant decrease in the ν(V=O) stretching frequency occurred, viz., 17 cm^{-1} in compound **2**, 21 cm^{-1} in compound **3**, and 15 cm^{-1} in compound **4**.

Oxidized products isolated from Compounds **1** and **3**.

FT IR spectroscopic data acquired for the oxidized products are shown in Table 9 B. Sulphur-containing ligands, such as DMSO, exhibit two potential donor sites and are therefore capable of coordinating to metal centers via the oxygen or sulphur atom present in the ligand.[188] Oxygen coordination is favored by smaller,

highly charged metal ions whereas heavier metals are known to coordinate via the sulphur atom.[188-190] According to Cotton *et al.*,[189] $[M(DMSO)_2Cl_2]$ (M = Pt and Pd) complexes are known to exhibit two strong spectral signals in the regions (1163 to 1116 cm^{-1}) and (1143 to 1117 cm^{-1}), attributed to the coordination of the DMSO ligand via the sulphur atom.[188] The FT IR spectra acquired for the oxidized products obtained from compounds **1** and **3**, both exhibited ν(S=O) stretching frequencies assigned to S-bonded DMSO ligand at 1164 and 1213 cm^{-1}, and 1133 and 1157 cm^{-1}, respectively.

Subsequent to aerial oxidation of compounds **1** and **3**, a decrease was observed in the indolic ν(N-H) stretching frequency from 3407 cm^{-1} for K[(Sal-*L*-tryp)] to 3185 cm^{-1} and 3201 cm^{-1} for the oxidized products obtained from compound **1** and **3**, respectively.

A similar spectral signal attributed to the ν(C=N) stretching frequency of the "free" *N*-Ethylmethocarbthio ligand was also observed in the FT IR spectrum acquired oxidized product obtained from compound **3**. This spectral signal, observed at 1666 cm^{-1}, was assigned to the ν(C=N) stretching frequency of the displaced "free" *N*-Ethhymethohcarbthio ligand, upon aerial oxidation of compound **3**. FT IR spectroscopic data therefore confirms that the oxidized product consisted of a mixture of the "free" displaced thiosemicarbazone ligand, as well as [VO(Sal-*L*-tryp)(DMSO)(OH)].

Spectral signals corresponding to ν(C=N) stretching frequencies of the Sal-*L*-tryp moiety were also observed at 1581 cm^{-1} and 1590 cm^{-1} for the products obtained from oxidized solutions of compounds **1** and **3**, respectively. The FT IR spectra of

both oxidzed products also demonstarted an increase in the ν(V=O) stretching frequency upon aerial oxidation. Comparison of the respective spectra illustrated a shift in the ν(V=O) from 997 cm^{-1} to 949 cm^{-1} for the product obtained from oxidized compound **1**, and from 976 cm^{-1} to 946 cm^{-1} for the product obtained from oxidized compound **3**. A broad spectral line attributed to the ν(OH) stretching frequency was also observed at 3194 cm^{-1} and 3193 cm^{-1} for the products obtained from oxidized solutions of compounds **1** and compound **3**, respectively.

NMR Spectral Studies

NMR spectra were acquired for the oxidized products derived from compounds **1** and **3** (see Appendix, Figures A29 and A30) using DMSO-d_6 as the solvent. Figure 36 shows the lettering system used for the assignments of protons for the oxidized complexes (see the experimental section for the lettering in the NMR data).

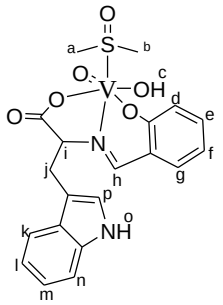

[VO(Sal-*L*-tryp)(DMSO)(OH)]

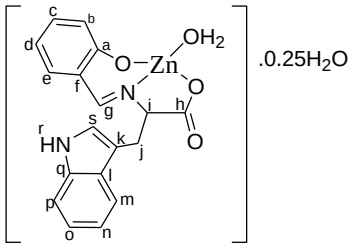

[Zn(Sal-*L*-tryp)(H_2O)].0.25H_2O

Figure 36. Assignments used for NMR data of complexes in the experimental section.

Both ^1H NMR spectra acquired for the oxidized products (isolated from compounds **1** and **3**) exhibited broad signals (see Appendix, Figures A24 and A25). These broad signal were suggested to be due to the formation of a paramagnetic vanadium(IV) species, [VO(Sal-*L*-tryp)(OH)]$^-$, which was identified by ESI MS as discussed above.

The resonance signals most useful for determining the binding mode of DMSO was reported to occur at δ = 2.7 ppm for O-bonded DMSO and at δ = 3.0 - 3.6 ppm for S-bonded DMSO.[147] The absence of a resonance signal at δ = 2.7 ppm suggested that the DMSO ligand was coordinated via the of sulfur atom and therefore confirms previous assignments made in the FT IR spectroscopic analysis.[147] The NMR spectra of the oxidized products both exhibited a singlet in the region δ = 3.0 to 3.6 ppm: δ = 3.36 ppm for the oxidized product isolated from compound **1** and at δ = 3.34 for the product isolated from compound **3**.

The ^{1}H NMR spectrum acquired for the oxidized product isolated from precursor **3** exhibited resonance signals at δ = 1.17 ppm and δ = 3.79 ppm, assigned to the methyl and methylene protons of the "free" *N*-Ethhymethohcarbthio ligand, respectively. Multiplets were also observed in the range δ = 6.87 - 7.43 ppm in the spectrum acquired for the oxidized product isolated from precursor **3**. These resonance signals were attributed to the aromatic protons present in the "free" *N*-Ethhymethohcarbthio ligand and the oxidized complex.

The ^{1}H NMR spectrum acquired for the oxidized product isolated from compound **1** exhibited resonance signals in the region δ = 7.06 to 7.52 ppm, which were assigned to aromatic protons of the oxidized product. Resonance signals attributed azomethine proton of the indole ring present in the *L*-tryptophan moiety were also observed at in the region δ = 7.82 to 8.09 ppm, and δ = 7.06 to 10.43 ppm, for the oxidized products isolated from compound **1** and compound **3**, respectively. In the ^{1}H NMR spectrum acquired for the oxidized product isolated from compound **3**, the previously mentioned resonance signal

was suggested to be overlapped with the signal attributed to the N(2)-H proton of the "free" *N*-Ethhymethohcarbthio ligand.

*UV-Visible and Fluorescence Spectroscopic Studies of Compound **1-4***

UV-visible spectral data were acquired for compounds **1**-**4** using DMSO as solvent. The respective UV-visible spectra acquired for compounds **1**-**4** are shown in figures 36-39 (See Appendix, Figures A31-A33), and the assignments are shown in Table 9. The UV-Visible spectra acquired for compounds **2-4** all exhibited charge transfer bands in the region 266-292 nm, assigned to π→π* transitions associated with the thioamide moiety. [152,154] These spectral bands were observed at 266 nm and 292 nm (shoulder) for compound **2**, at 270 nm and 288 nm (both as shoulders) for compound **3**, and at 276 nm for compound **4**. Previous spectroscopic studies has proven that charge transfer bands attributed to n→π* transitions of aromatic rings usually exist in the region 316-352 nm.[152,154,184,191,192] Similar spectral bands were also observed in the UV-Vis spectra of compounds **2-4**. The respective bands were observed as a shoulder at 316 nm for compound **2**, at 330 nm for compound **3**, and 352 nm for compound **4**.

According to Cavaco *et al*.,[60] oxovanadium(IV) complexes derived from salicylaldehyde ligands are known to exhibit a low-energy spectral band around 375 nm, attributed to π→π* transitions associated with the azomethine chromophore.[60] Similar spectral bands were also observed at 388 nm for compound **2**, as a shoulder at 390 nm for compound **3** and hidden beneath the n→π* transition for compound **4**. The UV-Visible spectra acquired for compounds **1-4** all exhibited spectral bands in the region 550-558 nm, attributed to p→d LMCT transitions (where p represents the lone

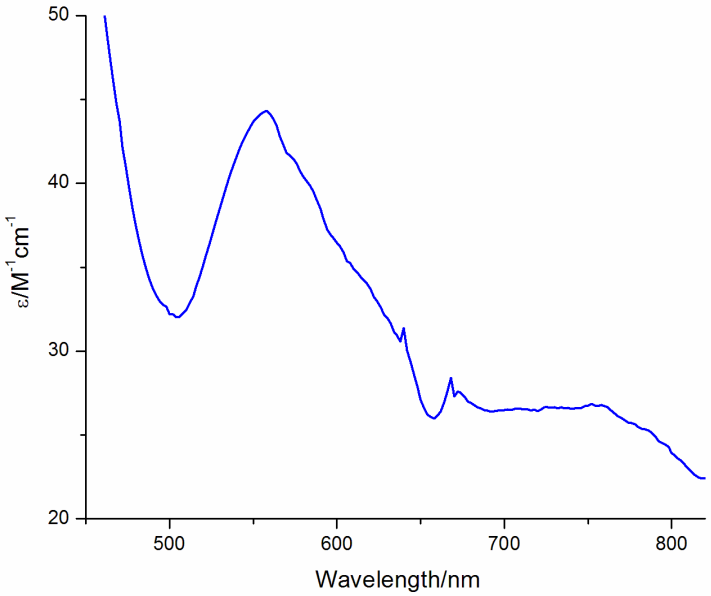

Figure 37. A UV-visible spectrum of compound **1** in DMSO.

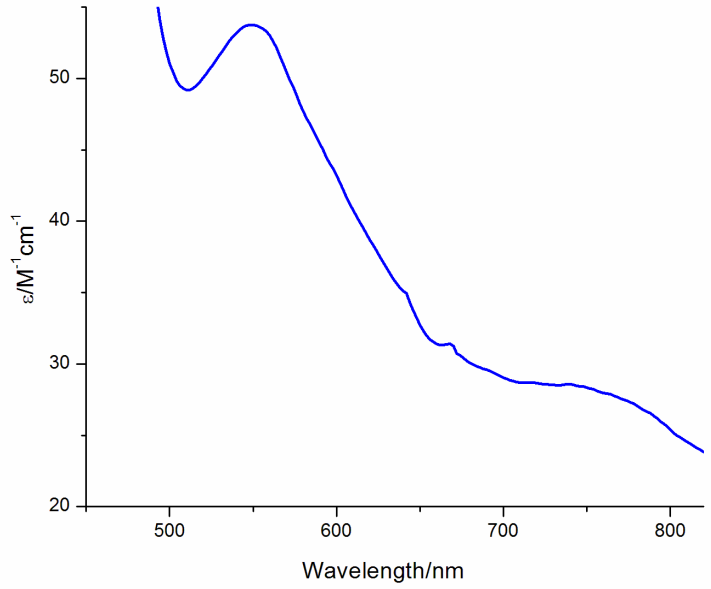

Figure 38. A UV-visible spectrum of compound **2** in DMSO.

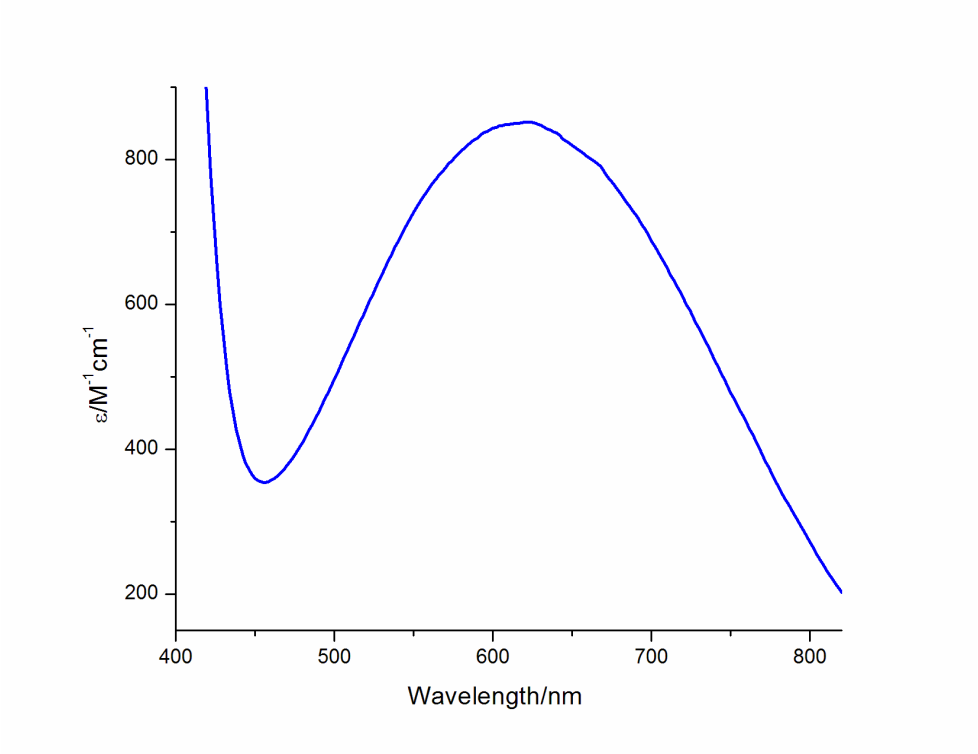

Figure 39. A UV-visible spectrum of compound **3** in DMSO.

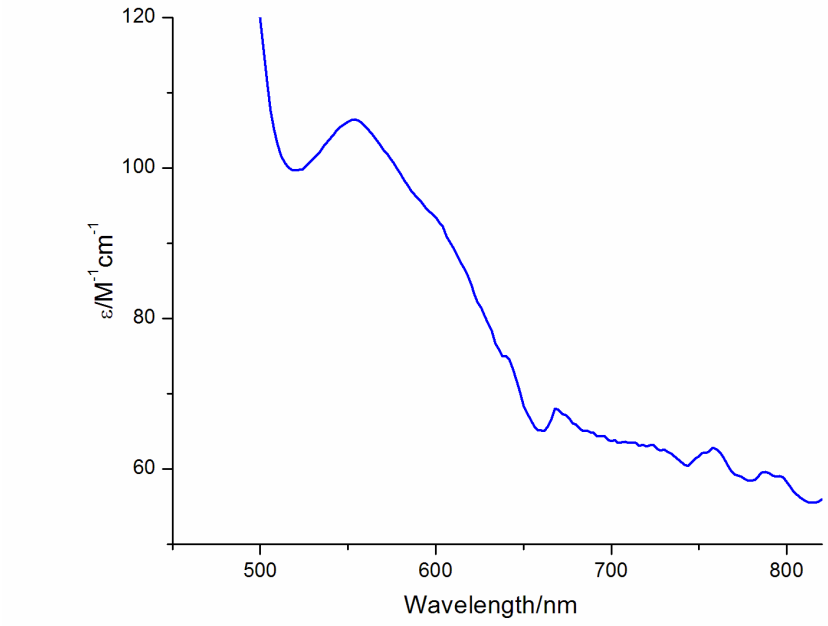

Figure 40. A UV-visible spectrum of compound **4** in DMSO.

Table 9

*UV-visible spectral data for compounds **1-4**.*

Complex	λ/nm	ε/$M^{-1}cm^{-1}$	Assignments
1	558	44	LMCT ($p \rightarrow d$ transition)
	758	27	d → d transition
2	266	74835	π → π* (thioamide moiety)
	292 (sh)	17954	π → π* (thioamide moiety)
	316 (sh)	10046	n → π* (aromatic rings)
	388	15013	π → π* (azomethine chromophore)
	550	54	LMCT ($p \rightarrow d$ transition)
	592 (sh)	45	d → d transition
	756	28	d → d transition
3	270 (sh)	10984	π → π* (thioamide moiety)
	288 (sh)	13874	π → π* (thioamide moiety)
	330	24837	n → π* (aromatic rings)
	390 (sh)	18250	π → π* (azomethine chromophore)
	620	852	d → d transition
4	276	21969	π → π* (thioamide moiety)
	352	14227	n → π* (aromatic rings)
	558	80	LMCT ($p \rightarrow d$ transition)
	590 (sh)	70	d → d transition
	756	38	d → d transition

pair of electrons on the phenolato oxygen, and d represents the 3d orbitals of the vanadium metal center).[193,194] Similar spectral bands were observed at 558 nm for compound 1, 550 nm for compound **2**, and 558 nm for compound **4**. A similar spectral band was absent in the UV-Visible spectrum acquired for compound **3** since it is believed to be hidden under the spectral band assigned to d→d transitions.

According to Pessoa *et al*., the UV-Visible spectral bands observed in the region 756-758 nm are attributed to d-d transitions of the metal center.[187] In our case, similar spectral bands were observed at 758 nm for compound **1** and at 756 nm for compounds **2** and **4**. Spectral bands assigned to d→d transitions also appeared as shoulders (of the much stronger LMCT band in the region 550-558 nm) at 592 nm and 590 nm for compounds **2** and **4**, respectively.

Fluorescence spectral data were acquired for compounds **2-4** in DMSO (see appendix, Figures A26-A28). Compounds **2**, **3**, and **4** were excited at 400, 330, and 340 nm, respectively. The highest fluorescence intensity was observed in the fluorescence spectrum of compound **2** due to the presence of an anthracene moiety in the MEATSC ligand while compounds **3** and **4** produced the lower intensities.

Electrochemical Studies

*Compounds **1-4** and [Zn(Sal-L-tryp)(H_2O)].0.25H_2O.* CV and square wave voltammograms were acquired for Compound **1-4** and [Zn(Sal-*L*-tryp)(H_2O)].0.25H_2O as shown in figures 40 and 41 (see Appendix, Figures A34 and A35). The data collected from electrochemical studies are shown in Table 10. The Zn(II) metal center is known to be redox inactive.[195] Electrochemical data acquired for [Zn(Sal-*L*-tryp)(H_2O)].0.25H_2O was therefore used to confirm the electrochemical data due to metal-based electron transfer in compounds **1-4**.

An irreversible anodic redox peak attributed to the oxidation of the *L*-

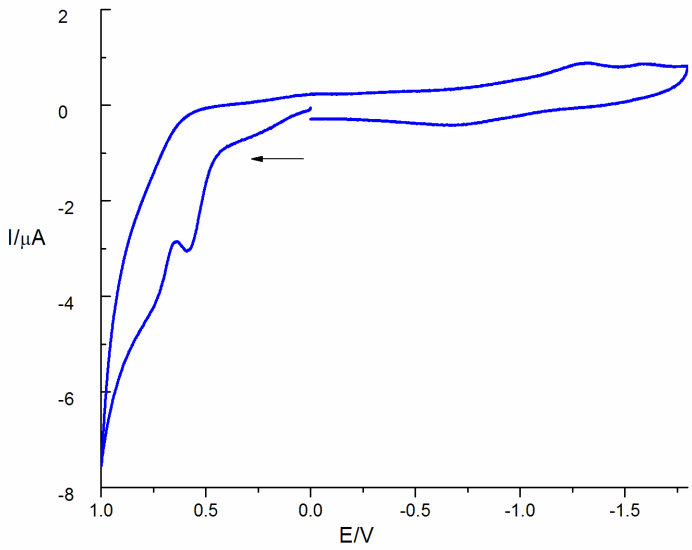

Figure 41. A cyclic voltammogram of a 1.0 mM solution of **[**Zn(Sal-*L*-tryp)(H_2O)].0.25H_2O in DMSO. Electrodes: platinum working electrode, platinum auxiliary electrode and Ag/Ag^+ (0.01 M $AgNO_3$ and 0.10 M TBAP in acetonitrile) reference electrode. Supporting electrolyte = 0.1 M TBAP. Scan rate = 100 mV s^{-1}.

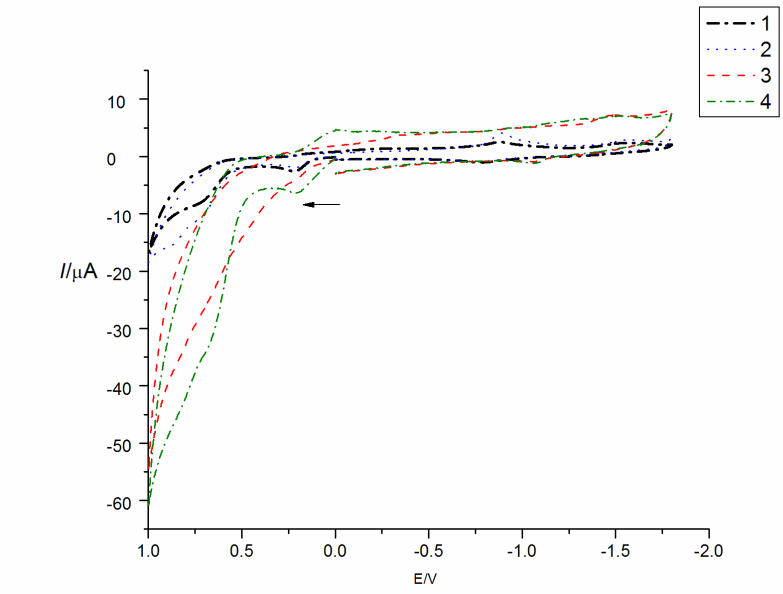

Figure 42. Cyclic voltammograms of 1.0 mM solutions of compounds **1-4** in DMSO. Electrodes: platinum working electrode, platinum auxiliary electrode and Ag/Ag^+ (0.01 M $AgNO_3$ and 0.10 M TBAP in acetonitrile) reference electrode. Supporting electrolyte = 0.1 M TBAP. Scan rate = 100 mV s^{-1}.

Table 10

*Electrochemical data of 1.0 mM solutions of compounds **1**-**4**, product isolated from oxidized compound **1**, and [Zn(Sal-L-tryp)(H_2O)].0.25H_2O in DMSO.*

A) Compounds **1**-**4**

Species	*E*/V	Assignment
1	E_{pa} = +0.71	*L*-tryp$^{0/+}$
	E_{pa} = +0.22	$V^{IV/V}$
	E_{pa} = -0.78	$V^{III/IV}$
	E_{pa} = -1.28	-
	E_{pc} = -0.88	$V^{IV/III}$
	E_{pc} = -1.57	*L*-tryp$^{+/0}$
2	E_{pa} = +0.87	Oxidation of anthracene moiety
	E_{pa} = +0.73	*L*-tryp$^{0/+}$
	E_{pa} = +0.21	$V^{IV/V}$
	E_{pa} = -0.78	$V^{III/IV}$
	E_{pa} = -1.24	CH_2-NH/ HC=N
	E_{pc} = -0.89	$V^{IV/III}$
	E_{pc} = -1.57	*L*-tryp$^{+/0}$
3	E_{pa} = +0.81	-
	E_{pa} = +0.64	*L*-tryp$^{0/+}$
	E_{pa} = +0.43	Oxidation of phenolate in vanillin moiety
	E_{pa} = +0.21	$V^{IV/V}$
	E_{pa} = -0.16	-
	E_{pa} = -1.07	$V^{III/IV}$
	E_{pa} = -1.36	CH_2-NH/ HC=N
	E_{pc} = -0.34	-
	E_{pc} = -0.88	$V^{IV/III}$
	E_{pc} = -1.17	-
	E_{pc} = -1.65	*L*-tryp$^{+/0}$

Table 10 (continued).

Species	*E*/V	Assignment
4	E_{pa} = +0.82	-
	E_{pa} = +0.66	*L*-tryp$^{0/+}$
	E_{pa} = +0.21	$V^{IV/V}$
	E_{pa} = -0.12	-
	E_{pa} = -1.07	$V^{III/IV}$
	E_{pa} = -1.31	CH_2-NH/ HC=N
	E_{pa} = -1.67	-
	E_{pc} = -0.68	-
	E_{pc} = -0.92	$V^{IV/III}$
	E_{pc} = -1.13	-
	E_{pc} = -1.51	*L*-tryp$^{+/0}$

B) Oxidized product obtained from compound **1** and [Zn(Sal-*L*-tryp)(H_2O)].0.25H_2O.

Species	*E*/V	Assignment
Oxidized Compound **1**	E_{pa} = +0.66	*L*-tryp$^{0/+}$
	E_{pa} = +0.22	$V^{IV/V}$
	E_{pa} = -0.12	-
	E_{pa} = -1.06	$V^{III/IV}$
	E_{pa} = -1.39	-
	E_{pa} = -1.66	-
	E_{pc} = -0.17	-
	E_{pc} = -0.48	-
	E_{pc} = -0.96	$V^{IV/III}$
	E_{pc} = -1.15	-
	E_{pc} = -1.30	$V^{V/IV}$
	E_{pc} = -1.50	*L*-tryp$^{+/0}$

Table 10 (continued).

Species	*E*/V	Assignment
[Zn(Sal-*L*-tryp)(H_2O)].0.25 H_2O	E_{pa} = +0.71	*L*-tryp$^{0/+}$
	E_{pa} = +0.59	$PhO^{-\cdot}$
	E_{pa} = -0.67	-
	E_{pa} = -1.34	-
	E_{pc} = -0.84	-
	E_{pc} = -1.30	-
	E_{pc} = -1.59	*L*-tryp$^{+/0}$

Note. Electrodes: platinum working electrode, platinum auxiliary electrode and Ag/Ag^+ (0.01 M $AgNO_3$ and 0.10 M TBAP in acetonitrile) reference electrode. Supporting electrolyte = 0.1 M TBAP. Scan rate = 100 mV s^{-1}.

tryptophan moiety of the Schiff base ligand (salicylaldehyde) was observed in the CV of each complex. Upon coordintion of the Schiff base ligand (salicylaldehyde moiety) to the respective metal center, a decrease in the redox potential attributed to the oxidation of the *L*-tryptophan moiety was generally observed. This redox potential decreased from +0.75 V in K[(Sal-*L*-tryp)] to +0.71 V for [Zn(Sal-*L*-tryp)(H_2O)].0.25H_2O and compound **1**, to +0.73 V for compound **2**, to +0.64 V for compound **3**, and to +0.66 V for compound **4**. The respective aniodic redox peaks were also confirmed using square wave voltammetry. The square voltammograms (see Appendix, Figures A38 and A39) of all complexes exhibited anodic redox peaks at +0.70 V for [Zn(Sal-*L*-tryp)(H_2O)].0.25H_2O, at +0.67 V for compounds **1**, **2**, and **3**, and at +0.62 V for compound **4**. These redox peaks were all attributed to the oxidation of the *L*-tryptophan moiety.

The CV acquired for [VO(salen)] exhibited an irreversible anodic redox peak at +0.50 V, attributed to the V(IV)/V(V) redox couple as reported by Kianfar and Mohebbi.[196] According to Maia *et al*.,[197] electrochemical data acquired for V(IV)

complexes were also shown to exhibit irreversible anodic redox peaks in the region +0.60 V to +0.65 V, attributed to the V(IV)/V(V) redox couple.[197] Similar redox peaks attributed to the V(IV)/V(V) redox couple were also observed in the CV's acquired for our complexes. The irreversible anodic redox peaks attributed to the V(IV)/V(V) redox couple were observed at +0.22 V for compound **1** and at +0.21 V for compounds **2-4**. Redox peaks attributed to the V(IV)/V(V) redox couple were observed at +0.18 V for compounds **1** and **3** and at +0.17 V in the square wave voltammograms of compounds **2** and **4**.

CV acquired for oxovanadium(IV) complexes are also known to display cathodic quasi-reversible voltammetric responses attributed to the V(IV)/V(III) redox couple in the potential range -0.9 V to -1.3 V.[191] In our case, simiar cathodic quasi-reversible redox peaks were observed at -0.88 V, -0.89 V, -0.88 V and -0.92 for compounds **1**, **2**, **3**, and **4**, respectively. The corresponding anodic quasi-reversible redox peak were observed at -0.78 V for compounds **1** and **2** and at -1.07 V compounds **3** and **4**. All other cathodic peaks observed in the voltammograms acquired for each complex were assigned to the reduction of cation radicals

*Oxidized products isolated from Compounds **1***. The representative CV and square wave voltammogram acquired for the product isolated from the oxidized solution of compound **1** is shown in figures 43 and 44. Products obtained from oxidized DMSO solutions of compounds **2-4** are proposed to exhibit similar electrochemical properties.

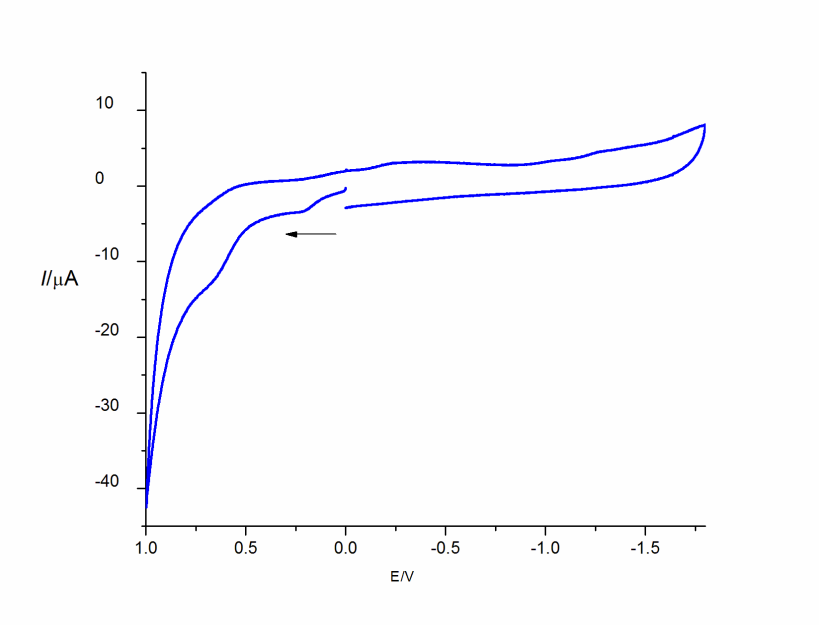

Figure 43. A cyclic voltammogram of a 1.0 mM solution of the oxidized product isolated from compound **1** in DMSO. Electrodes: platinum working electrode, platinum auxiliary electrode and Ag/Ag^{+} (0.01 M $AgNO_3$ and 0.10 M TBAP in acetonitrile) reference electrode. Supporting electrolyte = 0.1 M TBAP. Scan rate = 100 mV s^{-1}.

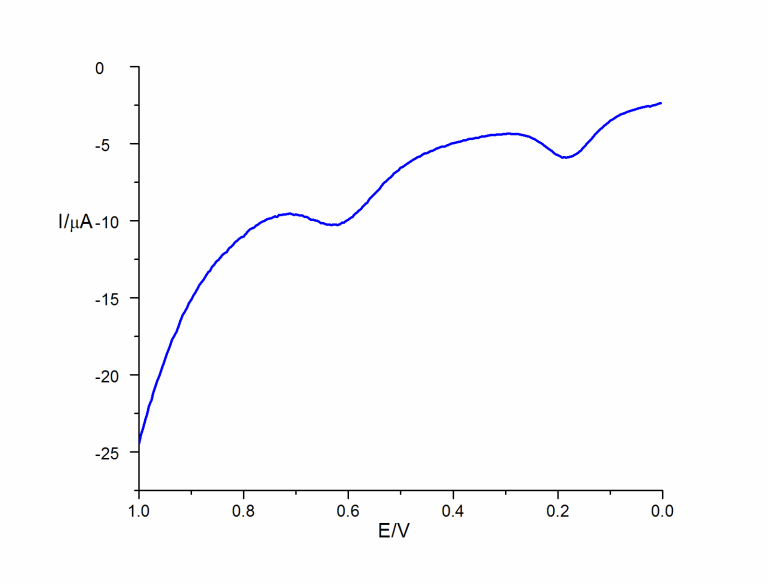

Figure 44. A square wave voltammogram: The oxidation of a 1.0 mM solution of the oxidized product isolated from compound **1** in DMSO. Electrodes: platinum working electrode, platinum auxiliary electrode and Ag/Ag^{+} (0.01 M $AgNO_3$ and 0.10 M TBAP in acetonitrile) reference electrode. Supporting electrolyte = 0.1 M TBAP. Initial potential = 0 V, final potential = +1.0 V, step E = 4 mV, S.W. amplitude = 25 mV, S.W. frequency = 15 Hz, filter = 100 Hz, and quiet time = 2 s.

Anodic redox peaks attributed to the oxidation of the *L*-tryptophan moiety, were observed at +0.66 V and at +0.63 V in the CV and square wave voltammogram (of the product isolated from the oxidized solution of compound **1**), respectively. Redox couples were observed at +0.22 V and 0.18 V in the CV and square wave voltammogram, respectively. The observance of a redox peak corresponding to the V(IV)/V(V) redox couple suggested that the product isolated from the oxidized solution of compound **1** was actually a mixture V(IV) and V(V) species. The CV of this oxidized product also exhibited a quasi-reversible redox wave (E_{pc} = -0.96 V and E_{pa} = -1.06 V) attributed to the V(IV)/V(III) redox couple.[191]

In vitro Studies

The data aquired from *in vitro* studies are presented in Table 11. The aim of these *in vitro* studies is to evaluate the antiproliferative activity of compounds **1-4** against colon cancer cell lines (HTC-116, Caco-2, and HT-29) and to compare the anti-proliferative activity with that of one non-cancerous colon cell line (CCD18-Co). Colorimetric assay (MTS assay), a technique that measures mitochondrial dehydrogenase activity as an indication of cell viability was used to evaluate the cytotoxicity of compounds **2-4** on three different cancer colon cell lines (HCT116, Caco-2 and HT-29). The effects of the compounds on the viability of these cells were evaluated after continuous incubation (24, 48, and 72 hours).

A comparison between the growth inhibition effect of the respective compounds against non-cancerous colonic myofibroblasts CCD-18Co cells and cancer colon cell lines were investigated. The results indicated a large difference in the inhibition of cell proliferation between cancer lines and the non-cancerous CCD-18Co

Table 11

*Anti-proliferative effects of compounds **2-4**, cisplatin, and etoposide on different cells lines after 24, 48 and 72 hours treatment.*

Species	HT-29			Caco-2		
	24 hrs	48 hrs	72 hrs	24 hrs	48 hrs	72 hrs
	$IC_{50}/\mu M$	$IC_{50}/\mu M$	$IC_{50}/\mu M$	$IC_{50}/\mu M$	$IC_{50}/\mu M$	$IC_{50}/\mu M$
2	277.1±10.2	239.6±7.9	100.3±5.1	349.1±19.5	277.1±16.3	147.1±10.8
3	244.2±8.8	169.6±15.1	87.9±0.5	367.0±21.5	281.6±14.4	152.5±12.7
4	128.6±10.7	82.4±9.6	47.8±5.5	242.1±25.1	166.2±15.3	85.4±14.0
Cisplatin	84.7±1.9	80.6±1.6	69.1±3.2	32.0±1.6	22.8±1.5	17.9±1.8
Etoposide	19.2±0.8	17.3±1.9	15.8±2.4	47.6±0.8	46.2±1.9	40.9±1.5
Species	HCT-116			CCD-18Co		
	24 hrs	48 hrs	72 hrs	24 hrs	48 hrs	72 hrs
	$IC_{50}/\mu M$	$IC_{50}/\mu M$	$IC_{50}/\mu M$	$IC_{50}/\mu M$	$IC_{50}/\mu M$	$IC_{50}/\mu M$
2	203.4±7.7	181.3±9.2	115.0±6.5	495.6±23.5	339.2±16.7	208.0±11.9
3	227.4±6.8	192.7±11.6	110.3±10.1	490.6±27.6	329.5±15.4	203.6±12.5
4	161.3±4.6	134.9±3.9	89.5±14.5	382.7±21.9	246.2±11.4	152.2±12.0
Cisplatin	53.8±2.1	49.7±1.3	41.0±2.7	83.0±1.1	72.0±1.5	64.1±1.6
Etoposide	40.8±0.5	36.2±2.0	38.4±1.2	82.5±3.1	79.2±1.2	73.2±1.9

cells. The growth inhibition effect of the respective compounds were shown to be time dependent as shown in Table 11.

Compounds **2**-**4** have been shown to time-dependently decrease cell viability of HCT-116, Caco-2, and more potently, in HT-29 cells (Table 11). While compounds **2** and **3** showed similar activities in both cancer cell lines, compound **4** was shown to be the most active of the three compounds tested. A plot of percentage cell viability

versus concentration of compound **4** against the HT-29 cancer cell line were plotted as shown in Figure 45 while the IC_{50} values for inhibition of cell proliferation for compounds **2-4**. After 72 hours, the IC_{50} values for compounds **2** and **3** were generally around 100 μM concentration. Although our compounds did not exhibit better efficacy against any of the cancer cell lines when compared to etoposide, compound **4** was shown to have a better efficacy on the HT-29 cancer cell line when compared to cisplatin (Table 11).

The possibility of cytotoxic selectivity towards colon cancer cells is suggested since all three compounds exhibited less inhibitory effects in human normal CCD-

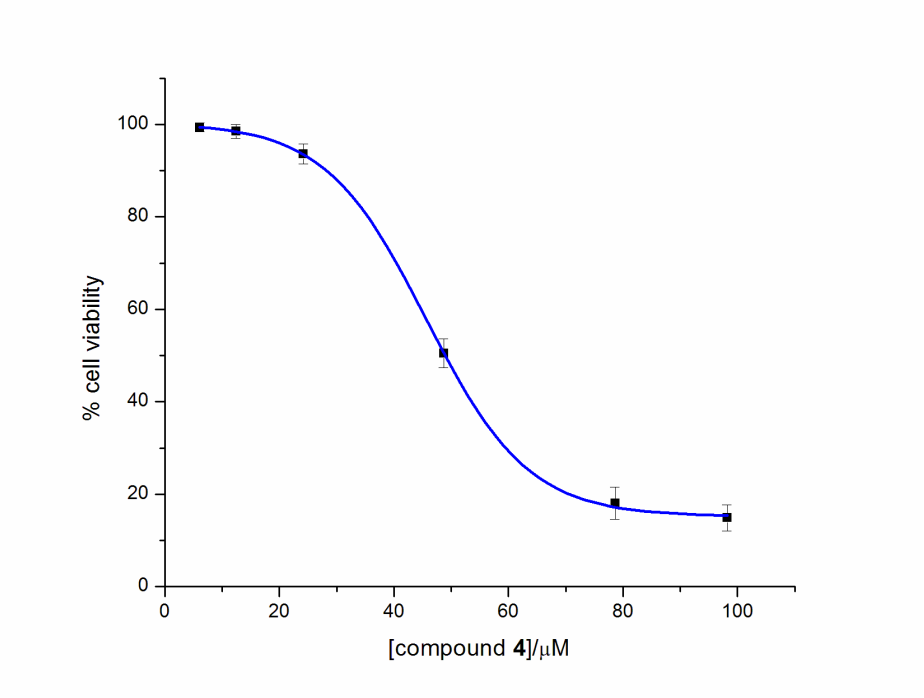

Figure 45. MTT cell proliferation assay of compound **4** against the HT-29 cancer cell line.

18Co cells. The IC_{50} values obtained for CCD-18Co were observed to be 3-fold and 2-fold than HT-29 and Caco-2 and HCT-116, respectively. The cytotoxic selectivity of

cisplatin (a positive control) towards the cancer colon cells (except on Caco-2 cells) was observed to be slightly lower than our synthesized compounds (Table 11). Cisplatin was previously reported to inhibit cell proliferation by about 70% in both cell lines (cancer and normal colon cells).[198] Overall, due to the fact that compounds **2**-**4** had no effect on non-cancerous cells but exhibited properties of potential growth suppressors of cancer cells, these compounds are proposed to be potential chemotherapeutic agents.

Although metal complexes are currently being investigated as probes and therapeutics, the various pathways and uptake mechanisms for metal complexes into cells are are sparse in literature. A review of the cellular accumulation of cisplatin has recently been reported.[199,200] Platinum-containing drugs are capable of entering the cell by passive diffusion, by organic cation transporters, by the copper transporter Ctr1, and possibly by endocytosis.[200] Ruthenium(II) complex containing lipophilic cations, for example the lipophilic 4,7-diphenyl-1,10-phenanthroline ligand, has been shown to passively diffuse across the plasma membrane in a membrane-potential dependent manner.[200] The excellent efficacy of the ruthenium(II) complexes with thiosemicarbazones as reported in a study by Beckford and co-workers[128] is also suggested to be due to the lipophilic nature of the respective complexes. Similarly, lipophilic cations, such as $[(bpy)_2Ru(thiosemicarbazone)](PF_6)_2$ and $[(phen)_2Ru(thiosemicarbazone)](PF_6)_2$ (where thiosemicarbazone = 9-anthraldehydethiosemicarbazone, 9-anthraldehyde-N(4)-methylthiosemicarbazone, and 9-anthraldehyde-N(4)-ethylthiosemicarbazone),[128] are also observed to have better efficacies against HT-29 and HCT-116 cell lines *versus* our neutral vanadium(IV) complexes for similar reasons.

In order to accurately conclude, a systematic study of ruthenium(II) complexes and compounds **2**-**4**, all under the same conditions, is needed. Apart from such a study, a more detailed emphasis will be placed on the methods used to examine cellular accumulations in order to identify the mechanism(s) of uptake, and to monitor possible efflux compounds **2**-**4**, and their analogues in the near future.[201]

CHAPTER IV

CONCLUSIONS AND FUTURE WORK

Conclusions

Two novel thiosemicarbazone ligands, MeATSC and *N*-Ethhymethohcarbthio were successfully synthesized and characterized. A reduced Schiff base and K[Sal-*L*-tryp)] ligand was also synthesized and characterized. Each thiosemicarbazone ligand was then coordinated to [VO(Sal-*L*-tryp)] (**1**) to form three novel V(IV) complexes. Thiosemicarbazones are known to exhibit thione-thiol tautomerism and can coordinate to metal centers either as a neutral (thione) or as a mono-anionic (thiolate) ligand. Due to the absence of a υ((S-H) spectral band in the FT IR spectra, the ligands were said to exist as neutral (thione) ligands.

Upon aerial oxidation, DMSO solutions of compounds **1-4** were readily oxidized to form V(V) species. All compounds are believed to behave similarly; hence, for this study, we focused on compounds **1** and **3** only. ESI MS data was used to identify the species formed in solution upon oxidation. The proposed mechanism (Scheme 14) suggests that the ligands are first substituted by DMSO solvent molecules followed by the dimerization of the solvated complexes to form binuclear species.

In this study, all four V(IV) compounds were shown to exhibit anti-cancer effects against three colon cancer cell lines, HTC-116, Caco-2, and HT-29. A comparative anti-proliferative study on non-cancerous colonic myofibrolasts, CCD18-Co, indicated that our novel compounds had no effect on these non-cancerous colorectal cells. The novel V(IV) compounds were also shown to exhibit cytotoxic selectivity towards colon cancer

cells. Cytotoxic selectivity was evident since compounds 2-3 exhibited less inhibitory effects in human non-cancerous CCD-18Co cells.

Overall, although compounds **1**-**4** are relatively unstable, compounds **2-3** exhibited interesting anti-proliferative activity on colon cancer cells. Due to existence of several species in solution (upon oxidation), the identity of the active species still remains unclear. A thorough investigation is therefore needed in order to identify the active species responsible for anti-proliferative activity. We are therefore suggesting that these compounds might be effective as chemotherapeutic agents.

Future Work

The synthesis and characterization of these novel thiosemicarbazone ligands and V(IV) compounds has paved the way for a series of interesting research with similar compounds. These compounds were shown to exhibit anti-cancer activity against colon cancer cell lines. This area of research can be expanded by synthesizing a series of similar V(IV) complexes containing varying thiosemicarbazone ligands. It is also important to investigate the effect of varying thiosemicarbazone ligands on the stability of the respective complexes.

During this study compounds **1**-**4** were shown to be readily oxidized to V(V) species upon aerial oxidation. The question as to the identity of the species solely responsible for antiproliferative activity is therefore asked. ESI MS data has provided information allowing us to formulate a proposed mechanism for the identity of the species formed upon oxidation. An in depth study is therefore needed in order to confirm the identity of the oxidized species and to study the relative stability and anti-proliferative effects of such oxidized species.

APPENDIX A

A MASS SPECTRUM OF THE REDUCED SCHIFF BASE (2-(2-HYDROXYBENZYLAMINO)-3-(1H-INDOL-3-YL)PROPANOIC ACID) IN THE POSITIVE MODE

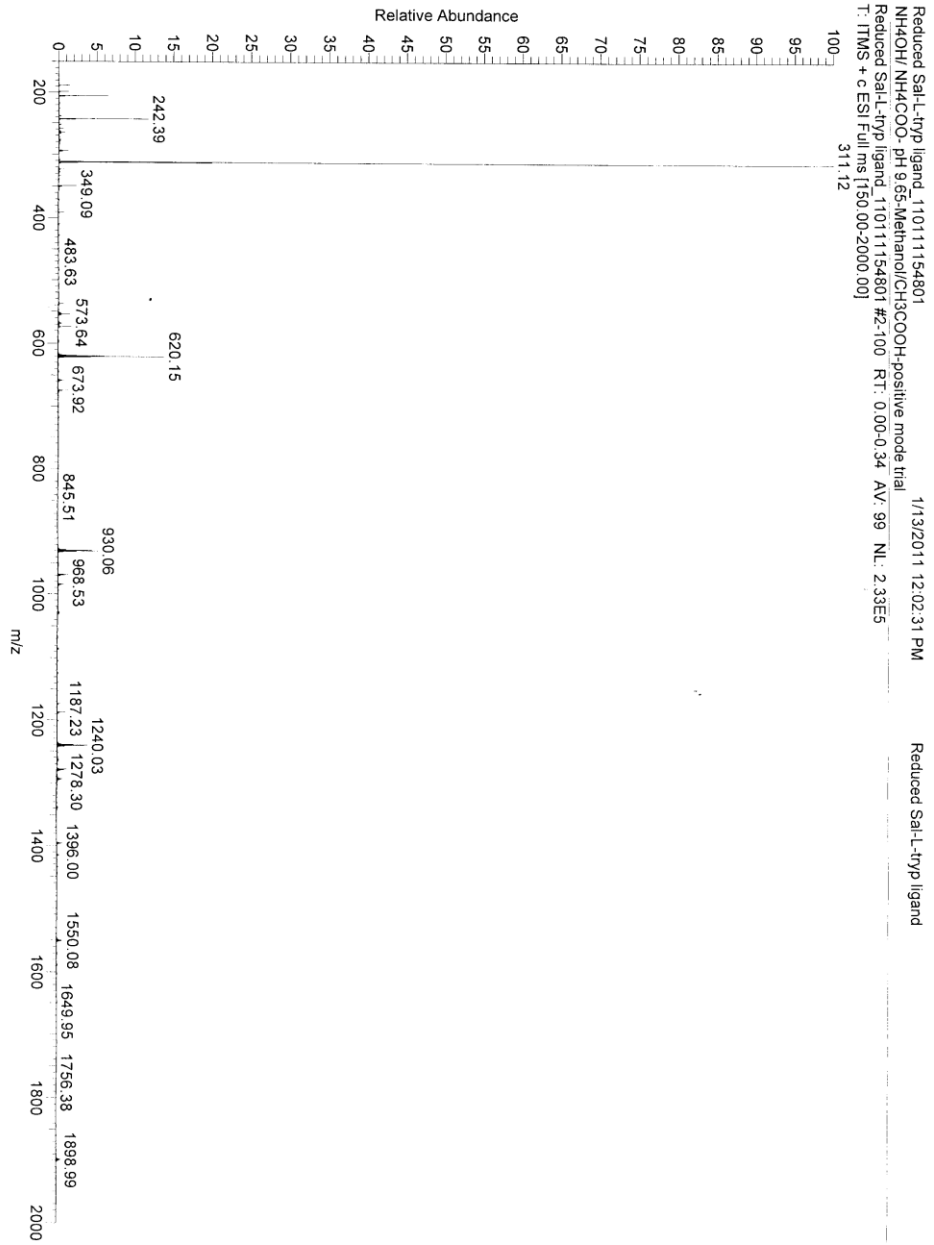

APPENDIX B

A MASS SPECTRUM OF K[(Sal-*L*-tryp)] IN THE POSITIVE MODE

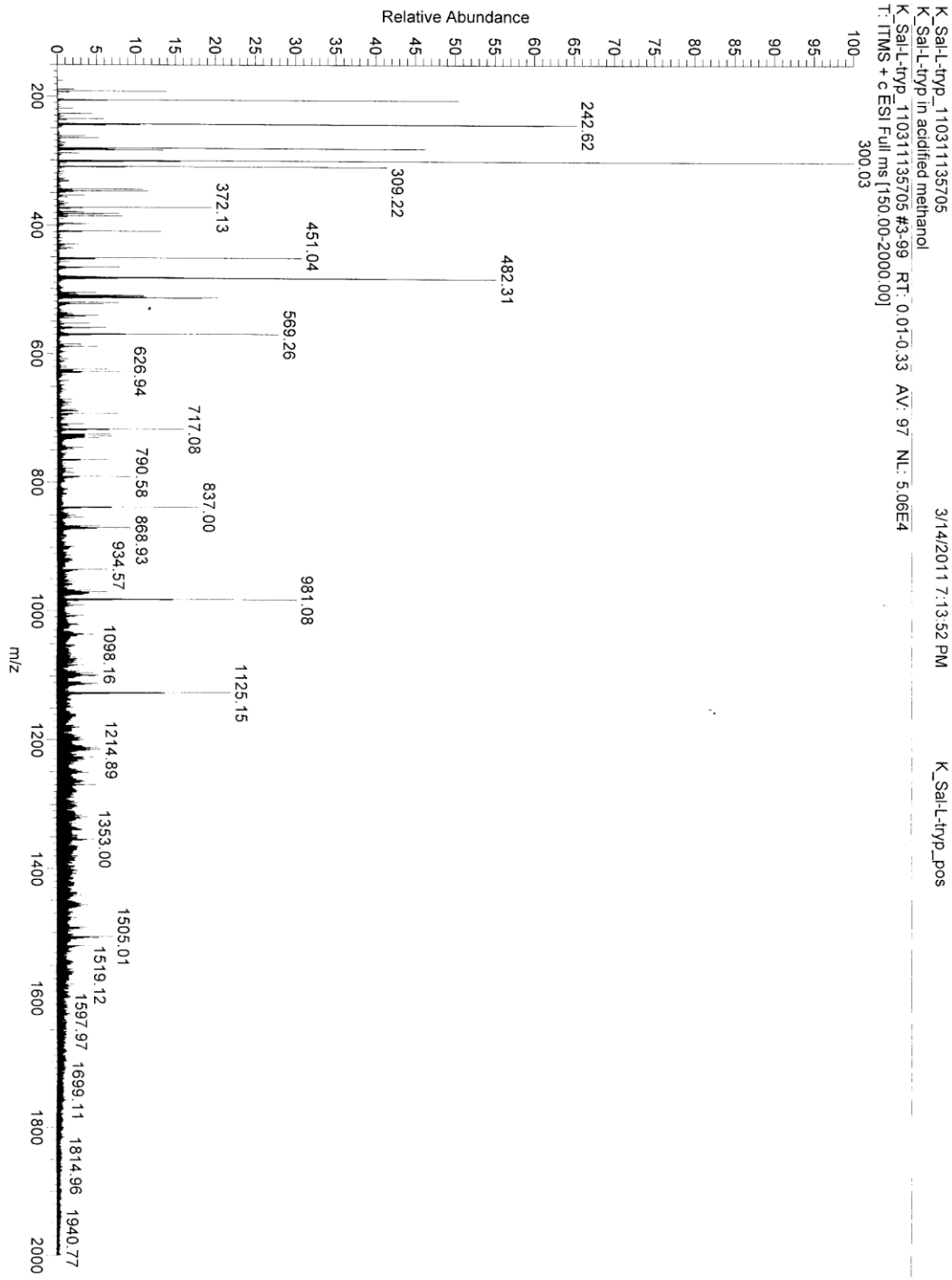

APPENDIX C

AN FT IR SPECTRUM OF MEATSC

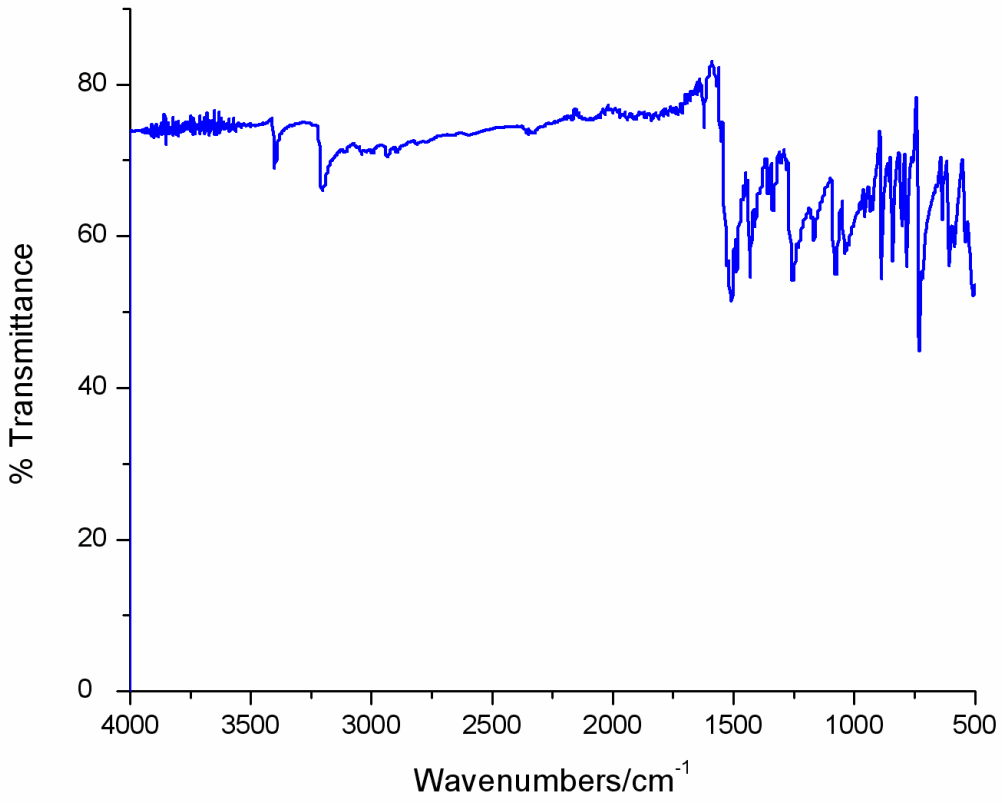

APPENDIX D

AN FT IR SPECTRUM OF *N*-ETHHYMETHOHCARBTHIO

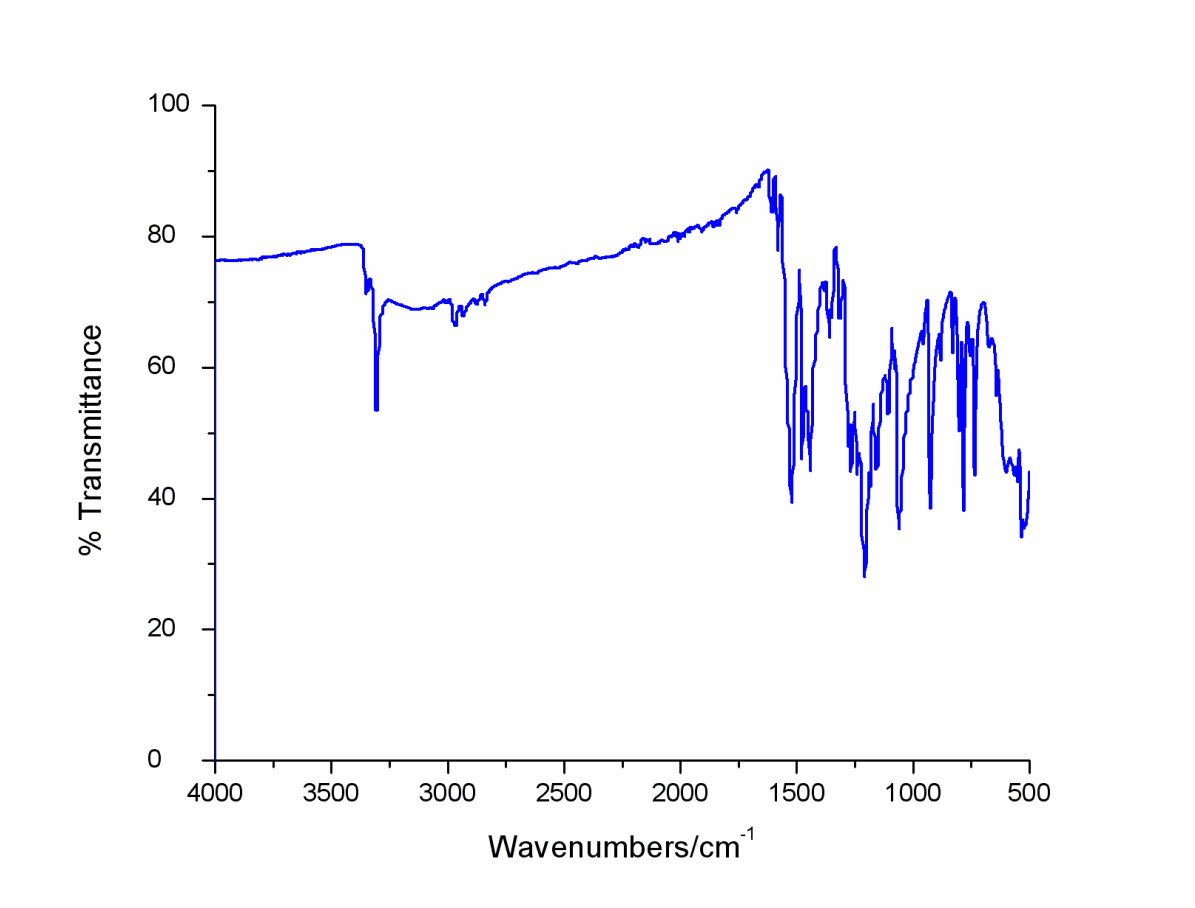

APPENDIX E

AN FT IR SPECTRUM OF ACETYLETHTSC

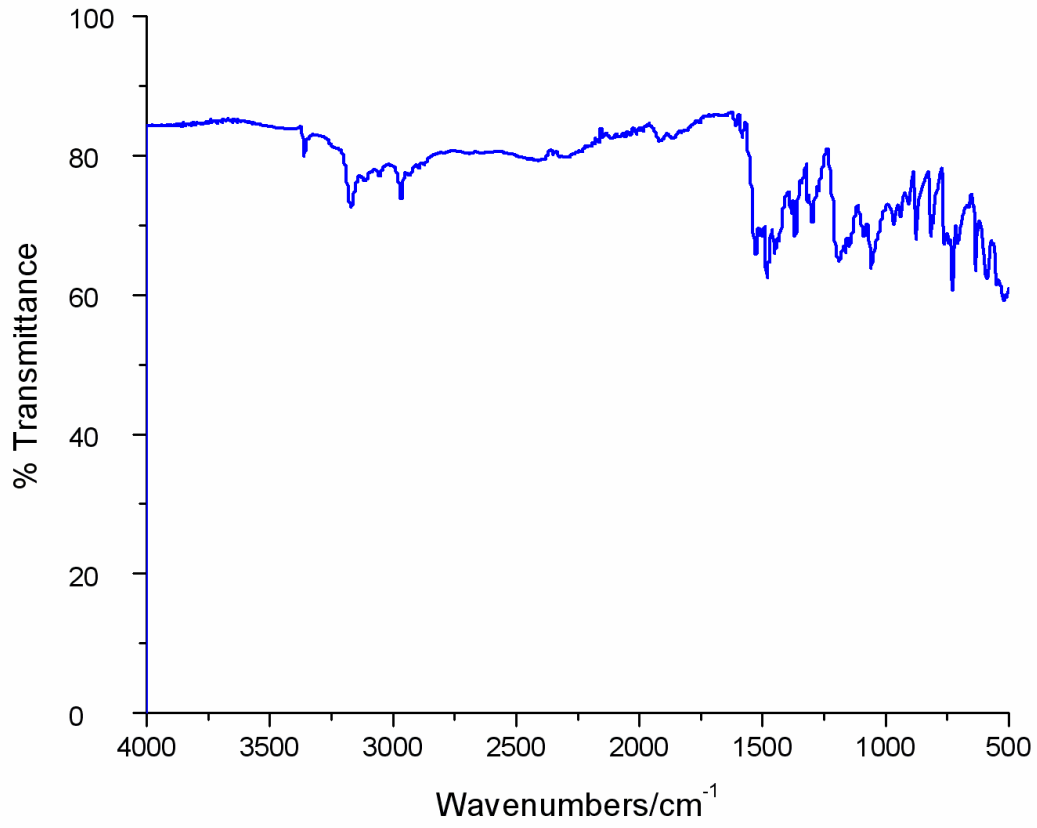

APPENDIX F

FT IR SPECTRUM OF THE REDUCED SCHIFF BASE

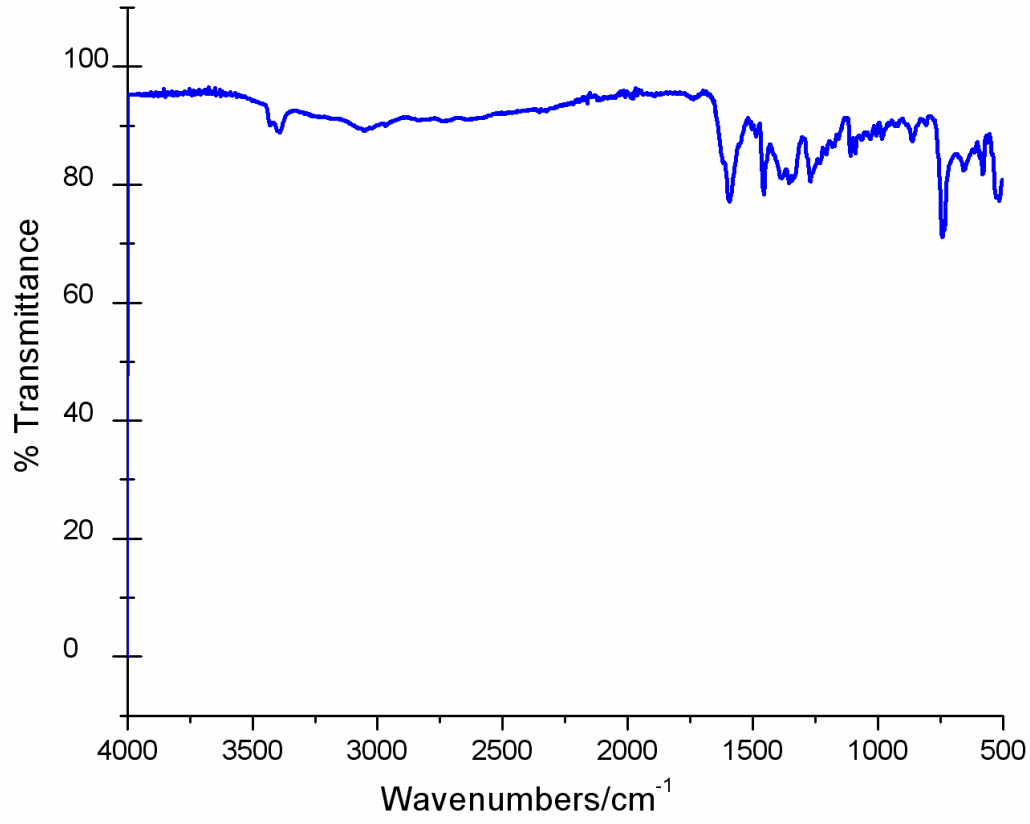

APPENDIX G

AN FT IR SPECTRUM OF K[(Sal-*L*-tryp)]

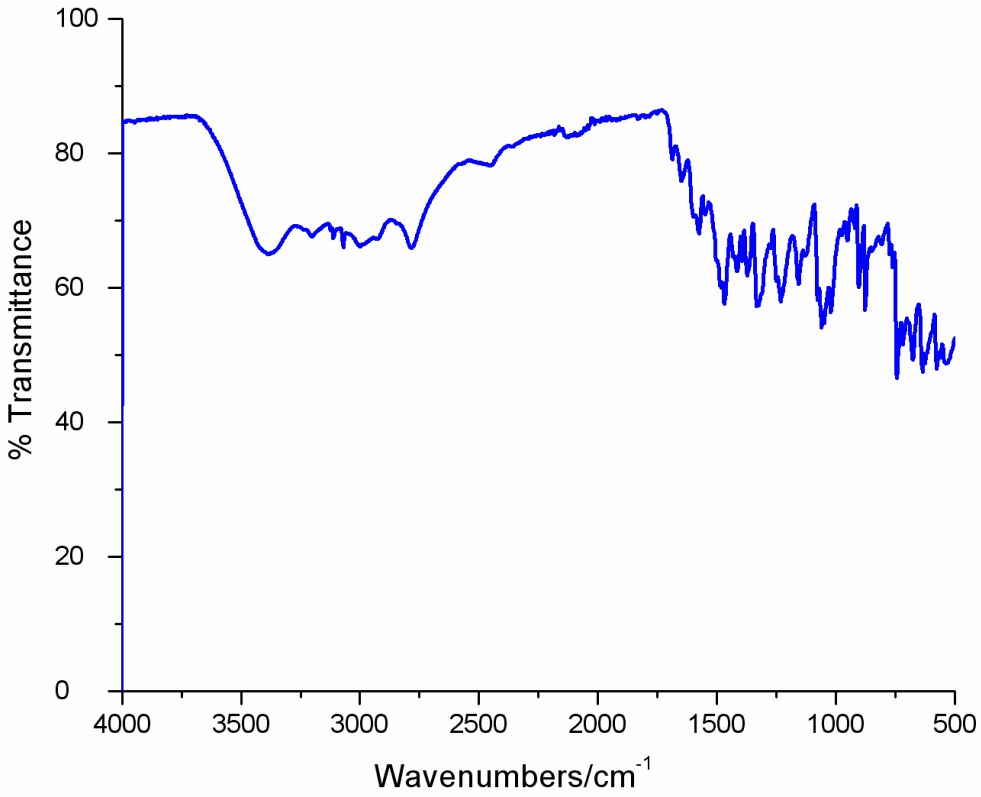

APPENDIX H

A ^{1}H NMR SPECTRUM OF THE REDUCED SCHIFF BASE IN NAOD/D_2O (PH = 9.0)

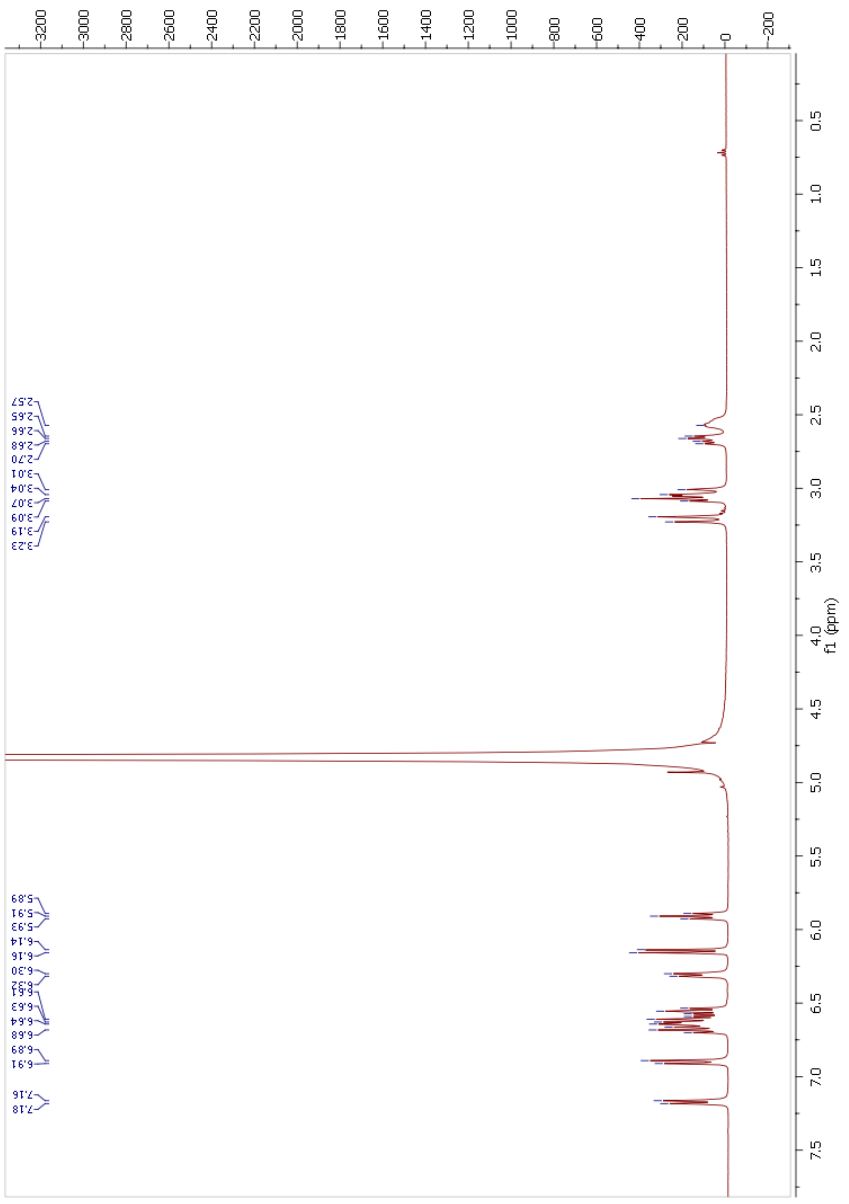

APPENDIX I

A ^{1}H NMR SPECTRUM OF K[(Sal-*L*-tryp)] IN DMSO-d_6

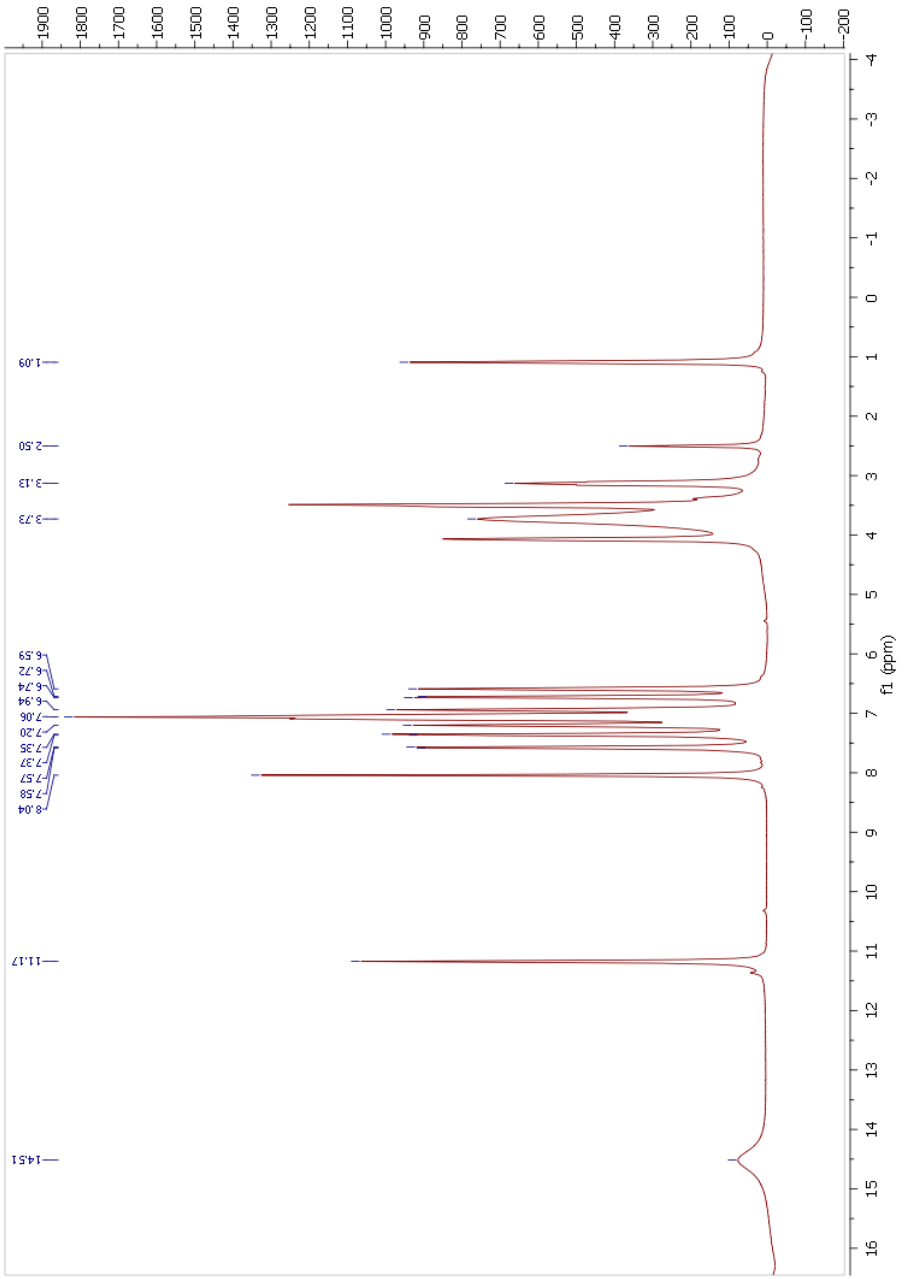

APPENDIX J

A ^{13}C NMR SPECTRUM OF THE REDUCED SCHIFF BASE IN NAOD/D_2O (PH = 9.0)

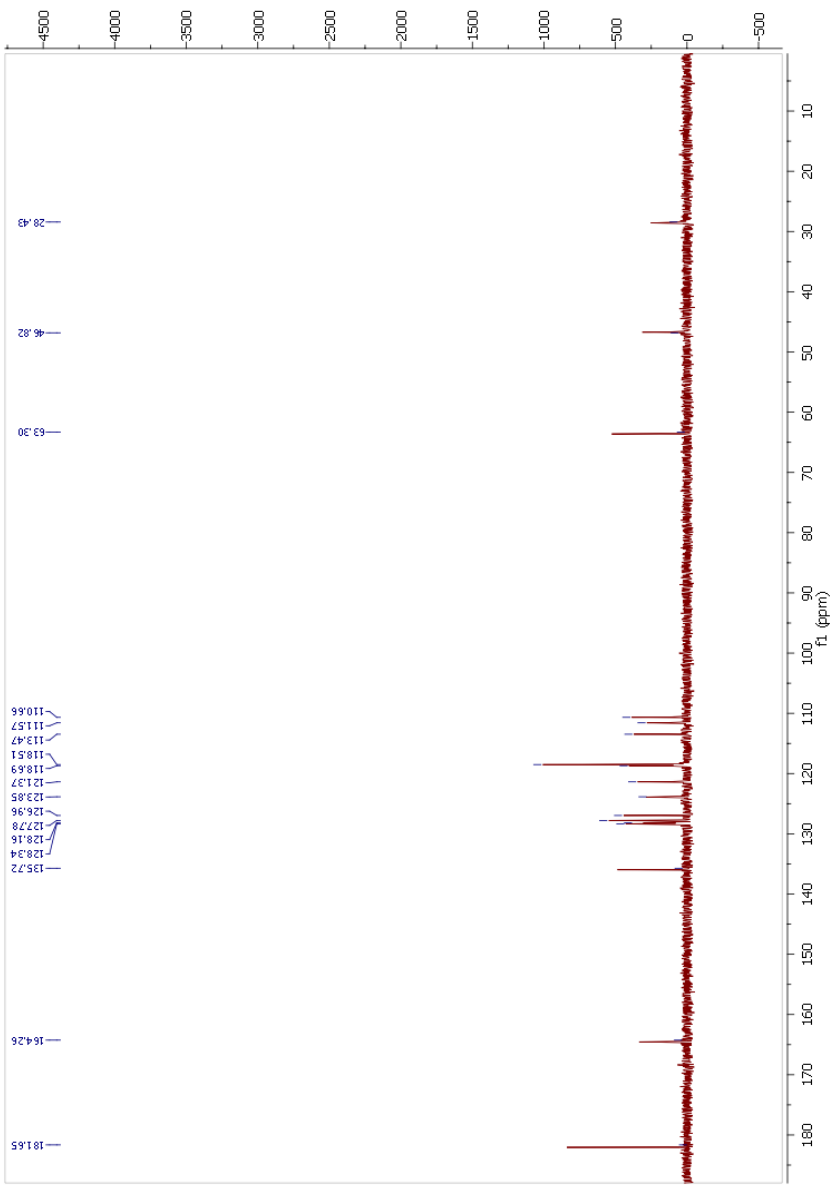

APPENDIX K

A ^{13}C NMR SPECTRUM OF K[(Sal-*L*-tryp)] IN DMSO-D_6

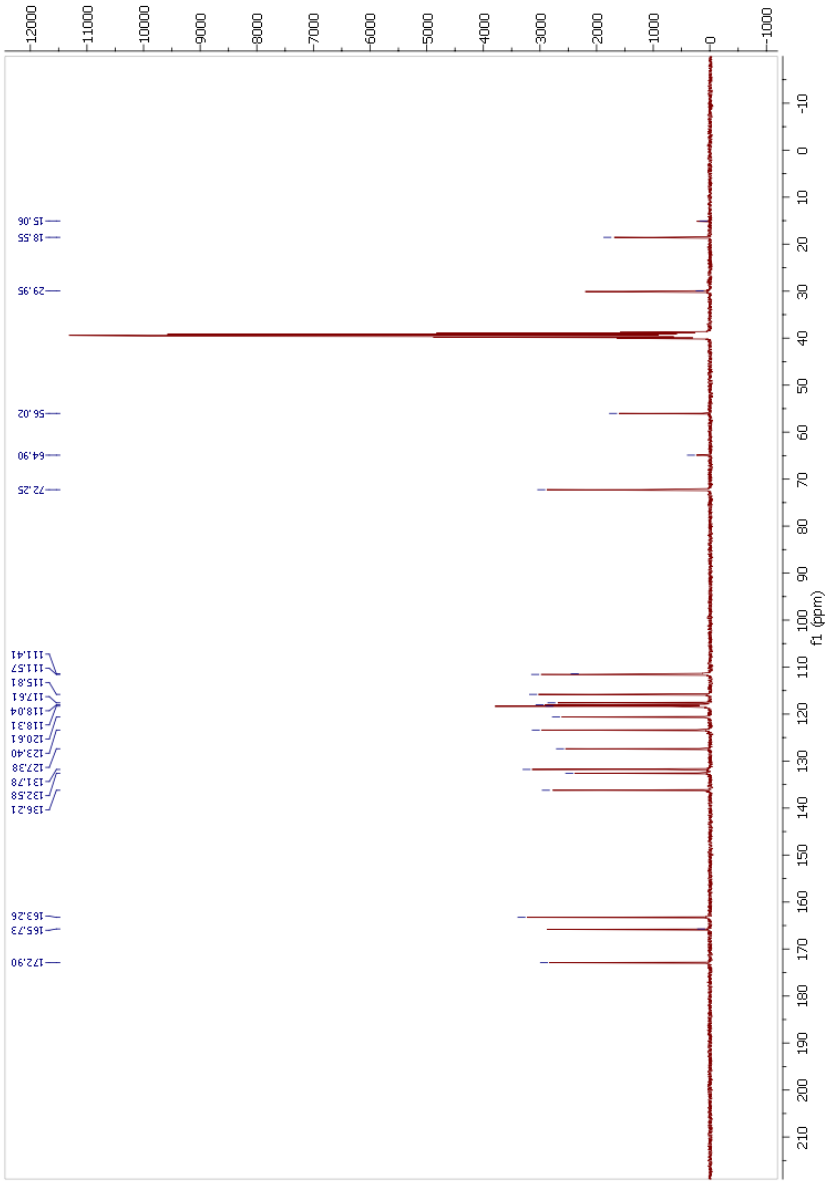

APPENDIX L

A ^{13}C NMR SPECTRUM OF *N*-ETHHYMETHOHCARBTHIO IN DMSO-d_6

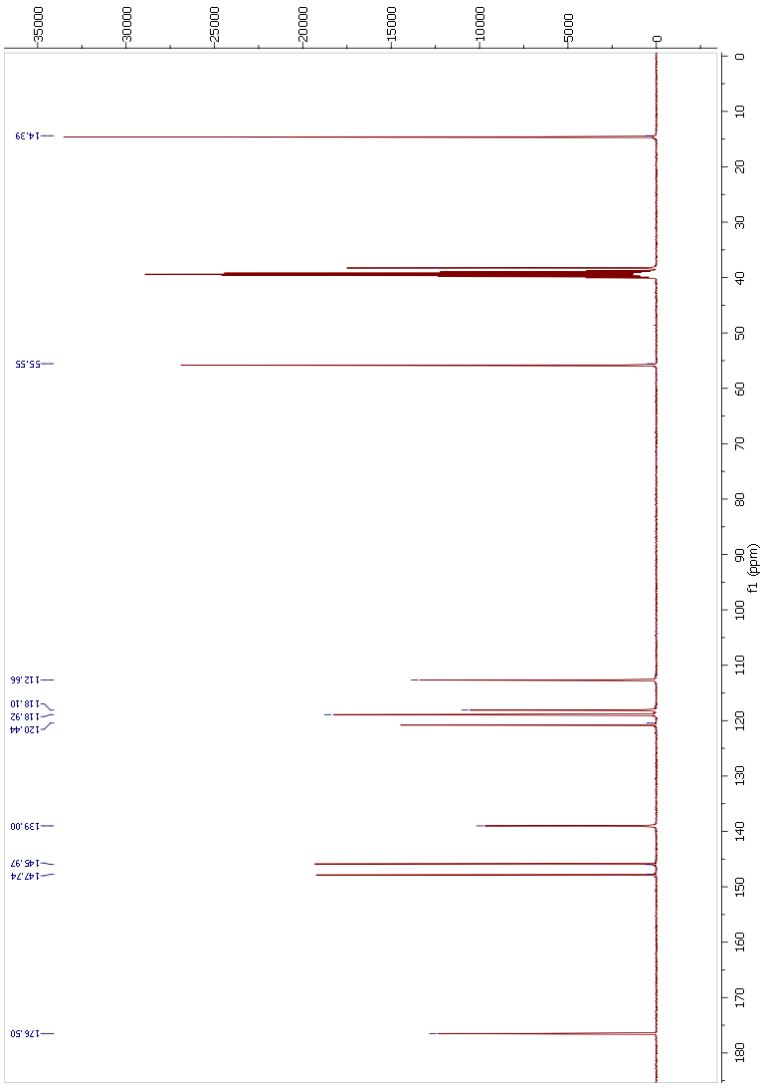

APPENDIX M

A SQUARE WAVE VOLTAMMOGRAM. THE OXIDATION OF A 1.0 MM SOLUTION OF K[(Sal-*L*-tryp)] IN DMSO. ELECTRODES: PLATINUM WORKING ELECTRODE, PLATINUM AUXILIARY ELECTRODE AND Ag/Ag^{+} (0.01 M $AgNO_3$ AND 0.10 M TBAP IN ACETONITRILE) REFERENCE ELECTRODE. SUPPORTING ELECTROLYTE = 0.1 M TBAP. INITIAL POTENTIAL = 0 V, FINAL POTENTIAL = +1.0 V, STEP E = 4 mV, S.W. AMPLITUDE = 25 mV, S.W. FREQUENCY = 15 Hz, filter = 100 Hz, AND QUIET TIME = 2 s

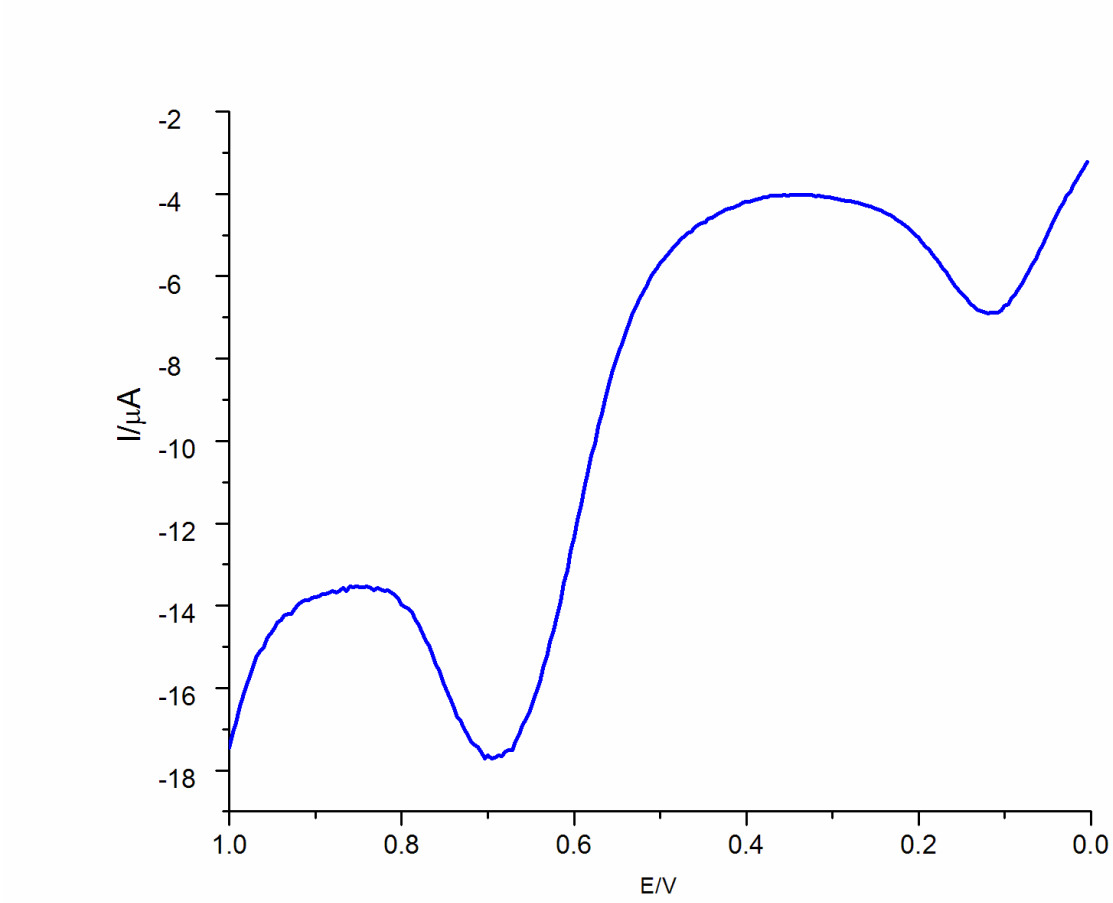

APPENDIX N

SQUARE WAVE VOLTAMMOGRAMS: THE OXIDATION OF 1.0 MM SOLUTIONS OF THIOSEMICARBAZONE LIGANDS IN DMSO. ELECTRODES: PLATINUM WORKING ELECTRODE, PLATINUM AUXILIARY ELECTRODE AND Ag/Ag^{+} (0.01 M $AgNO_3$ AND 0.10 M TBAP IN ACETONITRILE) REFERENCE ELECTRODE. SUPPORTING ELECTROLYTE = 0.1 M TBAP. INITIAL POTENTIAL = 0 V, FINAL POTENTIAL = +1.0 V, STEP E = 4 mV, S.W. AMPLITUDE = 25 mV, S.W. FREQUENCY = 15 Hz, FILTER = 100 Hz, AND QUIET TIME = 2 s

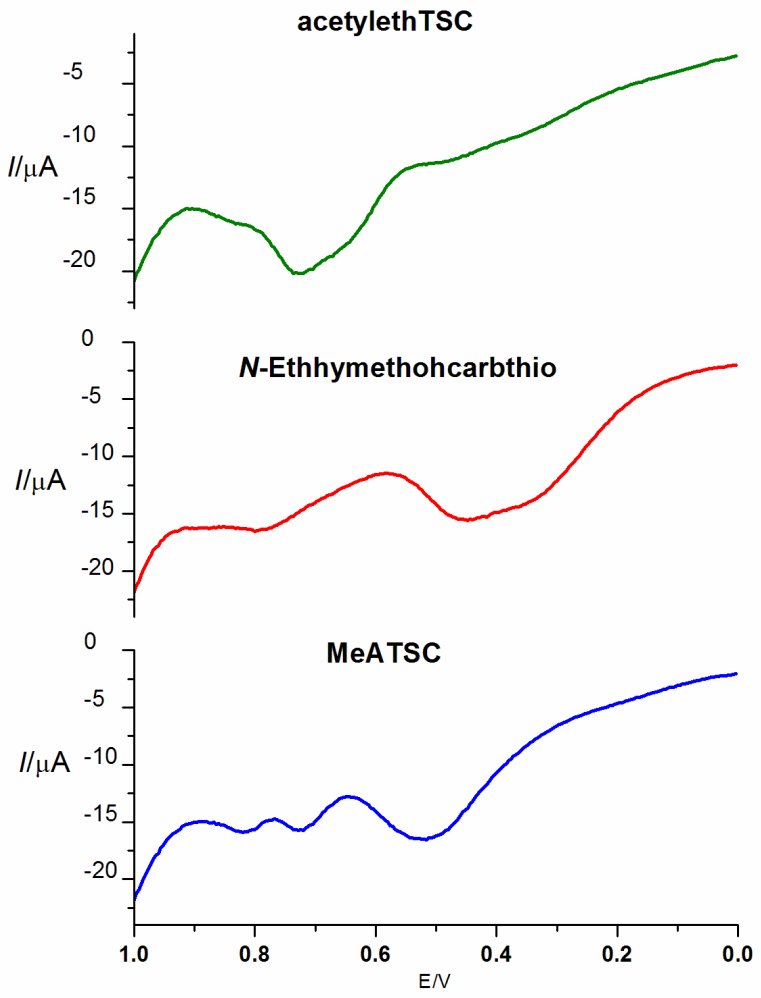

APPENDIX O

A MASS SPECTRUM OF COMPOUND **2** IN THE POSITIVE MODE

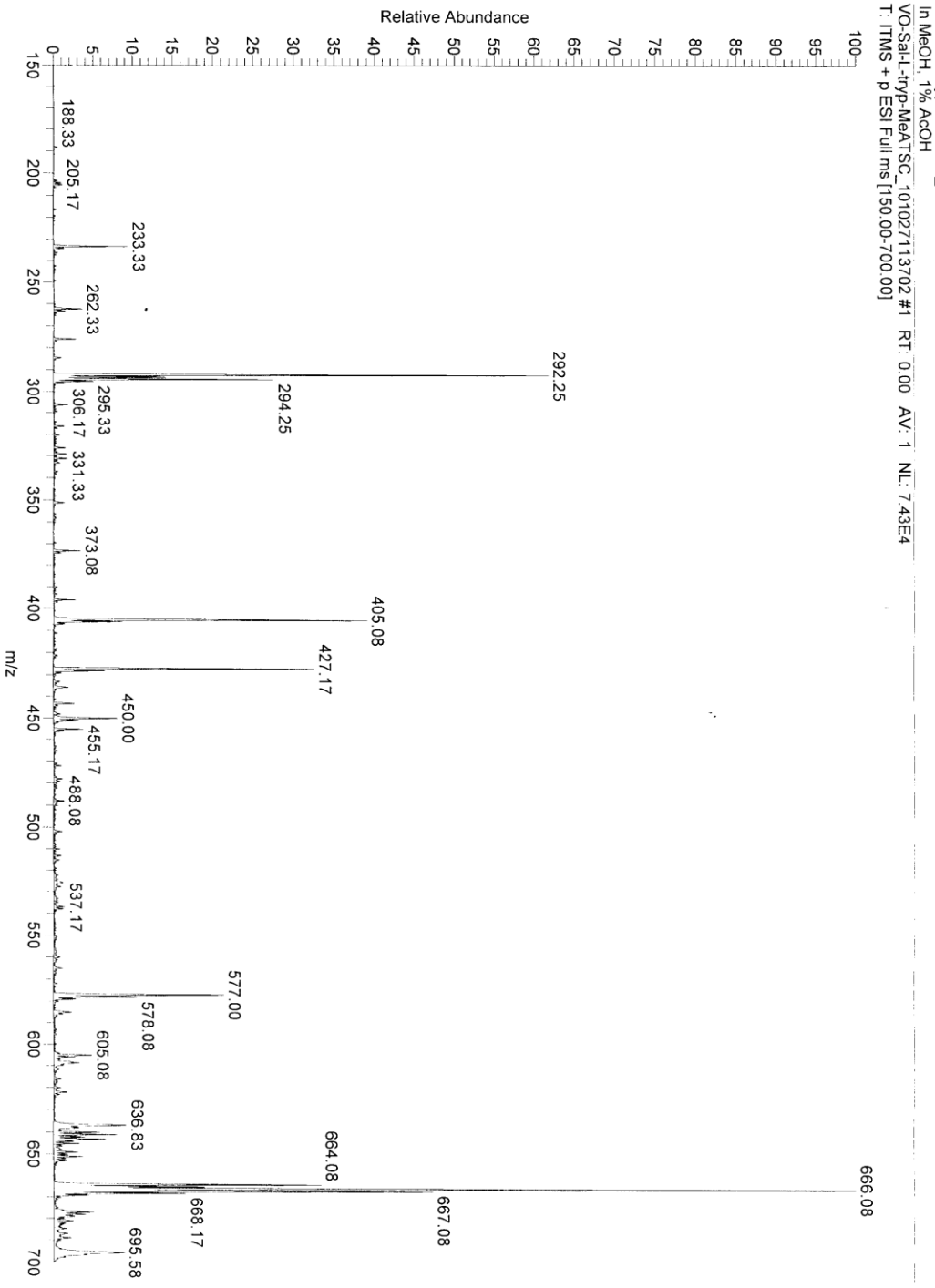

APPENDIX P

A MASS SPECTRUM OF COMPOUND **3** IN THE NEGATIVE MODE

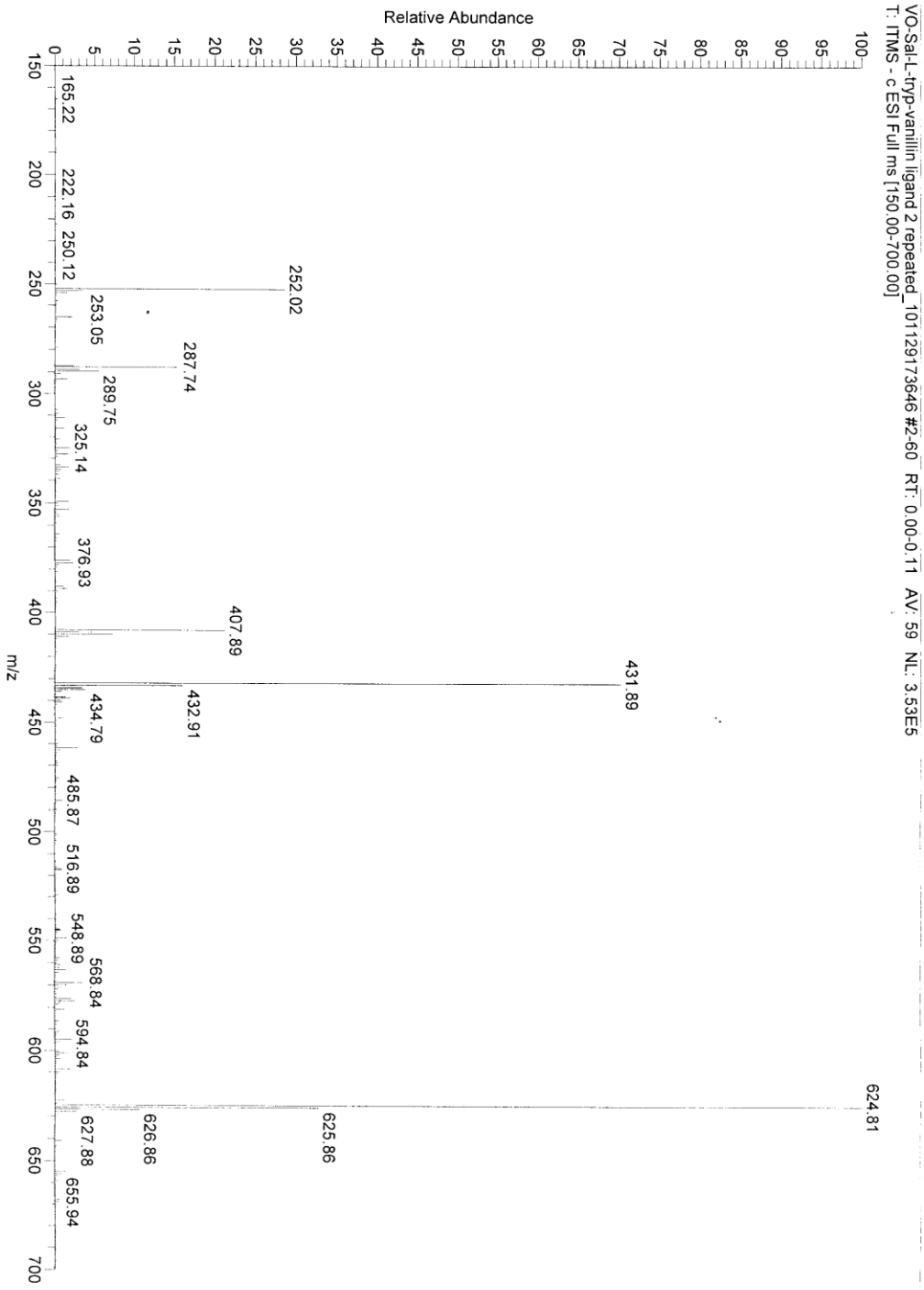

APPENDIX Q

A MASS SPECTRUM OF COMPOUND **4** IN THE POSITIVE MODE

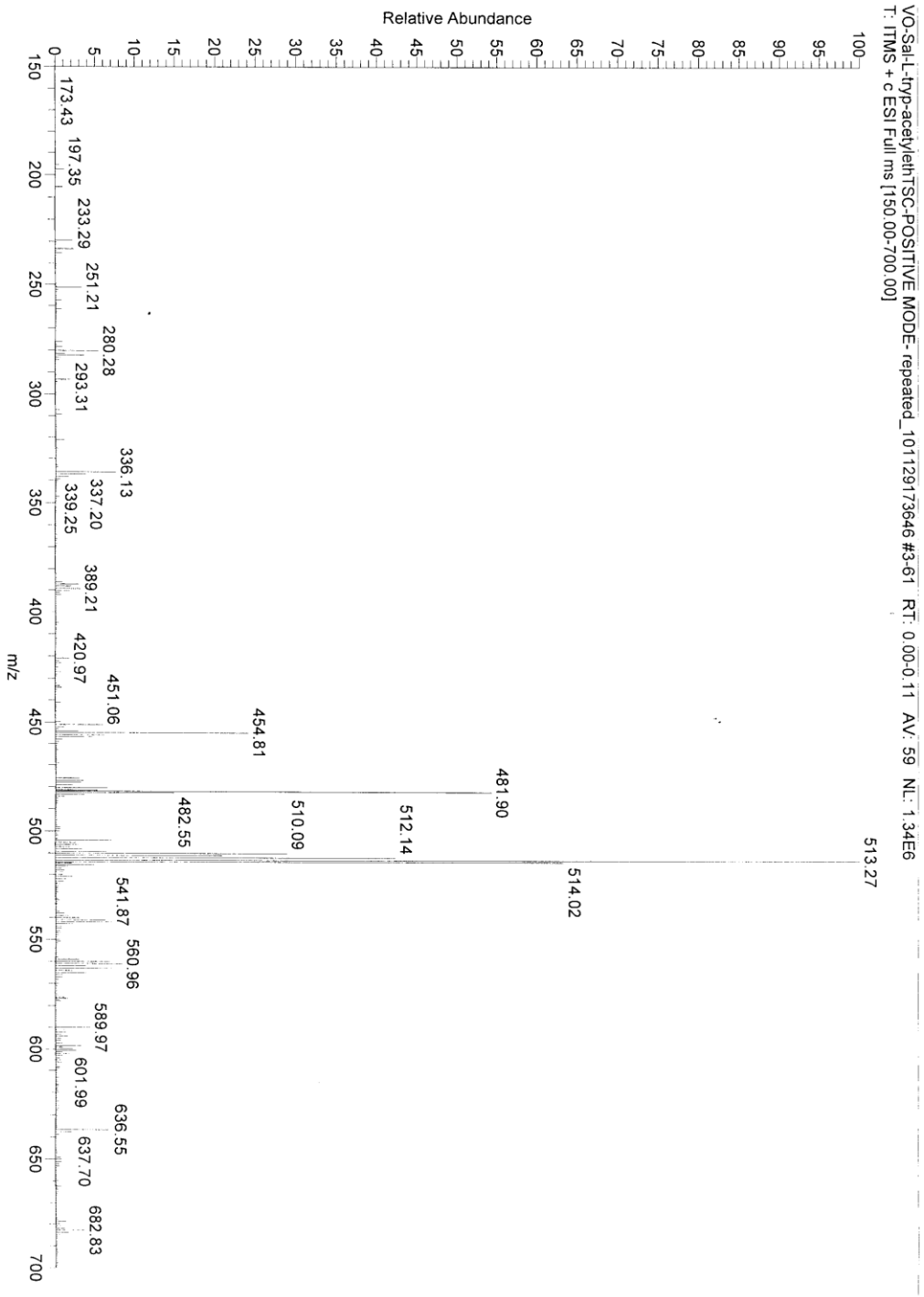

APPENDIX R

A MASS SPECTRUM OF [Zn(Sal-*L*-tryp)(H_2O)].0.25H_2O IN THE POSITIVE MODE

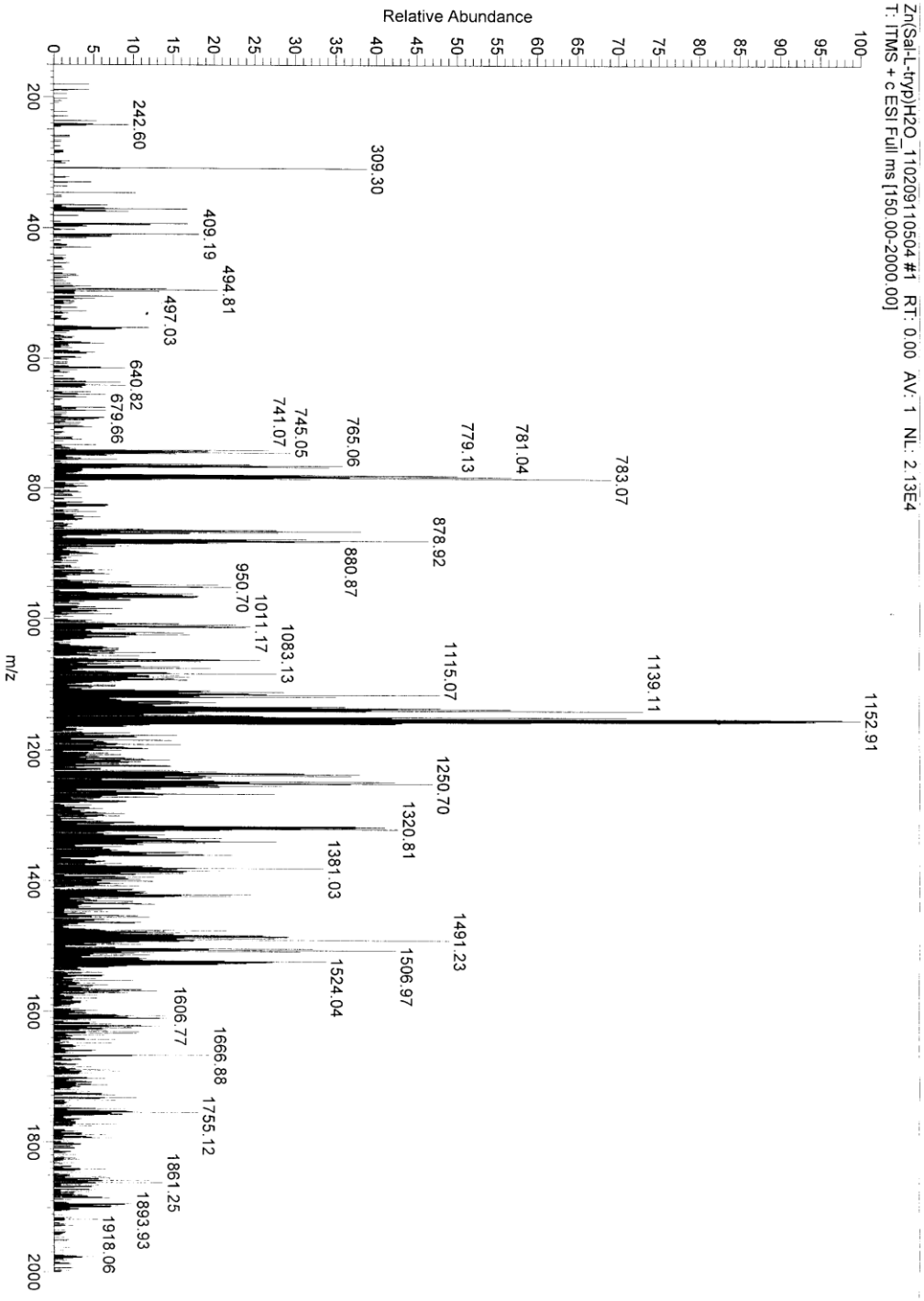

APPENDIX S

A MASS SPECTRUM OF OXIDISED PRODUCT ISOLATED FROM COMPOUND **1** IN THE POSITIVE MODE

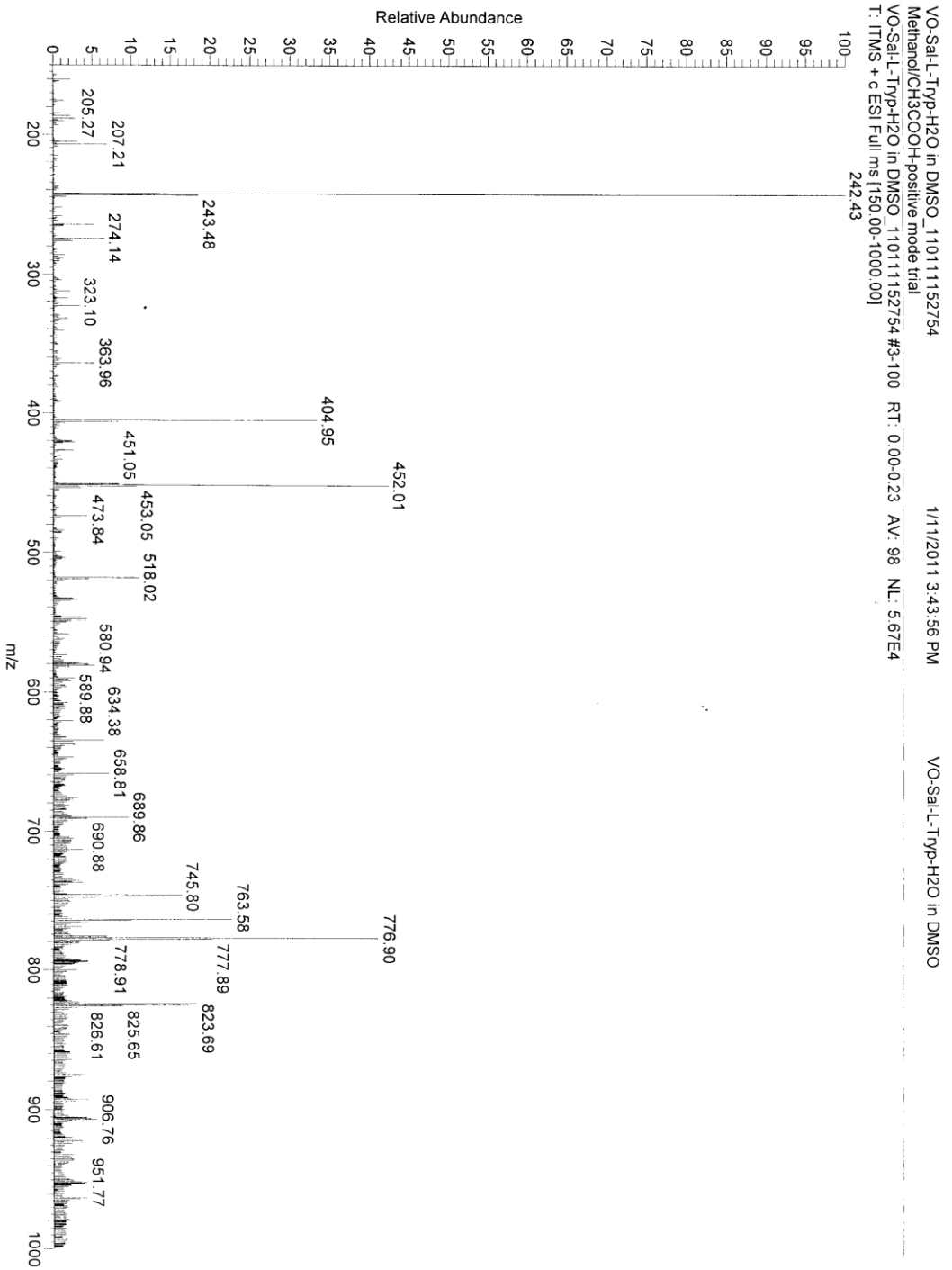

APPENDIX T

A MASS SPECTRUM OF OXIDIZED PRODUCT ISOLATED FROM COMPOUND **1** IN THE NEGATIVE MODE

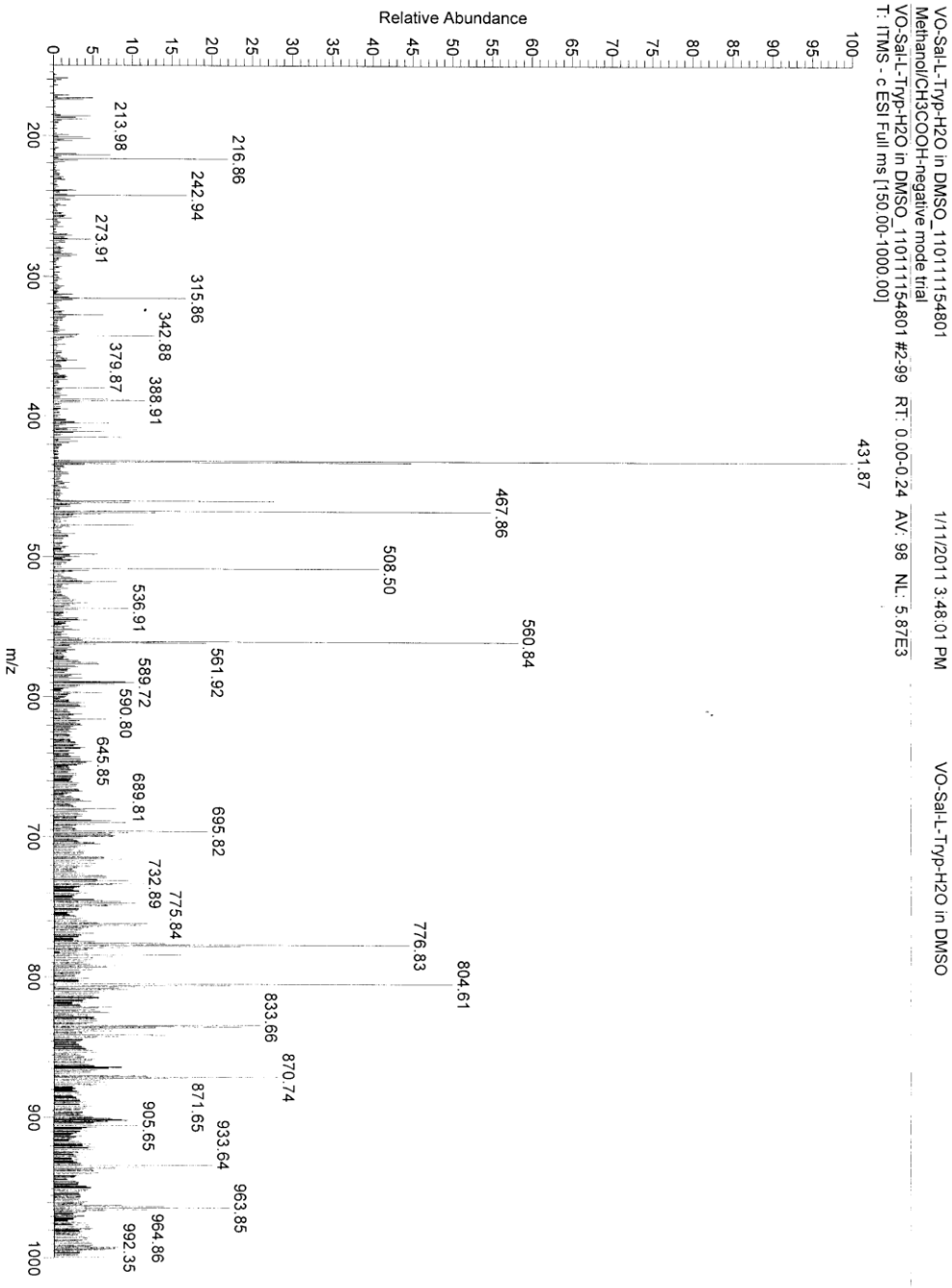

APPENDIX U

A MASS SPECTRUM OF OXIDIZED PRODUCT ISOLATED FROM COMPOUND **3** IN THE POSITIVE MODE

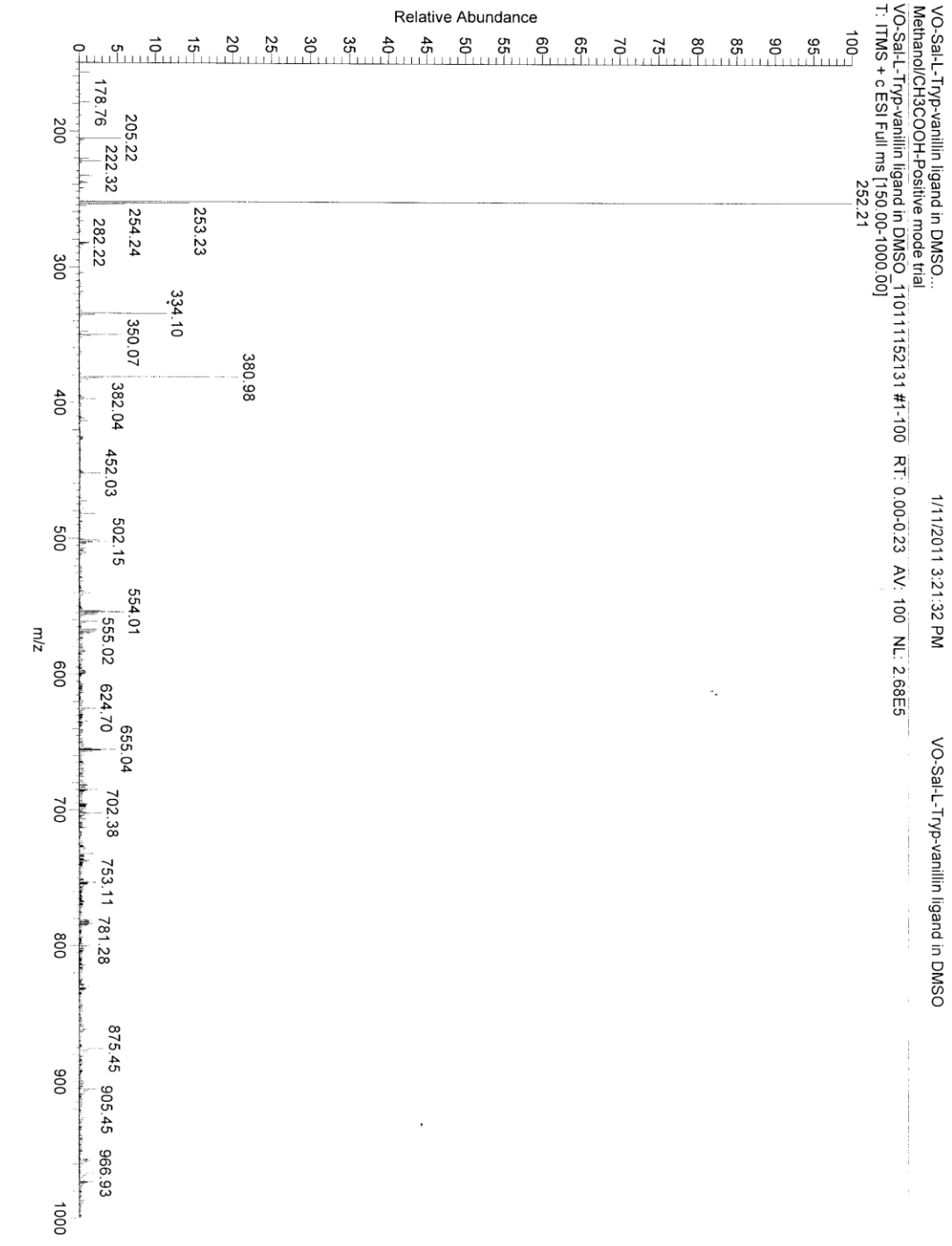

APPENDIX V

A MASS SPECTRUM OF OXIDIZED PRODUCT ISOLATED FROM COMPOUND 3 IN THE NEGATIVE MODE

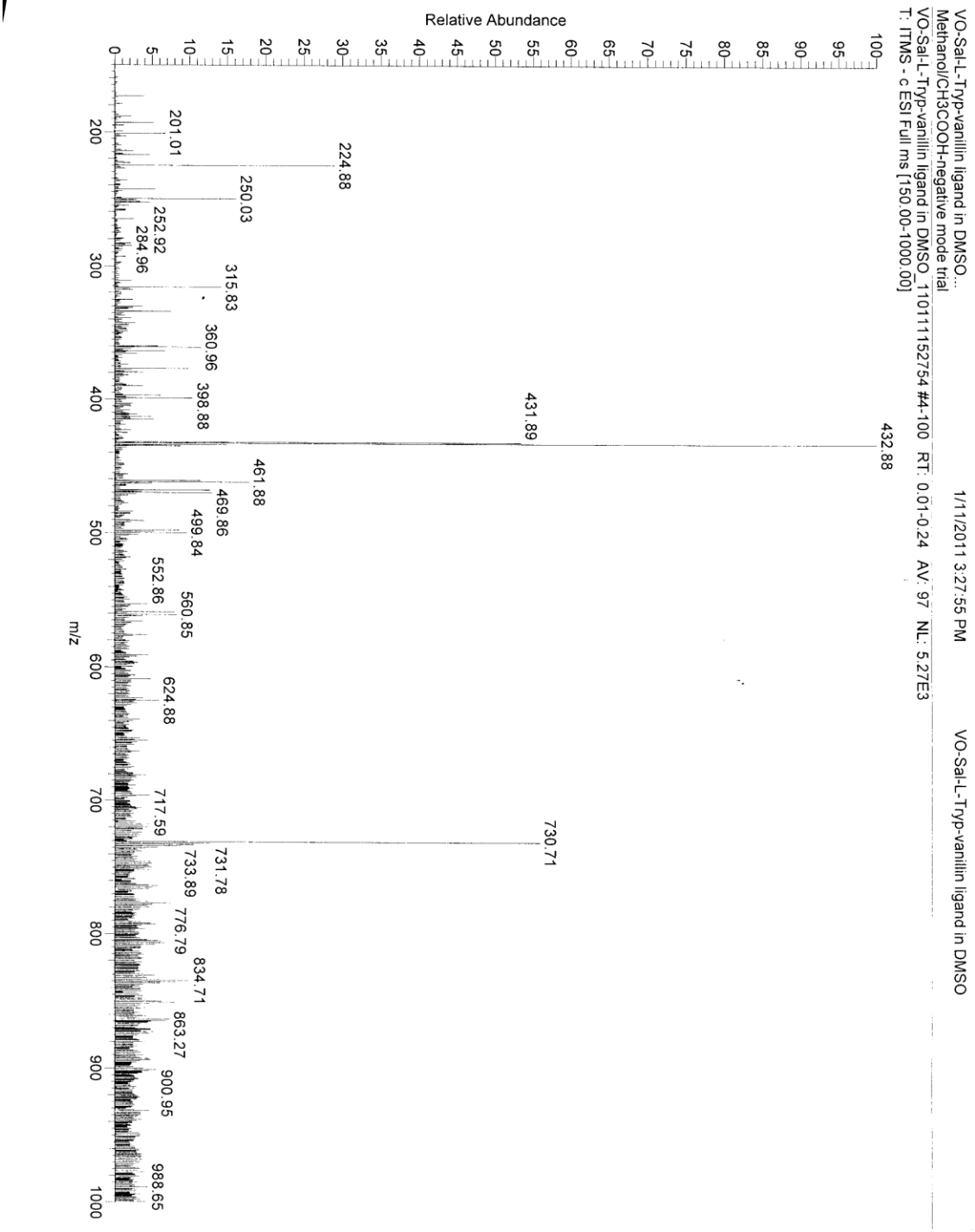

APPENDIX W

AN FT IR SPECTRUM OF COMPOUND

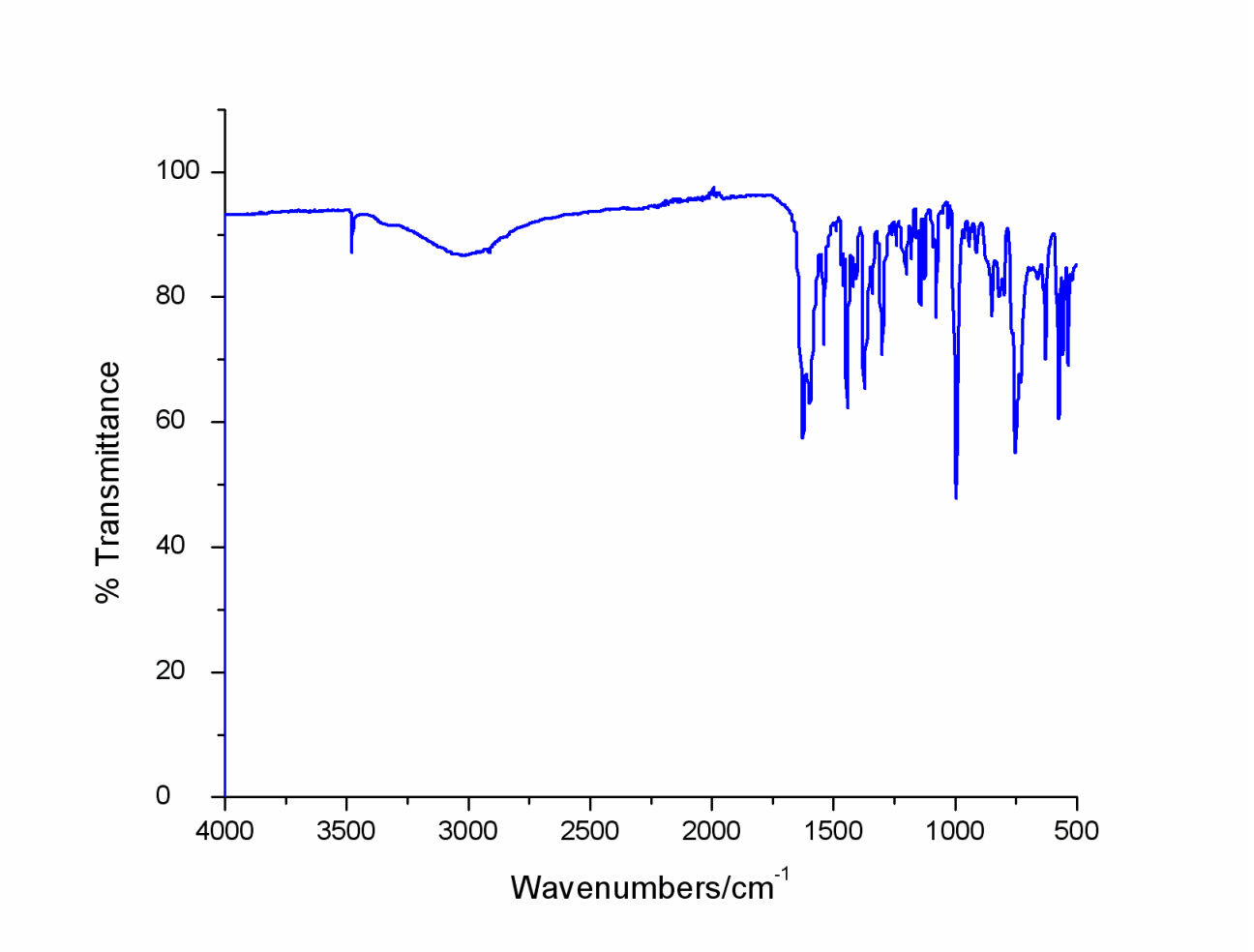

APPENDIX X

AN FT IR SPECTRUM OF COMPOUND **2**

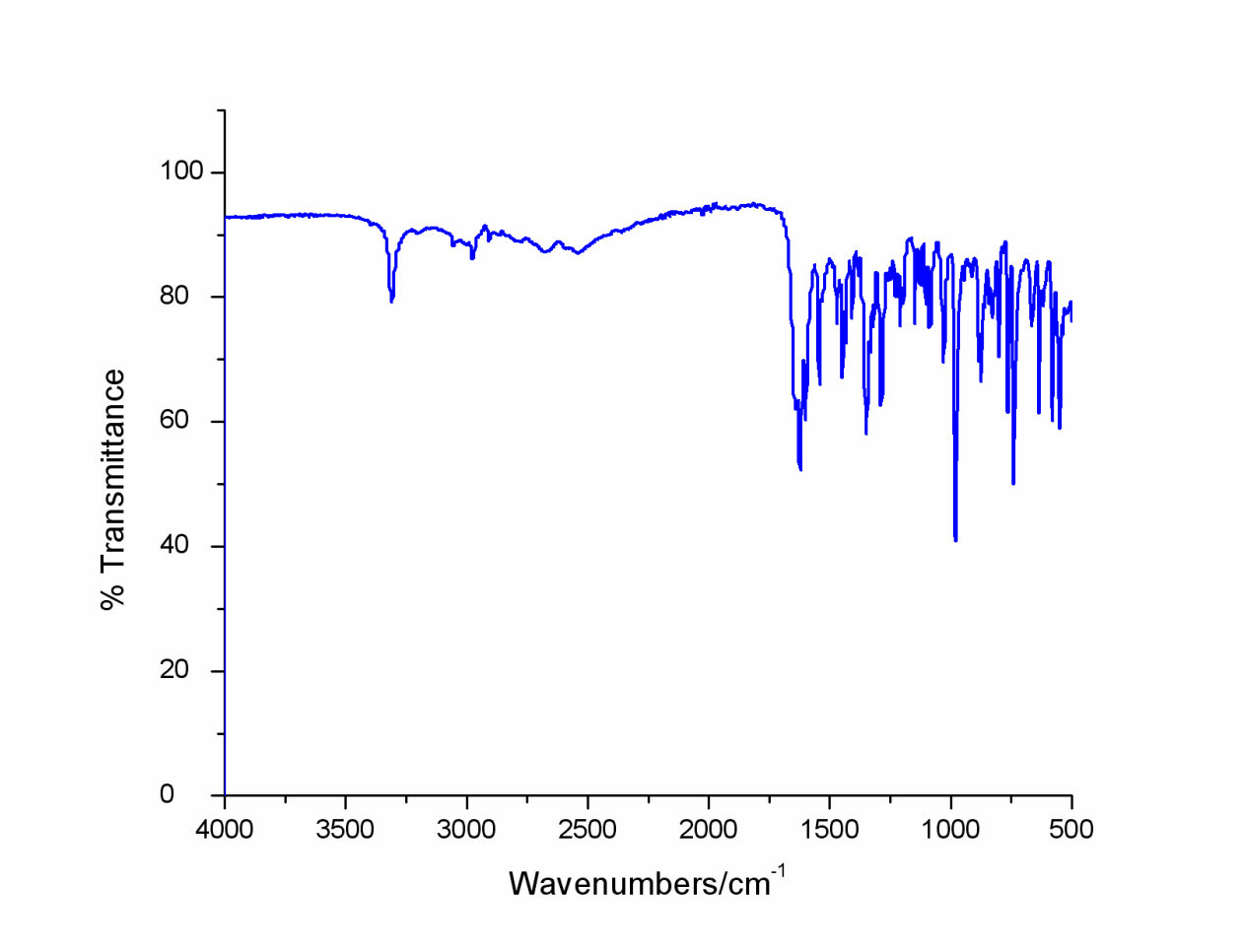

APPENDIX Y

AN FT IR SPECTRUM OF COMPOUND **3**

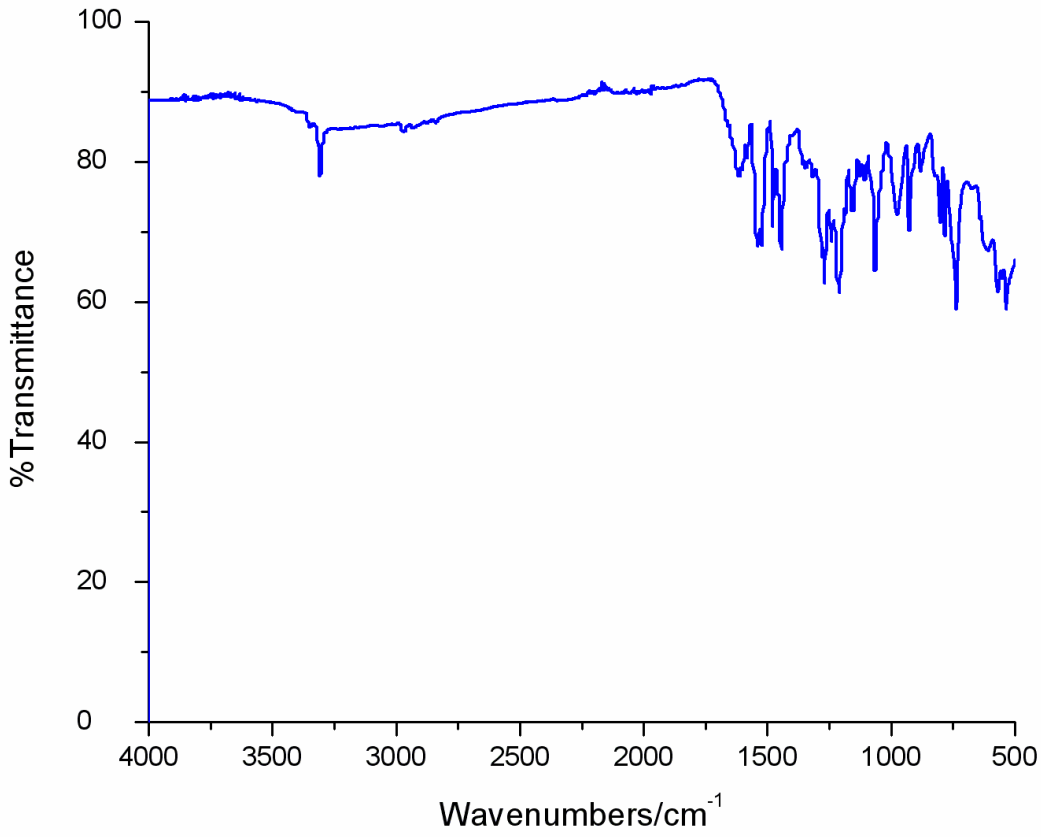

APPENDIX Z

AN FT IR SPECTRUM OF COMPOUND **4**

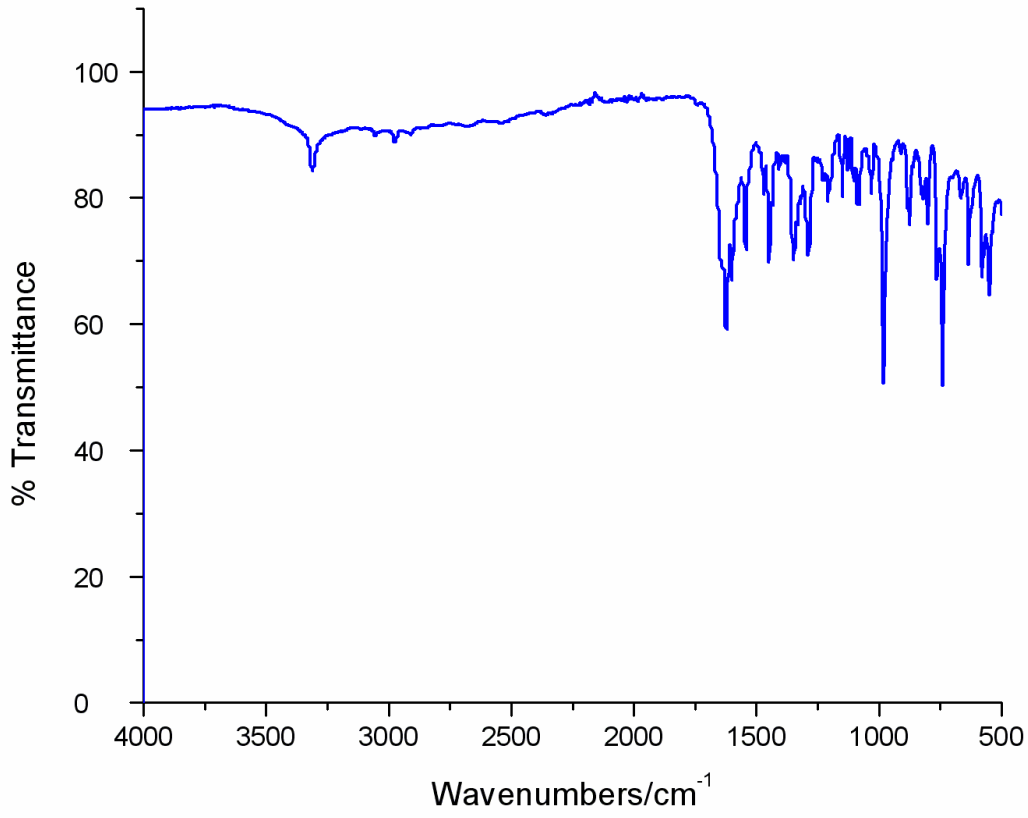

APPENDIX AA

AN FT IR SPECTRUM OF [Zn(Sal-*L*-tryp)(H_2O)].0.25H_2O

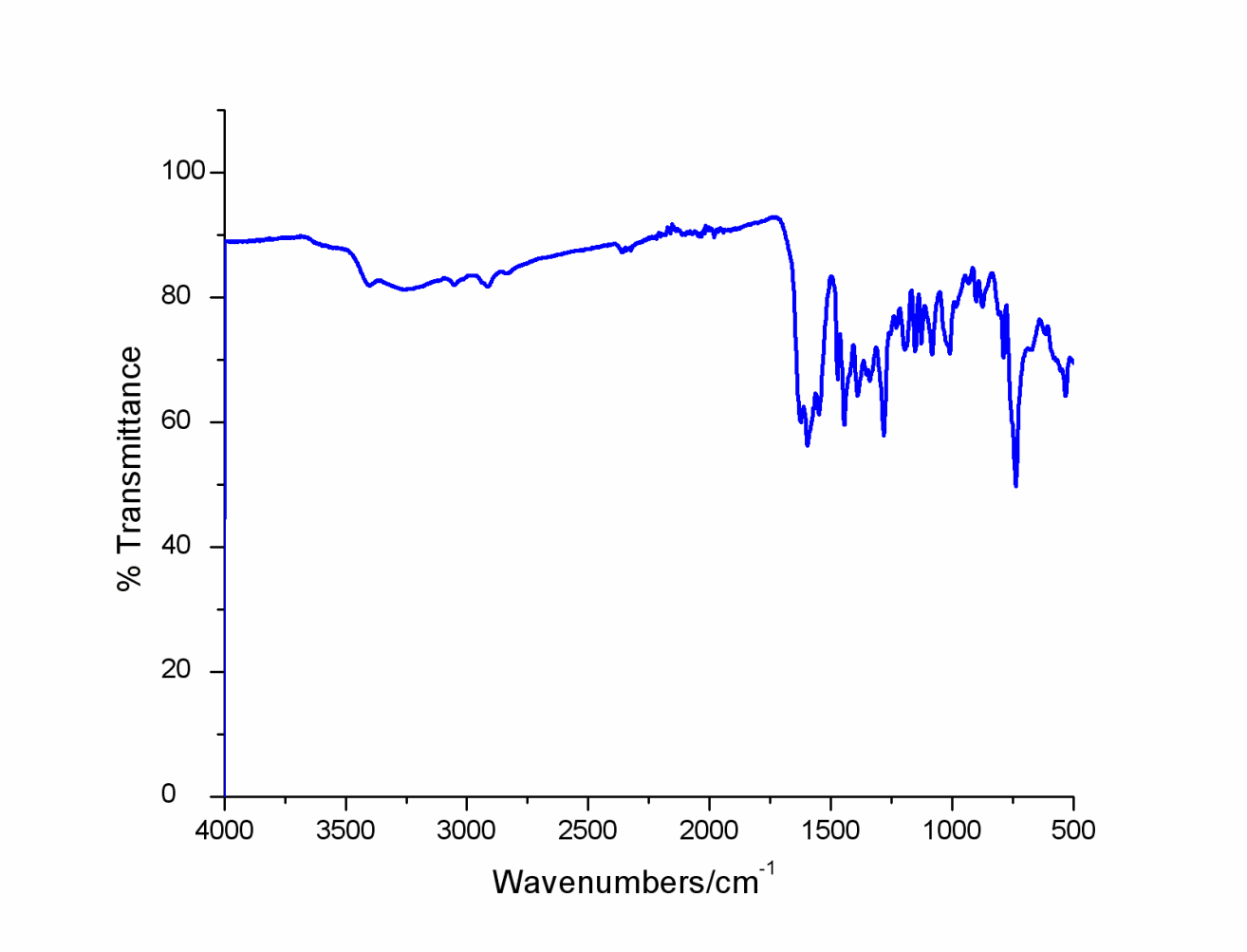

APPENDIX BB

A ^{1}H NMR SPECTRUM OF [Zn(Sal-*L*-tryp)(H_2O)].0.25H_2O IN DMSO-d_6

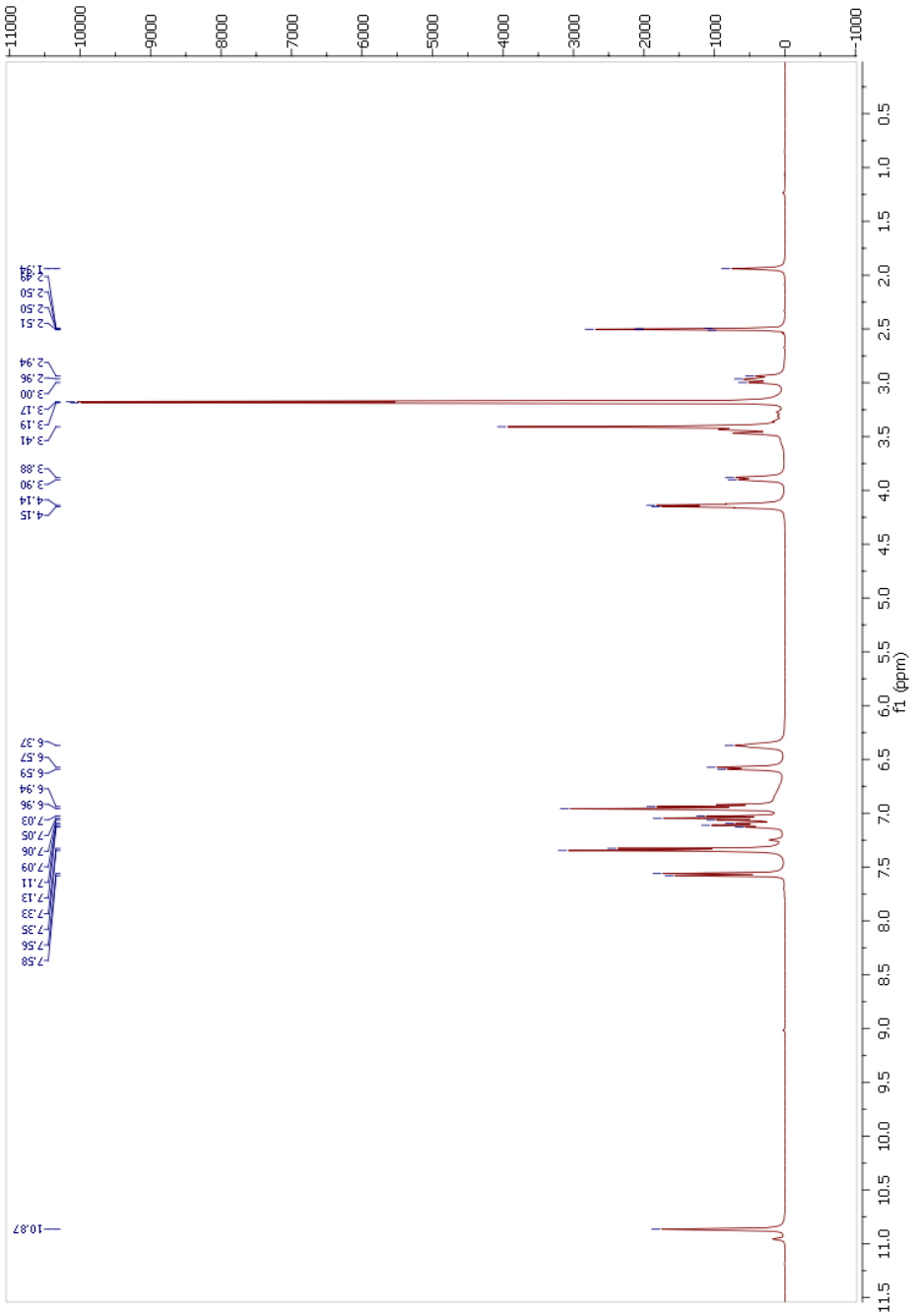

APPENDIX CC

A ^{1}H NMR SPECTRUM OF THE OXIDIZED PRODUCT OBTAINED FROM COMPOUND **1** IN DMSO-d_6

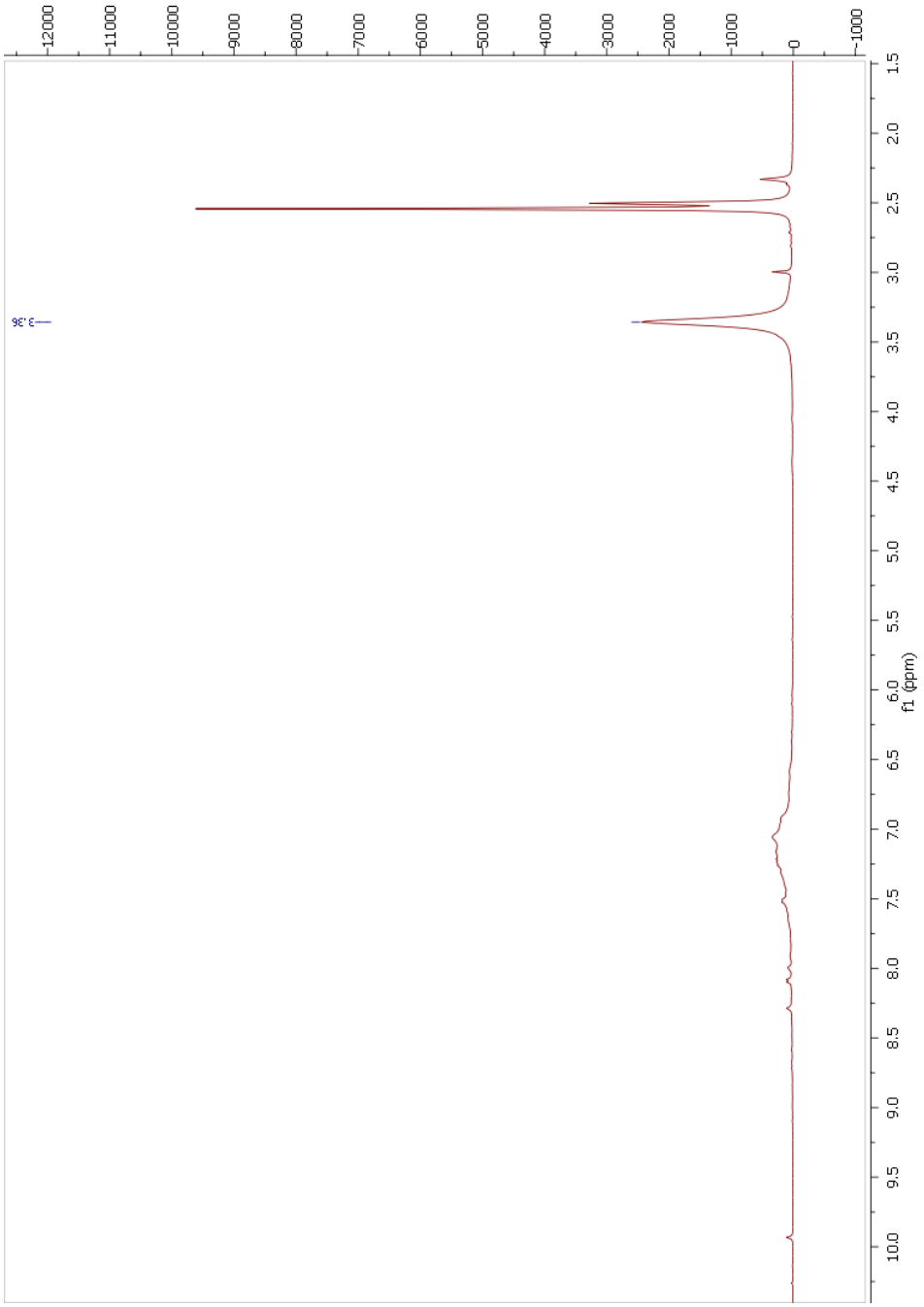

APPENDIX DD

A ^{1}H NMR SPECTRUM OF THE OXIDIZED COMPLEX DERIVED FROM COMPOUND **3** IN DMSO-d_6

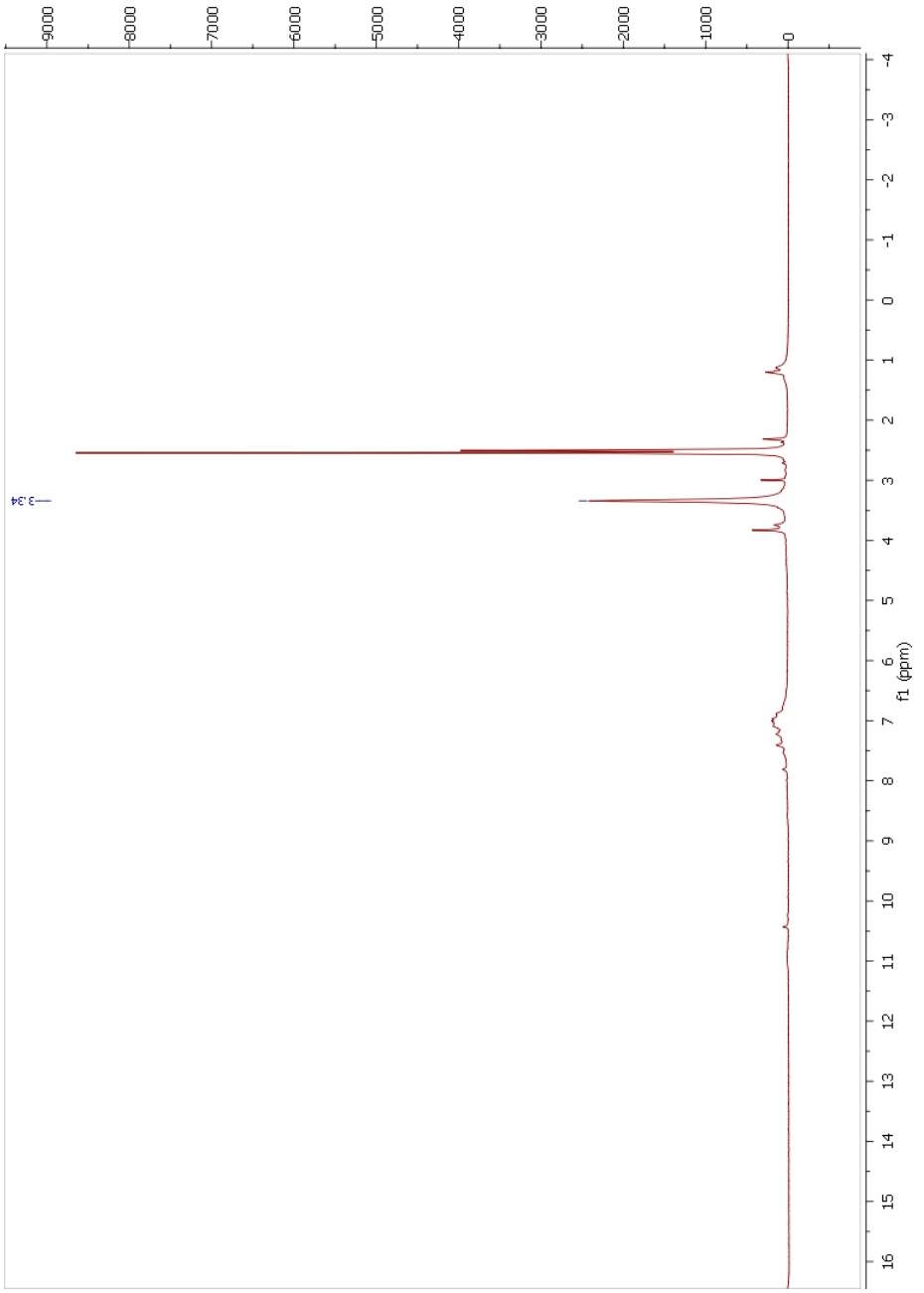

APPENDIX EE

UV-VISIBLE AND FLUORESCENCE SPECTRA FOR A 20 μM SOLUTION OF COMPOUND 2 IN DMSO. EXCITATION WAVELENGTH = 400 nm

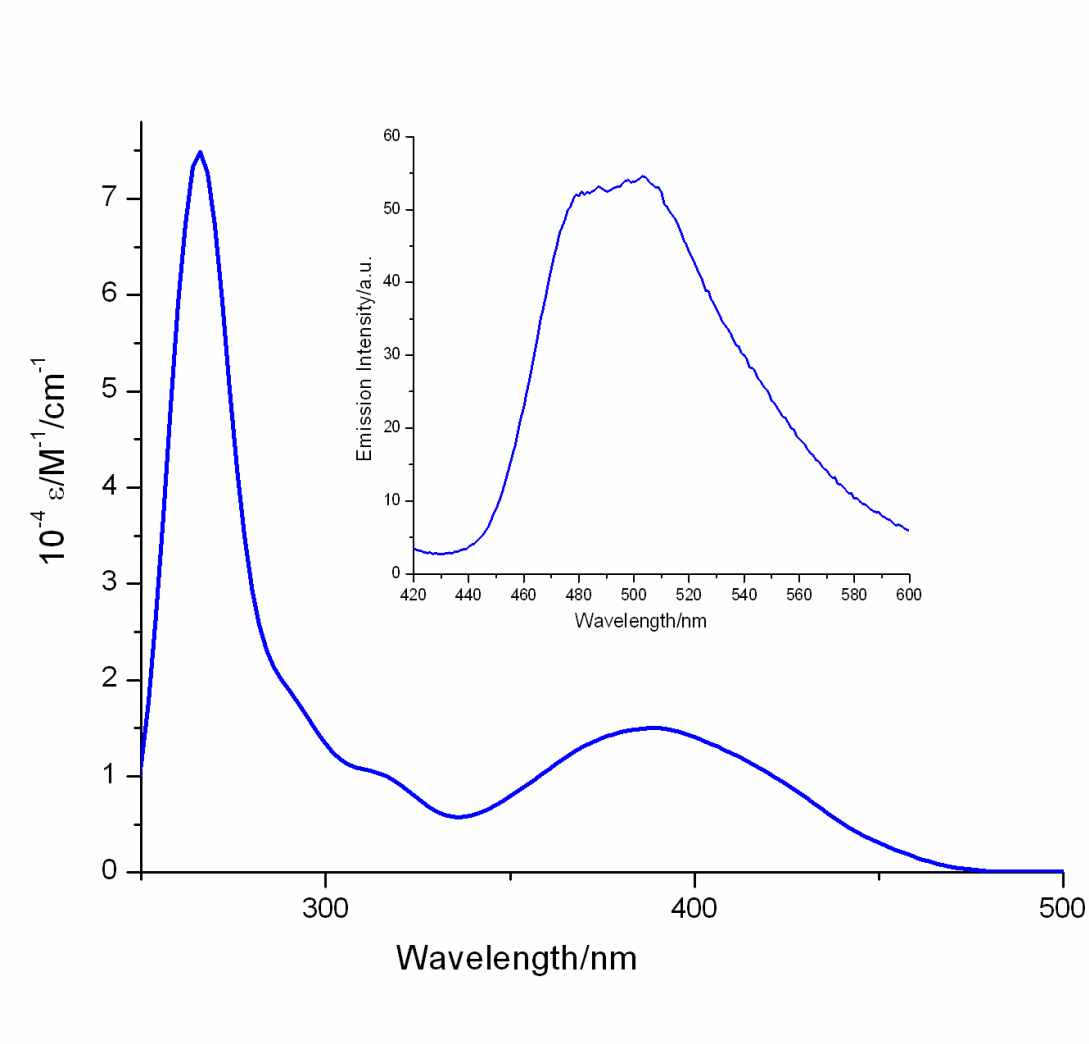

APPENDIX FF

UV-VISIBLE AND FLUORESCENCE SPECTRA FOR A 20 μM SOLUTION OF COMPOUND **3** IN DMSO. EXCITATION WAVELENGTH = 330 nm

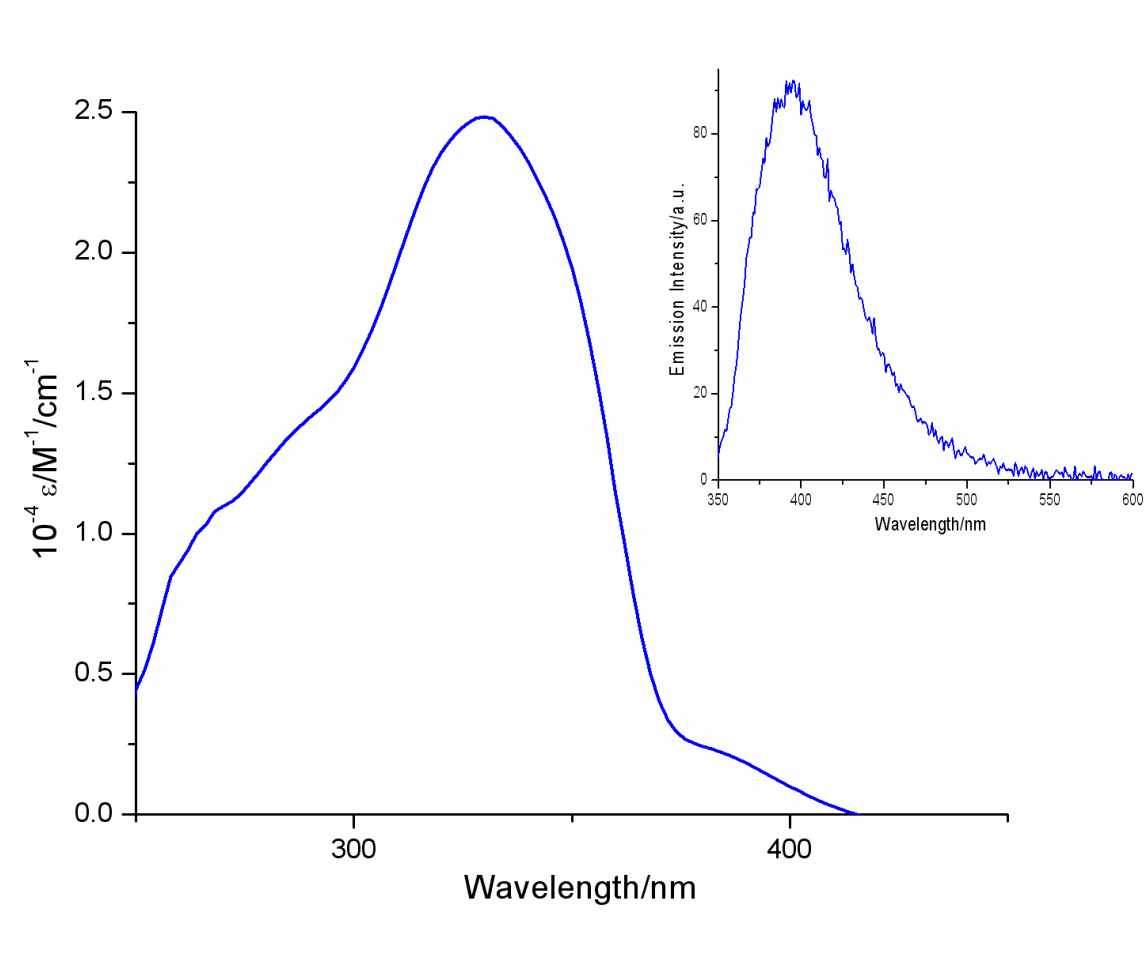

APPENDIX GG

UV-VISIBLE AND FLUORESCENCE SPECTRA FOR A 20 μM SOLUTION OF COMPOUND **4** IN DMSO. EXCITATION WAVELENGTH = 340 nm

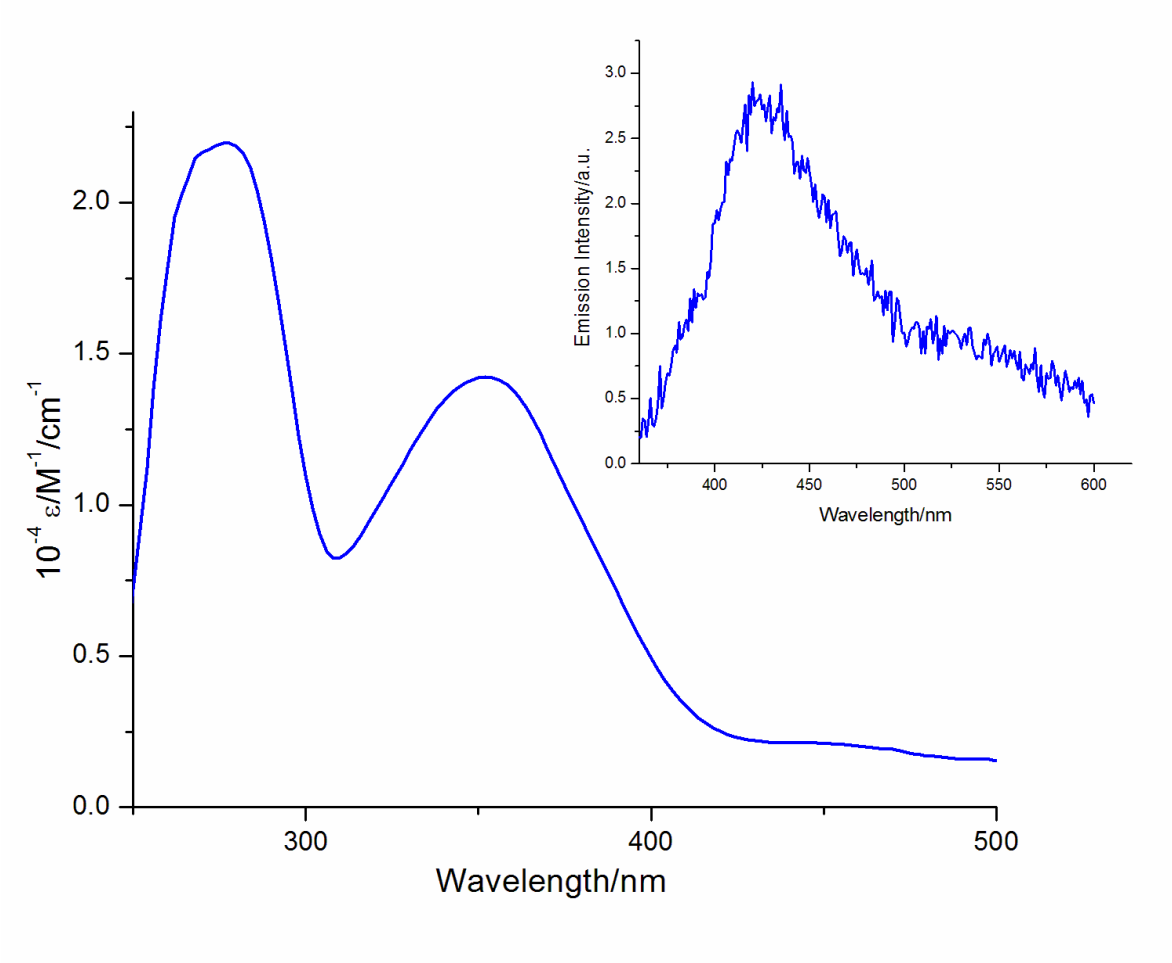

APPENDIX HH

SQUARE WAVE VOLTAMMOGRAMS: THE OXIDATION OF 1.0 mM SOLUTIONS COMPOUNDS 1-4 IN DMSO. ELECTRODES: PLATINUM WORKING ELECTRODE, PLATINUM AUXILIARY ELECTRODE AND Ag/Ag+ (0.01 M AgNO3 AND 0.10 M TBAP IN ACETONITRILE) REFERENCE ELECTRODE. SUPPORTING ELECTROLYTE = 0.1 M TBAP. INITIAL POTENTIAL = 0 V, FINAL POTENTIAL = +1.0 V, STEP E = 4 mV, S.W. AMPLITUDE = 25 mV, S.W. FREQUENCY = 15 Hz, FILTER = 100 Hz, AND QUIET TIME = 2 s

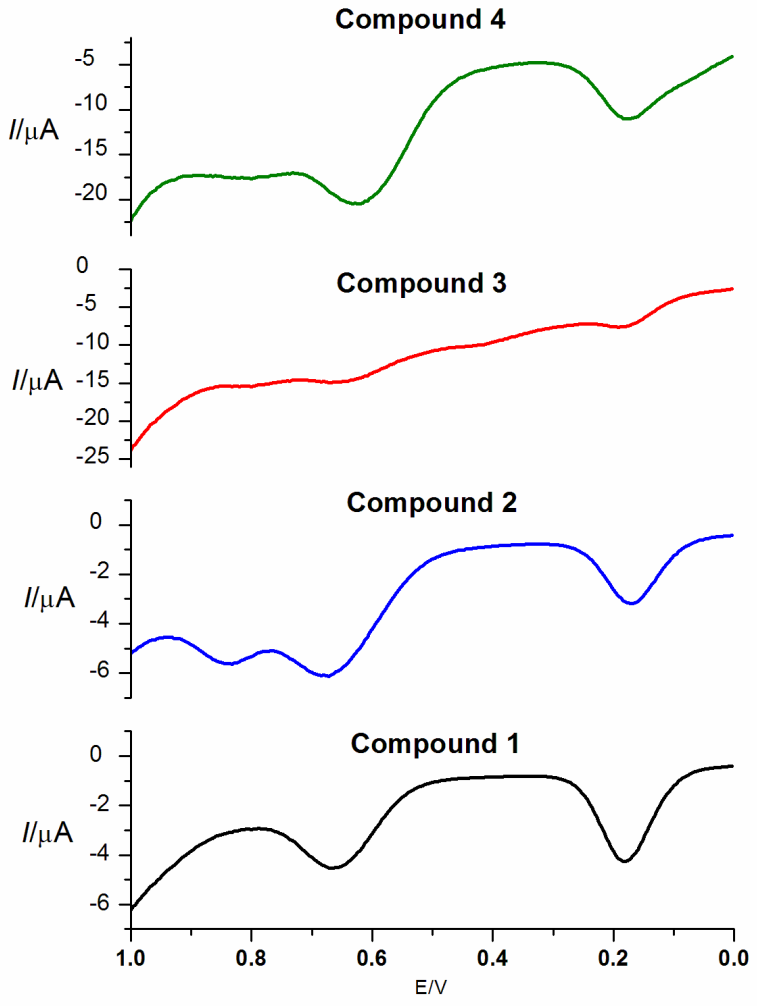

APPENDIX II

A SQUARE WAVE VOLTAMMOGRAM: THE OXIDATION OF A 1.0 MM SOLUTION [Zn(Sal-*L*-tryp)(H2O)].0.25H2O IN DMSO. ELECTRODES: PLATINUM WORKING ELECTRODE, PLATINUM AUXILIARY ELECTRODE AND Ag/Ag+ (0.01 M AgNO3 AND 0.10 M TBAP IN ACETONITRILE) REFERENCE ELECTRODE. SUPPORTING ELECTROLYTE = 0.1 M TBAP. INITIAL POTENTIAL = 0 V, FINAL POTENTIAL = +1.0 V, STEP E = 4 mV, S.W. AMPLITUDE = 25 mV, S.W. FREQUENCY = 15 Hz, FILTER = 100 Hz, AND QUIET TIME = 2 s

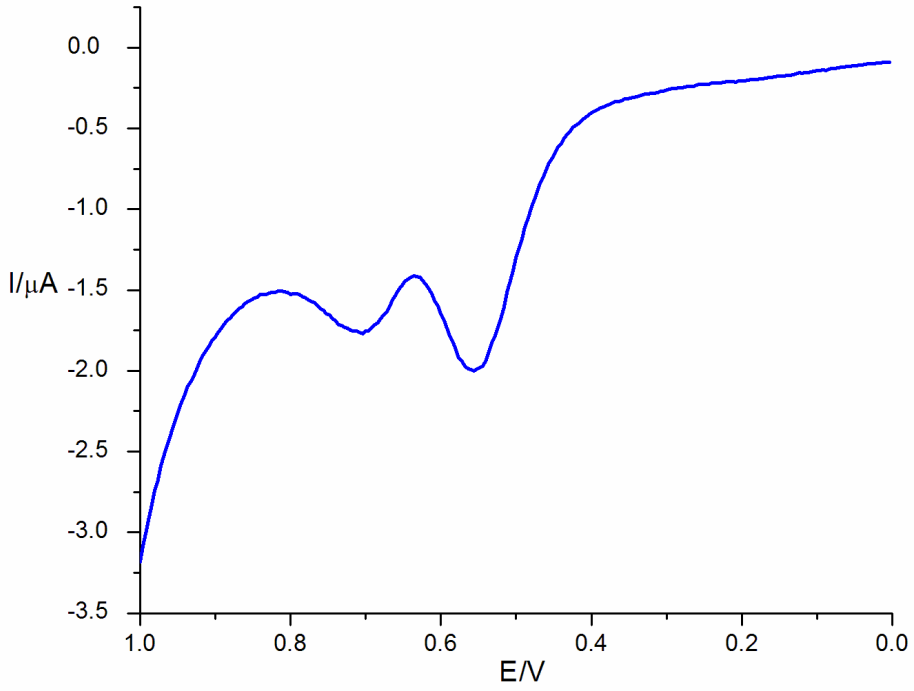

APPENDIX JJ

ATOMIC COORDINATES ($x\ 10^4$) AND EQUIVALENT ISOTROPIC DISPLACEMENT PARAMETERS ($A^2\ x\ 10^3$) FOR VENKAT35. U(eq) IS DEFINED AS ONE THIRD OF THE TRACE OF THE ORTHOGONALIZED Uij TENSOR

	x	y	z	U(eq)
S(1)	7608(1)	4402(1)	4836(1)	26(1)
S(2)	3123(1)	4067(1)	7194(1)	23(1)
N(1)	5081(1)	3382(1)	6207(1)	20(1)
N(2)	6001(1)	3320(1)	5703(1)	21(1)
N(3)	6006(1)	5421(1)	5737(1)	20(1)
N(4)	3033(2)	1718(1)	7328(1)	30(1)
C(1)	6484(2)	4402(2)	5460(1)	19(1)
C(2)	4599(2)	2389(2)	6452(1)	24(1)
C(3)	3608(2)	2598(2)	6982(1)	23(1)
C(4)	2174(2)	2220(2)	7788(1)	31(1)
C(5)	2091(2)	3456(2)	7789(1)	27(1)
C(6)	4934(2)	1099(2)	6252(1)	41(1)
C(7)	6390(2)	6658(2)	5541(1)	23(1)
C(8)	5569(2)	7599(2)	5915(1)	27(1)

APPENDIX KK

BOND LENGTHS [Å] AND ANGLES [°] FOR VENKAT35

S(1)-C(1)	1.6814(16)
S(2)-C(5)	1.7094(17)
S(2)-C(3)	1.7282(17)
N(1)-C(2)	1.284(2)
N(1)-N(2)	1.3691(18)
N(2)-C(1)	1.366(2)
N(2)-H(2N)	0.86(2)
N(3)-C(1)	1.329(2)
N(3)-C(7)	1.457(2)
N(3)-H(3N)	0.81(2)
N(4)-C(3)	1.312(2)
N(4)-C(4)	1.376(2)
C(2)-C(3)	1.474(2)
C(2)-C(6)	1.498(2)
C(4)-C(5)	1.349(3)
C(4)-H(4)	0.9500
C(5)-H(5)	0.9500
C(6)-H(6A)	0.9800
C(6)-H(6B)	0.9800
C(6)-H(6C)	0.9800
C(7)-C(8)	1.521(2)
C(7)-H(7A)	0.9900
C(7)-H(7B)	0.9900
C(8)-H(8A)	0.9800
C(8)-H(8B)	0.9800
C(8)-H(8C)	0.9800

C(5)-S(2)-C(3)	89.03(8)
C(2)-N(1)-N(2)	119.74(14)
C(1)-N(2)-N(1)	117.46(13)
C(1)-N(2)-H(2N)	118.7(13)
N(1)-N(2)-H(2N)	123.5(13)
C(1)-N(3)-C(7)	124.42(14)
C(1)-N(3)-H(3N)	117.4(15)
C(7)-N(3)-H(3N)	118.1(15)
C(3)-N(4)-C(4)	109.59(15)
N(3)-C(1)-N(2)	116.37(14)
N(3)-C(1)-S(1)	123.34(12)
N(2)-C(1)-S(1)	120.29(12)
N(1)-C(2)-C(3)	113.65(14)

N(1)-C(2)-C(6)	127.15(15)
C(3)-C(2)-C(6)	119.19(14)
N(4)-C(3)-C(2)	124.04(15)
N(4)-C(3)-S(2)	114.99(12)
C(2)-C(3)-S(2)	120.97(12)
C(5)-C(4)-N(4)	116.11(16)
C(5)-C(4)-H(4)	121.9
N(4)-C(4)-H(4)	121.9
C(4)-C(5)-S(2)	110.27(13)
C(4)-C(5)-H(5)	124.9
S(2)-C(5)-H(5)	124.9
C(2)-C(6)-H(6A)	109.5
C(2)-C(6)-H(6B)	109.5
H(6A)-C(6)-H(6B)	109.5
C(2)-C(6)-H(6C)	109.5
H(6A)-C(6)-H(6C)	109.5
H(6B)-C(6)-H(6C)	109.5
N(3)-C(7)-C(8)	110.14(14)
N(3)-C(7)-H(7A)	109.6
C(8)-C(7)-H(7A)	109.6
N(3)-C(7)-H(7B)	109.6
C(8)-C(7)-H(7B)	109.6
H(7A)-C(7)-H(7B)	108.1
C(7)-C(8)-H(8A)	109.5
C(7)-C(8)-H(8B)	109.5
H(8A)-C(8)-H(8B)	109.5
C(7)-C(8)-H(8C)	109.5
H(8A)-C(8)-H(8C)	109.5
H(8B)-C(8)-H(8C)	109.5

Symmetry transformations used to generate equivalent atoms:

APPENDIX LL

ANISOTROPIC DISPLACEMENT PARAMETERS (A^2 x 10^3) FOR VENKAT35. THE ANISOTROPIC DISPLACEMENT FACTOR EXPONENT TAKES THE FORM: -2 π^2 [h^2 a*^2 U11 + ... + 2 h k a* b* U12]

	U11	U22	U33	U23	U13	U12
S(1)	25(1)	18(1)	37(1)	3(1)	18(1)	0(1)
S(2)	30(1)	14(1)	28(1)	1(1)	13(1)	1(1)
N(1)	23(1)	18(1)	21(1)	1(1)	9(1)	-1(1)
N(2)	24(1)	14(1)	24(1)	-1(1)	12(1)	0(1)
N(3)	20(1)	16(1)	25(1)	2(1)	10(1)	-2(1)
N(4)	38(1)	17(1)	37(1)	1(1)	23(1)	0(1)
C(1)	17(1)	18(1)	22(1)	1(1)	3(1)	-1(1)
C(2)	30(1)	16(1)	27(1)	-1(1)	13(1)	0(1)
C(3)	29(1)	13(1)	28(1)	0(1)	13(1)	1(1)
C(4)	39(1)	20(1)	37(1)	2(1)	25(1)	0(1)
C(5)	32(1)	20(1)	30(1)	-2(1)	17(1)	3(1)
C(6)	52(1)	16(1)	58(1)	-2(1)	42(1)	-3(1)
C(7)	20(1)	15(1)	33(1)	2(1)	8(1)	-1(1)
C(8)	27(1)	17(1)	38(1)	1(1)	9(1)	0(1)

APPENDIX MM

HYDROGEN COORDINATES (x 10^4) AND ISOTROPIC DISPLACEMENT

PARAMETERS (A^2 x 10^3) FOR VENKAT35

	x	y	z	U(eq)
H(2N)	6339(19)	2640(20)	5564(10)	25
H(3N)	5438(19)	5345(19)	6017(10)	24
H(4)	1668	1725	8088	38
H(5)	1538	3919	8079	33
H(6A)	4809	992	5737	62
H(6B)	4381	525	6503	62
H(6C)	5830	936	6386	62
H(7A)	6294	6763	5018	27
H(7B)	7302	6787	5678	27
H(8A)	4669	7479	5772	41
H(8B)	5839	8427	5783	41
H(8C)	5670	7495	6433	41

REFERENCES

(1) Tsaramyrsi, M.; Kavousanaki, D.; Raptopoulou, C. P.; Terzis, A.; Salifoglou, A. *Inorg. Chim. Acta* **2001**, *320*, 47.

(2) Barceloux, D. G. *J. Toxicol. Clin. Toxicol.* **1999**, *37*, 265.

(3) Crans, D. C.; Smee, J. J.; Gaidamauskas, E.; Yang, L. *Chem. Rev.* **2004**, *104*, 849.

(4) Crans, D. C. *Pure Appl. Chem.* **2005**, *77*, 1497.

(5) Roman's Dieties. http://www.candlesandwicksmydeities.blogspot.com/ (accessed 11/27/11).

(6) Willsky, G. R.; Takeuchi, E. S.; Tracey, A. S. In *Vanadium*; CRC Press: 2007, 1.

(7) Evangelou Angelos, M. *Crit.Rev. Oncol. Hematol.* **2002**, *42*, 249.

(8) Pawlik, J. R. *Chem. Rev.* **1993**, *93*, 1911.

(9) Willsky, G. R.; Goldfine, A. B.; Kostyniak, P. J.; McNeill, J. H.; Yang, L. Q.; Khan, H. R.; Crans, D. C. *J. Inorg. Biochem.* **2001**, *85*, 33.

(10) Zhang, X.; Tracey, A. S. *Acta Chem. Scand.* **1992**, *46*, 1170.

(11) Willsky, G. R.; Goldfine, A. B.; Kostyniak, P. J. *ACS Symp. Ser.* **1998**, *711*, 278.

(12) Taylor, P. D. *Chem. Commun.* **1996**, 405.

(13) Ten, B. H. B.; Schoemaker, H. E.; Wever, R. *Eur. J. Biochem.* **2001**, *268*, 132.

(14) Nagesh, K. S. *VIVECHAN IJR* **2010**, *1*, 10.

(15) Weckhuysen, B. M.; Keller, D. E. *Catal. Today* **2003**, *78*, 25.

(16) Cotton, F. A.; Wilkinson, G.; Murillo, C. A.; Bochmann, M. *Advanced Inorganic Chemistry*, 6 th ed., John Wiley & Sons Inc., New York, NY, **1999**.

(17) Buglyo, P.; Crans, D. C.; Nagy, E. M.; Lindo, R. L.; Yang, L.; Smee, J. J.; Jin, W.; Chi, L.-H.; Godzala, M. E., III; Willsky, G. R. *Inorg. Chem.* **2005**, *44*, 5416.

(18) Meier, R.; Boddin, M.; Mitzenheim, S.; Kanamori, K. *Met. Ions Biol. Syst.* **1995**, *31*, 45.

(19) Rehder, D. *Coord. Chem. Rev.* **1999**, *182*, 297.

(20) Kanamori, K.; Ookubo, Y.; Ino, K.; Kawai, K.; Michibata, H. *Inorg. Chem.* **1991**, *30*, 3832.

(21) Fry, F. H.; Dougan, B. A.; McCann, N.; Ziegler, C. J.; Brasch, N. E. *Inorg. Chem.* **2005**, *44*, 5197.

(22) Vanadium Compounds. http://www.scribd.com/doc/30127991/Vanadium-Compounds (accessed 11/27/11).

(23) Cotton, F. A.; Wilkinson, G.; Murillo, C. A.; Bochmann, M. *Advanced Inorganic Chemistry*, 2 nd ed., John Wiley & Sons inc., New York, NY, **1999**.

(24) Kaul, E. *Experimental Investigation of New Low-Dimensional Spin Systems in Vanadium Oxides* **2005**.

(25) Bondareva, V. M.; Andrushkevich, T. V.; Lapina, O. B. *Catal. Today* **2000**, *61*, 173.

(26) Kanamori, K.; Teraoka, M.; Maeda, H.; Okamoto, K. *Chem. Lett.* **1993**, 1731.

(27) Crans, D. C.; Tracey, A. S. *ACS Symp. Ser.* **1998**, *711*, 2.

(28) Francavilla, J.; Chasteen, N. D. *Inorg. Chem.* **1975**, *14*, 2860.

(29) Boyd, D. W.; Kustin, K. *Adv. Inorg. Biochem.* **1984**, *6*, 311.

(30) Zhou, X.; Wei, C.; Li, M.; Qiu, S.; Li, X. *Hydrometallurgy* **2011**, *106*, 104.

(31) Iannuzzi, M. M.; Rieger, P. H. *Inorg. Chem.* **1975**, *14*, 2895.

(32) Livage, J. *Materials* **2010**, *3*, 4175.

(33) Cruywagen, J. J.; Heyns, J. B. B.; Westra, A. N. *Inorg. Chem.* **1996**, *35*, 1556.

(34) Naeem, A.; Westerhoff, P.; Mustafa, S. *Water Res.* **2007**, *41*, 1596.

(35) Baes, C. F., Jr.; Mesmer, R. E. *The Hydrolysis of Cations*; Wiley-Interscience, **1976**.

(36) Pourbaix, M. *Atlas of Electrochemical Equilibria in Aqueous Solutions*; Pergamon, 1966.

(37) Slebodnick, C.; Hamstra, B. J.; Pecoraro, V. L. *Struct. Bonding* **1997**, *89*, 51.

(38) Chasteen, N. D. *Struct. Bonding* **1983**, *53*, 105.

(39) Heath, E.; Howarth, O. W. *J. Chem. Soc., Dalton Trans.* **1981**, 1105.

(40) Greenwood, N. N.; Earnshaw, A. *Chemistry of the elements*, 2 nd ed., Pergamon Press plc, United Kingdom, Oxford, **1984**.

(41) Pettersson, L.; Hedman, B.; Andersson, I.; Ingri, N. *Chem. Scr*. **1983**, *22*, 254.

(42) Pettersson, L.; Andersson, I.; Hedman, B. *Chem. Scr.* **1985**, *25*, 309.

(43) Crans, D. C.; Mahroof-Tahir, M.; Keramidas, A. D. *Mol. Cell. Biochem.* **1995**, *153*, 17.

(44) Tracey, A. S.; Jaswal, J. S.; Angus-Dunne, S. J. *Inorg. Chem.* **1995**, *34*, 5680.

(45) Nath, M.; Saini, P. K. *J. Chem. Soc., Dalton Trans.* **2011**, *40*, 7077.

(46) Chavan, S. P.; Rasapalli, S. *Tetrahedron Lett.* **2004**, *45*, 3941.

(47) Rathelot, P.; Azas, N.; El-Kashef, H.; Delmas, F.; Di, G. C.; Timon-David, P.; Maldonado, J.; Vanelle, P. *Eur. J. Med. Chem.* **2002**, *37*, 671.

(48) Pawar, R. P.; Andurkar, N. M.; Vibhute, Y. B. *J. Indian Chem. Soc.* **1999**, *76*, 271.

(49) Bekhit, A. A.; Fahmy, H. T. Y.; Rostom, S. A. F.; Baraka, A. M. *Eur. J. Med. Chem.* **2003**, *38*, 27.

(50) Cakir, S.; Odabasoglu, M.; Bicer, E.; Yazar, Z. *J. Mol. Struct.* **2009**, *918*, 81.

(51) Williams, D. R. *Chem Rev* **1972**, *72*, 203.

(52) Pandeya, S. N.; Sriram, D.; Nath, G.; DeClercq, E. *Eur. J. Pharm. Sci.* **1999**, *9*, 25.

(53) Bain, G. A.; West, D. X.; Krejci, J.; Valdes-Martinez, J.; Hernandez-Ortega, S.; Toscano, R. A. *Polyhedron* **1996**, *16*, 855.

(54) Sen, S.; Talukder, P.; Dey, S. K.; Mitra, S.; Rosair, G.; Hughes, D. L.; Yap, G. P. A.; Pilet, G.; Gramlich, V.; Matsushita, T. *J. Chem. Soc., Dalton Trans.* **2006**, 1758.

(55) Maurya, M. R.; Bisht, M.; Kumar, A.; Kuznetsov, M. L.; Avecilla, F.; Pessoa, J. C. *J. Chem. Soc., Dalton Trans.* **2011**, *40*, 6968.

(56) Frausto da Silva, J. J. R.; Wootton, R.; Gillard, R. D. *J. Chem. Soc., Dalton Trans.* **1970**, 3369.

(57) Casella, L.; Gullotti, M.; Pintar, A.; Colonna, S.; Manfredi, A. *Inorg. Chim. Acta* **1988**, *144*, 89.

(58) Cavaco, I.; Pessoa, J. C.; Costa, D.; Duarte, M. T.; Gillard, R. D.; Matias, P. *J. Chem. Soc., Dalton Trans.* **1994**, 149.

(59) Pessoa, J. C.; Calhorda, M. J.; Cavaco, I.; Costa, P. J.; Correia, I.; Costa, D.; Vilas-Boas, L. F.; Felix, V.; Gillard, R. D.; Henriques, R. T.; Wiggins, R. *J. Chem. Soc., Dalton Trans.* **2004**, 2855.

(60) Cavaco, I.; Pessoa, J. C.; Duarte, M. T.; Henriques, R. T.; Matias, P. M.; Gillard, R. D. *J. Chem. Soc., Dalton Trans.* **1996**, 1989.

(61) Mondal, S.; Ghosh, P.; Chakravorty, A. *Inorg. Chem.* **1997**, *36*, 59.

(62) Mishra, A. P.; Soni, M. *Met Based Drugs* **2008**, *2008*, 875410.

(63) Prasad, K. S.; Kumar, L. S.; Shekar, S. C.; Prasad, M.; Revanasiddappa, H. D. *Chem. Sci. J.* **2011**, 1.

(64) Maggio, B.; Daidone, G.; Raffa, D.; Plescia, S.; Mantione, L.; Catena, C. V. M.; Mangano, N. G.; Caruso, A. *Eur. J. Med. Chem.* **2001**, *36*, 737.

(65) Rang, H. P.; Dale, M. M. *Pharmacology*, 2nd ed., Churchill Livingstone, Melbourne. **1991**.

(66) Priestman, T. J. *Cancer Chemotherapy: An Introduction*; 3rd ed; Springer-Verlag: London **1989**.

(67) Koepf-Maier, P.; Koepf, H. *Chem. Rev.* **1987**, *87*, 1137.

(68) Whittaker, J.; McFadyen, W. D.; Wickham, G.; Wakelin, L. P. G.; Murray, V. *Nucleic Acids Res.* **1998**, *26*, 3933.

(69) West, D. X.; Padhye, S. B.; Sonawane, P. B. *Struct. Bonding* **1991**, *76*, 1.

(70) Zhang, C. X.; Lippard, S. J. *Curr. Opin. Chem. Biol.* **2003**, *7*, 481.

(71) Rafique, S.; Idrees, M.; Nasim, A.; Akbar, H.; Athar, A. *Biotechnol. Mol. Biol. Rev.* **2010**, *5*, 38.

(72) Kostova, I. *Recent Pat. Anti-Cancer Drug Discovery* **2006**, *1*, 1.

(73) Kostova, I. *Anti-Cancer Agents Med. Chem.* **2009**, *9*, 827.

(74) Jakupec, M. A.; Galanski, M.; Arion, V. B.; Hartinger, C. G.; Keppler, B. K. *Dalton Trans.* **2008**, 183.

(75) Fricker, S. P. *Introduction, In Metal Compounds in Cancer Therapy; Fricker, S. Ed.; Chapman and Hall: London* **1994**, 1.

(76) English, L. H.; Macara, I. G.; Cantley, L. C. *J Cell Biol* **1983**, *97*, 1299.

(77) Thompson, H. J.; Chasteen, N. D.; Meeker, L. D. *Carcinogenesis* **1984**, *5*, 849.

(78) Desoize, B. *Anticancer Res.* **2004**, *24*, 1529.

(79) Narla, R. K.; Chen, C.-L.; Dong, Y.; Uckun, F. M. *Clin. Cancer Res.* **2001**, *7*, 2124.

(80) Morinville, A.; Maysinger, D.; Shaver, A. *Trends Pharmacol. Sci.* **1998**, *19*, 452.

(81) Djordjevic, C. *Met. Ions Biol. Syst.* **1995**, *31*, 595.

(82) Djordjevic, C.; Wampler, G. L. *J. Inorg. Biochem.* **1985**, *25*, 51.

(83) Kieler, J.; Gromek, A.; Nissen, N. I. *Acta. Chir. Scand. Suppl.* **1965**, *343*, 154.

(84) Ray, R. S.; Rana, B.; Swami, B.; Venu, V.; Chatterjee, M. *Chem.-Biol. Interact.* **2006**, *163*, 239.

(85) Bishayee, A.; Waghray, A.; Patel, M. A.; Chatterjee, M. *Cancer Lett.* **2010**, *294*, 1.

(86) Faure, R.; Vincent, M.; Dufour, M.; Shaver, A.; Posner, B. I. *J. Cell Biochem.* **1995**, *59*, 389.

(87) Faure, R.; Vincent, M.; Dufour, M.; Shaver, A.; Posner, B. I. *J. Cell. Biochem.* **1995**, *59*, 389.

(88) Zhang, Z.; Chen, F.; Huang, C.; Shi, X. *J. Environ. Pathol., Toxicol. Oncol.* **2002**, *21*, 223.

(89) Harding, M. M.; Mokdsi, G. *Curr. Med. Chem.* **2000**, *7*, 1289.

(90) D'Cruz Osmond, J.; Uckun Fatih, M. *Expert Opin. Investig. Drugs* **2002**, *11*, 1829.

(91) Dong, Y.; Narla, R. K.; Sudbeck, E.; Uckun, F. M. *J. Inorg. Biochem.* **2000**, *78*, 321.

(92) Narla, R. K.; Dong, Y.; D'Cruz, O. J.; Navara, C.; Uckun, F. M. *Clin. Cancer Res.* **2000**, *6*, 1546.

(93) Manning, F. C.; Patierno, S. R. *Cancer Invest* **1996**, *14*, 455.

(94) D'Cruz, O. J.; Dong, Y.; Uckun, F. M. *Anti-Cancer Drugs* **2000**, *11*, 849.

(95) Kulkarni, N. V.; Hegde, G. S.; Kurdekar, G. S.; Budagumpi, S.; Sathisha, M. P.; Revankar, V. K. *Spectrosc. Lett.* **2010**, *43*, 235.

(96) Hu, W.-X.; Zhou, W.; Xia, C.-N.; Wen, X. *Bioorg. Med. Chem. Lett.* **2006**, *16*, 2213.

(97) Sau, D. K.; Butcher, R. J.; Chaudhuri, S.; Saha, N. *Mol. Cell. Biochem.* **2003**, *253*, 21.

(98) Kasuga, N. C.; Sekino, K.; Ishikawa, M.; Honda, A.; Yokoyama, M.; Nakano, S.; Shimada, N.; Koumo, C.; Nomiya, K. *J. Inorg. Biochem.* **2003**, *96*, 298.

(99) Kovala-Demertzi, D.; Demertzis, M. A.; Miller, J. R.; Frampton, C. S.; Jasinski, J. P.; West, D. X. *J. Inorg. Biochem.* **2002**, *92*, 137.

(100) West, D. X.; Padhye, S. B.; Sonawane, P. B. *Struct. Bonding* **1991**, *76*, 1.

(101) Kowol, C. R.; Eichinger, R.; Jakupec, M. A.; Galanski, M.; Arion, V. B.; Keppler, B. K. *J. Inorg. Biochem.* **2007**, *101*, 1946.

(102) Grguric-Sipka, S.; Kowol, C. R.; Valiahdi, S.-M.; Eichinger, R.; Jakupec, M. A.; Roller, A.; Shova, S.; Arion, V. B.; Keppler, B. K. *Eur. J. Inorg. Chem.* **2007**, 2870.

(103) Abou-Hussen, A. A.; El-Metwally, N. M.; Saad, E. M.; El-Asmy, A. A. *J. Coord. Chem.* **2005**, *58*, 1735.

(104) Gomez-Saiz, P.; Garcia-Tojal, J.; Maestro, M.; Mahia, J.; Lezama, L.; Rojo, T. *Eur. J. Inorg. Chem.* **2003**, 2123.

(105) Yu, Y.; Kalinowski, D. S.; Kovacevic, Z.; Siafakas, A. R.; Jansson, P. J.; Stefani, C.; Lovejoy, D. B.; Sharpe, P. C.; Bernhardt, P. V.; Richardson, D. R. *J. Med. Chem.* **2009**, *52*, 5271.

(106) Brockman, R. W.; Thomson, J. R.; Bell, M. J.; Skipper, H. E. *Cancer Res.* **1956**, *16*, 167.

(107) Moore, E. C.; Sartorelli, A. C. *Pharmacol. Ther.* **1984**, *24*, 439.

(108) Cerqueira, N. M. F. S. A.; Fernandes, P. A.; Ramos, M. J. *Recent Pat. Anti-Cancer Drug Discov.* **2007**, *2*, 11.

(109) Reichard, P.; Baldesten, A.; Rutberg, L. *J. Biol. Chem.* **1961**, *236*, 1150.

(110) Jordan, A.; Reichard, P. *Annu. Rev. Biochem.* **1998**, *67*, 71.

(111) Sartorelli, A. C.; Booth, B. A. *Cancer Res.* **1967**, *27*, 1614.

(112) Li, J.; Luo, X.; Wang, Q.; Zheng, L. M.; King, I.; Doyle, T. W.; Chen, S. H. *Bioorg. Med. Chem. Lett.* **1998**, *8*, 3159.

(113) Cerqueira, N. M. F. S. A.; Pereira, S.; Fernandes, P. A.; Ramos, M. J. *Curr. Med. Chem.* **2005**, *12*, 1283.

(114) Eklund, H.; Uhlin, U.; Farnegardh, M.; Logan, D. T.; Nordlund, P. *Prog. Biophys. Mol. Biol.* **2001**, *77*, 177.

(115) French, F. A.; Blanz, E. J., Jr. *J. Med. Chem.* **1966**, *9*, 585.

(116) Thelander, L.; Graslund, A. *J. Biol. Chem.* **1983**, *258*, 4063.

(117) Baker, C. H.; Banzon, J.; Bollinger, J. M.; Stubbe, J.; Samano, V.; Robins, M. J.; Lippert, B.; Jarvi, E.; Resvick, R. *J. Med. Chem.* **1991**, *34*, 1879.

(118) Wright, J. A.; Chan, A. K.; Choy, B. K.; Hurta, R. A. R.; McClarty, G. A.; Tagger, A. Y. *Biochem. Cell Biol.* **1990**, *68*, 1364.

(119) Liu, M. C.; Lin, T. C.; Sartorelli, A. C. *J. Med. Chem.* **1992**, *35*, 3672.

(120) Finch, R. A.; Liu, M.-C.; Cory, A. H.; Cory, J. G.; Sartorelli, A. C. *Adv. Enzyme Regul.* **1999**, *39*, 3.

(121) Finch, R. A.; Liu, M. C.; Grill, S. P.; Rose, W. C.; Loomis, R.; Vasquez, K. M.; Cheng, Y. C.; Sartorelli, A. C. *Biochem. Pharmacol.* **2000**, *59*, 983.

(122) Kowol, C. R.; Berger, R.; Eichinger, R.; Roller, A.; Jakupec, M. A.; Schmidt, P. P.; Arion, V. B.; Keppler, B. K. *J. Med. Chem.* **2007**, *50*, 1254.

(123) Hedley, D. W.; Tripp, E. H.; Slowiaczek, P.; Mann, G. J. *Cancer Res.* **1988**, *48*, 3014.

(124) Chitambar, C. R.; Narasimhan, J.; Guy, J.; Sem, D. S.; O'Brien, W. J. *Cancer Res.* **1991**, *51*, 6199.

(125) Narasimhan, J.; Antholine, W. E.; Chitambar, C. R. *Biochem. Pharmacol.* **1992**, *44*, 2403.

(126) Patil, S. A.; Naik, V. H.; Kulkarni, A. D.; Kamble, U.; Bagihalli, G. B.; Badami, P. S. *J. Coord. Chem.* **2010**, *63*, 688.

(127) Sava, G.; Pacor, S.; Bergamo, A.; Cocchietto, M.; Mestroni, G.; Alessio, E. *Chemico-Biol. Interact.* **1995**, *95*, 109.

(128) Beckford, F. A.; Shaloski, M., Jr.; Leblanc, G.; Thessing, J.; Lewis-Alleyne, L. C.; Holder, A. A.; Li, L.; Seeram, N. P. *J. Chem. Soc., Dalton Trans.* **2009**, 10757.

(129) Clarke, M. J. *Coord. Chem. Rev.* **2003**, *236*, 209.

(130) Clarke, M. J.; Zhu, F.; Frasca, D. R. *Chem. Rev.* **1999**, *99*, 2511.

(131) Armitage, B. *Chem. Rev.* **1998**, *98*, 1171.

(132) Groessl, M.; Zava, O.; Dyson, P. J. *Metallomics* **2011**, *3*, 591.

(133) Ang, W. H.; Dyson, P. J. *Eur. J. Inorg. Chem.* **2006**, 4003.

(134) Sava, G.; Zorzet, S.; Turrin, C.; Vita, F.; Soranzo, M.; Zabucchi, G.; Cocchietto, M.; Bergamo, A.; DiGiovine, S.; Pezzoni, G.; Sartor, L.; Garbisa, S. *Clin. Cancer Res.* **2003**, *9*, 1898.

(135) Sava, G.; Bergamo, A. *Int. J. Oncol.* **2000**, *17*, 353.

(136) Maurya, M. R.; Kumar, A.; Abid, M.; Azam, A. *Inorg. Chim. Acta* **2006**, *359*, 2439.

(137) Sheldrick, G. M. *Acta Crystallogr., Sect. A: Found. Crystallogr.* **2008**, *A64*, 112.

(138) Sheldrick, G. M. *NATO ASI Series, Series E: Applied Sciences* **1997**, *347*, 219.

(139) Sheldrick, G. M.; Schneider, T. R. *Methods Enzymol.* **1997**, *277*, 319.

(140) Cory, A. H.; Owen, T. C.; Barltrop, J. A.; Cory, J. G. *Cancer Comm.* **1991**, *3*, 207.

(141) Koh, L. L.; Ranford, J.; Robinson, W.; Svensson, J. O.; Tan, A. L. C.; Wu, D. *Inorg. Chem.* **1996**, *35*, 6466.

(142) Vanco, J.; Svajlenova, O.; Marek, J. *Acta Crystallogr., Sect. C: Cryst. Struct. Commun.* **2003**, *C59*, m190.

(143) Garcia-Raso, A.; Fiol, J. J.; Lopez-Zafra, A.; Mata, I.; Espinosa, E.; Molins, E. *Polyhedron* **2000**, *19*, 673.

(144) Pessoa, J. C.; Duarte, M. T.; Gillard, R. D.; Madeira, C.; Matias, P. M.; Tomaza, I. *J. Chem. Soc., Dalton Trans.* **1998**, 4015.

(145) Viñuelas-Zahínos, E.; Luna-Giles, F.; Torres-García, P.; Fernández-Calderón, M. C. *Eur. J. Med. Chem.* **2011**, *46*, 150.

(146) Lobana, T. S.; Sharma, R.; Bawa, G.; Khanna, S. *Coord. Chem. Rev.* **2009**, *253*, 977.

(147) Mahalingam, V.; Chitrapriya, N.; Fronczek, F. R.; Natarajan, K. *Polyhedron* **2008**, *27*, 2743.

(148) Zhang, H.; Thomas, R.; Oupicky, D.; Peng, F. *J. Biol. Inorg. Chem.* **2008**, *13*, 47.

(149) Reddy, K. H.; Reddy, P. S.; Babu, P. R. *Transition Met. Chem. (Dordrecht, Neth.)* **2000**, *25*, 154.

(150) Chatterjee, M.; Ghosh, S. *Transition Met. Chem.* **1998**, *23*, 355.

(151) Bhattacharjee, S.; Bhattacharyya, R. *J. Chem. Soc., Dalton Trans.* **1993**, 1151.

(152) Kanoongo, N.; Singh, R.; Tandon, J. P. *Transition Met. Chem.* **1987**, *12*, 271.

(153) Belicchi-Ferrari, M.; Bisceglie, F.; Buschini, A.; Franzoni, S.; Pelosi, G.; Pinelli, S.; Tarasconi, P.; Tavone, M. *J. Inorg. Biochem.* **2009**, *104*, 199.

(154) Demirci, T. B.; Koseoglu, Y.; Guner, S.; Ulkuseven, B. *Cent. Eur. J. Chem.* **2006**, *4*, 149.

(155) Lobana, T. S.; Sharma, R.; Bawa, G.; Khanna, S. *Coord. Chem. Rev.* **2009**, *253*, 977.

(156) Cavaco, I.; Pessoa, J. C.; Duarte, M. T.; Gillard, R. D.; Matias, P. *Chem. Commun.* **1996**, 1365.

(157) Venkatraman, R.; Ameera, H.; Sitole, L.; Ellis, E.; Fronczek, F. R.; Valente, E. J. *J. Chem. Crystallogr.* **2009**, *39*, 711.

(158) Zhang, H.; Thomas, R.; Oupicky, D.; Peng, F. *JBIC, J. Biol. Inorg. Chem.* **2008**, *13*, 47.

(159) Raposo, M. M. M.; Garcia-Acosta, B.; Abalos, T.; Calero, P.; Martinez-Manez, R.; Ros-Lis, J. V.; Soto, J. *J. Org. Chem.* **2010**, *75*, 2922.

(160) West, D. X.; Swearingen, J. K.; Valdes-Martinez, J.; Hernandez-Ortega, S.; El-Sawaf, A. K.; Van, M. F.; Castineiras, A.; Garcia, I.; Bermejo, E. *Polyhedron* **1999**, *18*, 2919.

(161) Lobana, T. S.; Butcher, R. J.; Failes, T. W.; Turner, P. *J. Coord Chem.* **2005**, *58*, 1369.

(162) Lobana, T. S.; Castineiras, A. *Polyhedron* **2002**, *21*, 1603.

(163) Lobana, T. S.; Khanna, S.; Butcher, R. J.; Hunter, A. D.; Zeller, M. *Polyhedron* **2006**, *25*, 2755.

(164) Lobana, T. S.; Sanchez, A.; Casas, J. S.; Castineiras, A.; Sordo, J.; Garcia-Tasende, M. S.; Vazquez-Lopez, E. M. *J. of the Chem. Soc., Dalton Trans.* **1997**, 4289.

(165) Afrasiabi, Z.; Sinn, E.; Kulkarni, P. P.; Ambike, V.; Padhye, S.; Deobagakar, D.; Heron, M.; Gabbutt, C.; Anson, C. E.; Powell, A. K. *Inorg. Chim. Acta* **2005**, *358*, 2023.

(166) Frith, K. A.; Limson, J. L. *Electrochim. Acta* **2010**, *55*, 4281.

(167) Tang, X.; Liu, Y.; Hou, H.; You, T. *Talanta* **2010**, *80*, 2182.

(168) Babaei, A.; Zendehdel, M.; Khalilzadeh, B.; Taheri, A. *Colloids and Surf. B* **2008**, *66*, 226.

(169) Cakir, S.; Bicer, E. *J. Iran. Chem. Soc.* **2010**, *7*, 394.

(170) Cakir, S.; Bicer, E.; Eleman, A. *Transition Met. Chem.* **2001**, *26*, 89.

(171) Cakir, S.; Bicer, E.; Cakir, O. *Electrochem. Commun.* **2000**, *2*, 124.

(172) Thomas, F.; Arora, H.; Philouze, C.; Jarjayes, O. *Inorg. Chim. Acta* **2010**, *363*, 3122.

(173) Bollo, S.; Soto-Bustamante, E.; Nunez-Vergara, L. J.; Squella, J. A. *J. Electroanal. Chem.* **2000**, *492*, 54.

(174) Refaey, S. A. M.; Hassan, A. A.; Shehata, H. S. *Int. J. Electrochem. Sci.* **2008**, *3*, 325.

(175) Manming, Y.; Kun, L.; Zhiyu, J. *J. Electroanal. Chem.* **1996**, *408*, 225.

(176) Blankespoor, R. L.; Doyle, M. P.; Hedstrand, W. H.; Tamblyn, W. H.; Van Dyke, D. A. *J. Am. Chem. Soc.* **1981**, *103*, 7096.

(177) Sonawane, P.; Kumbhar, A.; Padhye, S.; Butcher, R. J. *Transition Met. Chem.* **1994**, *19*, 277.

(178) Padhye, S.; Chikate, R.; Kumbhar, A.; Shallom, J. M.; Chitnis, M. P. *BioMetals* **1992**, *5*, 67.

(179) Murugkar, A.; Padhye, S.; Guha-Roy, S.; Wagh, U. *Inorg. Chem. Commun.* **1999**, *2*, 545.

(180) Li, Q.; Batchelor-McAuley, C.; Compton, R. G. *J. Phys. Chem. B* **2010**, *114*, 97.

(181) Hammerich, O.; Parker, V. D. *J. Am. Chem. Soc.* **1974**, *96*, 4289.

(182) Majeski, E. J.; Stuart, J. D.; Ohnesorge, W. E. *J. Am. Chem. Soc.* **1968**, *90*, 633.

(183) Kovala-Demertzi, D.; Demertzis, M. A.; Miller, J. R.; Papadopoulou, C.; Dodorou, C.; Filousis, G. *J. Inorg. Biochem.* **2001**, *86*, 555.

(184) Mendes, I. C.; Botion, L. M.; Ferreira, A. V. M.; Castellano, E. E.; Beraldo, H. *Inorg. Chim. Acta* **2009**, *362*, 414.

(185) Beraldo, H.; Nacif, W. F.; Teixeira, L. R.; Reboucas, J. S. *Trans. Met. Chem.* **2002**, *27*, 85.

(186) West, D. X.; Swearingen, J. K.; Valdes-Martinez, J.; Hernandez-Ortega, S.; El-Sawaf, A. K.; Van Meurs, F.; Castineiras, A.; Garcia, I.; Bermejo, E. *Polyhedron* **1999**, *18*, 2919.

(187) Pessoa, J. C.; Cavaco, I.; Correia, I.; Tomaz, I.; Duarte, T.; Matias, P. M. *J. Inorg. Biochem.* **2000**, *80*, 35.

(188) Price, J. H.; Williamson, A. N.; Schramm, R. F.; Wayland, B. B. *Inorg. Chem.* **1972**, *11*, 1280.

(189) Cotton, F. A.; Francis, R. *J. Am. Chem. Soc.* **1960**, *82*, 2986.

(190) Cotton, F. A.; Francis, R.; Horrocks, W. D., Jr. *J. Phys. Chem.* **1960**, *64*, 1534.

(191) Sasmal, P. K.; Patra, A. K.; Nethaji, M.; Chakravarty, A. R. *Inorg. Chem.* **2007**, *46*, 11112.

(192) Toshima, K.; Takano, R.; Ozawa, T.; Matsumura, S. *Chem. Commun.* **2002**, 212.

(193) Rath, S. P.; Ghosh, T.; Mondal, S. *Polyhedron* **1997**, *16*, 4179.

(194) Bonadies, J. A.; Carrano, C. J. *J. Am. Chem. Soc.* **1986**, *108*, 4088.

(195) Guillo, P.; Hamelin, O.; Loiseau, F.; Pecaut, J.; Menage, S. *Dalton Trans.* **2010**, *39*, 5650.

(196) Kianfar, A. H.; Mohebbi, S. *J. Iran. Chem. Soc.* **2007**, *4*, 215.

(197) Maia, P. I. d. S.; Pavan, F. R.; Leite, C. Q. F.; Lemos, S. S.; de, S. G. F.; Batista, A. A.; Nascimento, O. R.; Ellena, J.; Castellano, E. E.; Niquet, E.; Deflon, V. M. *Polyhedron* **2009**, *28*, 398.

(198) Kan, W. L.; Cho, C. H.; Rudd, J. A.; Lin, G. *J. Ethnopharmacol.* **2008**, *120*, 36.

(199) Hall Matthew, D.; Okabe, M.; Shen, D.-W.; Liang, X.-J.; Gottesman Michael, M. *Annu, Rev, Pharmacol, Toxicol.* **2008**, *48*, 495.

(200) Puckett, C. A.; Ernst, R. J.; Barton, J. K. *Dalton Trans.* **2010**, *39*, 1159.

(201) Puckett, C. A.; Barton, J. K. *J. Am. Chem. Soc.* **2007**, *129*, 46.